The Application of the Computational Methods (Molecular Mechanics and Molecular Orbital Calculations) to the Studies of Insect Pheromones

December, 1993

DOCTOR OF ENGINEERING

Kazuko Shimazaki

TOYOHASHI UNIVERSITY OF TECHNOLOGY

(1)

The Application of the Computational Methods (Molecular Mechanics and Molecular Orbital Calculations) to the Studies of Insect Pheromones

December, 1993

DOCTOR OF ENGINEERING

Kazuko Shimazaki

TOYOHASHI UNIVERSITY OF TECHNOLOGY

要旨

計算化学の昆虫フェロモンの研究への適用

昆虫は、主に嗅覚を用いた感覚刺激に対する反応として摂食行動や配偶行動を起こすが、最近多くの昆虫がフェロモンと呼ばれる化学物質を分泌して同種間の情報伝達をおこなっていることが生理学的研究から明らかになってきた。特に雌が生産する性フェロモンは極く微量で雄を誘引することから、有効な害虫駆除剤としての利用が期待される。けれども、フェロモン研究には二つの大きな障害がある。一つは化学上の問題で、昆虫の雌が産生するフェロモンの量が極めて微量であるため、構造決定までに時間を要する点、もう一つは工業上の問題で、フェロモンの構造が複雑でキラル中心が多数あるため、合成による生産に不適な点である。特に後者に関しては、立体異性体がフェロモン活性を阻害することがあるとの報告もあるので、充分なエナンチオマー純度を持った製品が活性発現には要求される。

これらの問題の解決に計算化学は重要な役割をもって寄与することができる。一つはフェロモンの構造決定や配座解析において不足する試料を補足することであり、もう一つは合成可能な新規な類縁体の探索に有効な活性発現構造を同定することである。そこで2種類の生活害虫の性フェロモンについて計算化学を用いた研究を行い、その有効性を検討した。一つはタバコシバンムシの性フェロモン、セリコルニンの絶対立体配置の決定への適用(1)、もう一つはワモンゴキブリの性フェロモン、ペリプラノン類とその類縁体の活性発現構造の同定および構造活性相関の検討への適用(2)である。以下に結果を示す。

(1)鎖状、環状セリコルニンの絶対立体配置は、$^{3}J_{HH}$値の実測値と、

分子力場法での配座解析結果から求められる計算値との比較から、それぞれ（4*S**, 6*S**, 7*S**)、および(3*S**, 5*S**, 6*S**)と決定された。この結果から、計算化学的手法は天然物の立体配置の決定に役立つことが示された。

(2)ペリプラノンB(P-B)とその類縁体について、分子力場法による各化合物の配座解析から活性発現環配座が、分子軌道法による電子状態の検討から活性発現軌道が同定された。得られた2つの活性発現要素を組み合わせて、有効フロンティア指数（Effective Frontier Parameter ：$EF^{(N)}_{(S)}$）を考案し生理活性との相関を求めたところ、良い相関が得られた(*R*=0.929)。

次に$EF^{(N)}_{(S)}$の活性予測の信頼性を検証するため、ペリプラノンA(P-A)および類縁体について検討した。配座解析の結果、P-A には、先に活性発現環配座とした環配座と、活性発現軌道の存在する部分が良く重なる環配座が同程度の確率で存在していた。そこでこの二つを活性発現環配座として、P-Bとその類縁体について、再度$EF^{(N)}_{(S)}$と生理活性の相関を求め直したところ、さらに相関は良くなった(*R*=0.969)。新しく得られた相関式より求めたP-Aおよび類縁体の活性予測値は、実測値と一致した。これは活性予測の指標としての$EF^{(N)}_{(S)}$の信頼性を示すものである。

このように計算化学と実験化学の組み合わせた昆虫フェロモンに関する研究は、他の生理活性物質の分子認識機構の解明にも拡張されると考える。

summary

title;
The Application of the Computational Methods (Molecular Mechanics and Molecular Orbital Calculations) to the Studies of Insect Pheromones

Insects are believed to rely on their sense of olfaction when searching for food or mates. Physiological research has revealed that a number of species use molecules called 'pheromones' as signals for communication. In particular, the potency of sex pheromones produced by female insects to attract male is extremely high and it has been thought that they would serve as effective controlling agents for insect pests. There are, however, two major difficulties which have delayed the development of pheromone studies. The first is chemical in nature; female insects only produce a small amount of sex pheromones in nature, and it takes a long time to determine their stereochemical structure. The other is an engineering problem; the natural pheromones generally contain chiral carbons in their complex molecular structures and, therefore, known synthetic procedures are not compatible with their industrial production. In addition, it has been reported that some stereoisomers of pheromones display a strong inhibitory action against the pheromone activity. Therefore, a compound with high enantiomeric purity is required to induce the pheromone activity.

However, computational chemical methods can contribute to the industrial utilization of pheromones by playing an important role in determining answers to these problems. Firstly, these methods can complement the insufficient amount of natural pheromones in the structural determinations and the conformational analyses. The other is in the identification of the biologically active structure of pheromones and in searching for new analogues which are synthesized easily.

In this thesis, applications of computational methods to the stereochemical assignments of serricornin , the sex pheromone of cigarette beetle (1), and to the structure-activity relationship of periplanones, the sex pheromones of American cockroach (2), are described.

(1) The absolute configurations of acyclic and cyclic forms of serricornin are determined to be (*4S*,6S*,7S**) and (*3S*,5S*,6S**), respectively from comparison of the observed $^3J_{HH}$s values with those calculated for all possible diastereomers. It is revealed that the MM conformational analysis is useful in the determination of the unknown stereochemistry of natural products.

(2) X-ray crystallographic and NOE analyses have been performed on periplanone-A (**P-A**), -B (**P-B**) and their analogues. But, those observed results were insufficient to obtain the biologically active structures. In order to clarify their conformational properties, a complete analysis by molecular mechanics of **P-B** and its related analogues was carried out by CONFLEX/MM2 with an additional set of MM2 force field parameters for the epoxy functional group. The validity of the calculated

results was confirmed by comparison with X-ray and NMR results. The ring conformation of the global minimum of **P-B** is well superimposable on those of the analogues and of the third conformer of Germacrene-D. A hypothesis can be drawn as follows; the biological activities depend on the total population of the conformers having the same ring conformation as the global minimum of **P-B**. CONFLEX/MM2 study suggests that the ring conformation of the global minimum of **P-B** is the biologically important structure.

An AM1 study on the stable conformers obtained by CONFLEX/MM2 was carried out to investigate the correlation between the electronic properties and their pheromone activity. Only the population-weighted orbital energy of the frontier unoccupied molecular orbitals which are distributed around the 'upper' part of the ten-membered ring in the structural formula (abbreviated as $FUMO_{upper}$), shows a good correlation with biological activity (R=0.849). It suggests that the $FUMO_{upper}$ plays an important part in the biological activity.

A new parameter, effective frontier parameter ($EF^{(N)}(S)$), is proposed as an index for the evaluation of pheromone activity; this takes into account the electronic properties in $FUMO_{upper}$ and the geometries of the stable conformers of **P-B** and the analogues. The correlation between $EF^{(N)}(S)$ and biological activities (R=0.929) is improved.

The same conformational analyses are performed on **P-A** and the related analogues to confirm the reliability of $EF^{(N)}(S)$. A CONFLEX/MM2 calculation revealed the conformational properties of

those compounds. The conformation of the global minimum of **P-A** is well superimposable on that of **P-B**. However, the second conformer of **P-A**, of which exomethylene group is flapped upwards, exists in comparable concentration with the global minimum. A comparison of the ring structure of the global minimum with that of the second one shows that the geometries around the epoxy-carbonyl moiety and the high density regions in $FUMO_{upper}$ are similar to each other. Therefore, $EF^{(N)}(S)$ was reassessed for **P-B** and their analogues on the basis that these two ring structures are the biologically important ones. An even better correlation between improved $EF^{(N)}(S)$ and biological activities is obtained (R=0.969). The predicted value of the biological activity for **P-A** calculated from the new linear regression equation is in good agreement with that observed in the bioassay. The improved $EF^{(N)}(S)$ appears reliable as an index for the prediction of the biological activity of newly designed analogues.

Contents

Chapter 1

General Introduction

Insects are believed to rely on their sense of olfaction when searching for food or mates. Physiological research has revealed that a number of species use molecules called 'pheromones' as signals for communication. In particular, the potency of sex pheromones produced by female insects to attract male is extremely high and it has been thought that they would serve as effective controlling agents for insect pests. There are, however, two major difficulties which have delayed the development of pheromone studies. The first is chemical in nature; female insects only produce a small amount of sex pheromones in nature, and it takes a long time to determine their stereochemical structure. The other is an engineering problem; the natural pheromones generally contain chiral carbons in their complex molecular structures and, therefore, known synthetic procedures are not compatible with their industrial production. In addition, it has been reported that some stereoisomers of pheromones display a strong inhibitory action against the pheromone activity. Therefore, a compound with high enantiomeric purity is required to induce the pheromone activity.

However, computational chemical methods can contribute to the industrial utilization of pheromones by playing an important role in determining answers to these problems. Firstly, these methods can complement the insufficient amount of natural pheromones in the structural determinations and the conformational analyses. The other is in the identification

of the biologically active structure of pheromones and in searching for new analogues which are synthesized easily.

In this thesis, applications of computational methods to the stereochemical assignments of serricornin, the sex pheromone of cigarette beetle, and to the structure-activity relationship of periplanones, the sex pheromones of American cockroach, are described. The contents of this thesis are as follows.

In chapter 2, conformational analysis by molecular mechanics calculation is performed to determine the absolute configuration of serricornin.

In chapter 3, conformational properties of periplanones and their analogues are analyzed by the X-ray crystallography and ^1H NMR spectroscopy.

In chapters 4, 5, and 6, combined molecular mechanics and semiempirical molecular orbital calculations are applied to the investigation of the conformational and electronic properties of periplanones and their analogues. The structure-activity relation is discussed in some detail.

In chapter 7, the conclusions are described.

Chapter 2

Conformational Analysis of Serricornin. Application of Molecular Mechanics Calculations to Stereochemical Assignment of Serricornin, The Sex Pheromone of Cigarette Beetle (*Lasioderma serricorne* F.).

Abstract

Conformational analysis using molecular mechanics(MM) was performed for a determination of the stereochemistry of serricornin, the sex pheromone of the cigarette beetle (*Lasioderma serricorne* F.). An exhaustive conformational analysis using MM2 calculations with algorithms for covering torsional energy surfaces of flexible molecules furnishes coordinates and steric energies of all local energy minimum conformers of serricornin, both acyclic and the corresponding cyclic forms. These coordinates gave angles required for the calculation of vicinal H/H coupling constants($^3J_{HH}$s) of each energy mimima by Altona's modified Karplus equation. The Boltzmann distribution of all local energy minima were calculated from their steric energies to furnish populations of each energy minimum conformer. Population-weighted averaged $^3J_{HH}$s of four enantiomeric pairs, (*S*,S*,S**), (*S*,S*,R**), (*S*,R*,S**), and (*R*,S*,S**)-serricornins were calculated from the data above. The observed $^3J_{HH}$s of the naturally occurring serricornin, both acyclic and cyclic forms, are fitted best to calcd. $^3J_{HH}$s of (*4S*,6S*,7S**)-acyclic and (*3S*,5S*,6S**)-cyclic serricornin, respectively, among those of four enantiomeric pairs of serricornin.

Introduction

Serricornin, a female-produced sex pheromone of the cigarette beetle, was isolated and structurally elucidated to be an equilibrating mixture of 4,6-dimethyl-7-hydroxynonan-3-one and the corresponding cyclic hemiketal (Figure 1) (Chuman et al., 1985). Many efforts on synthetic studies of the diastereomeric mixture (Chuman et al., 1979), (*4RS,6S,7R*)- (Chuman et al., 1981), (*4RS,6R,7R*)- (Mori K. et al., 1981), (*4RS,6S,7S*)- (Hoffmann et al., 1982), (*4S,6R,7R*)- (Mori M. et al., 1982a), and (*4S,6S,7S*)- acyclic serricornins (Mori M. et al., 1982b; Mori K. and Watanabe, 1985) were required to established the absolute configuration of naturally occurring serricornin to be (*4S,6S,7S*) as the acyclic form and (*3S,5S,6S*) as the cyclic form (Chuman et al., 1985). The determination of the absolute configuration is important to develop an effective lure for the pest, because only (*S,S,S*)- serricornin elicits pheromonal activity among eight possible stereoisomers (Chuman et al., 1985).

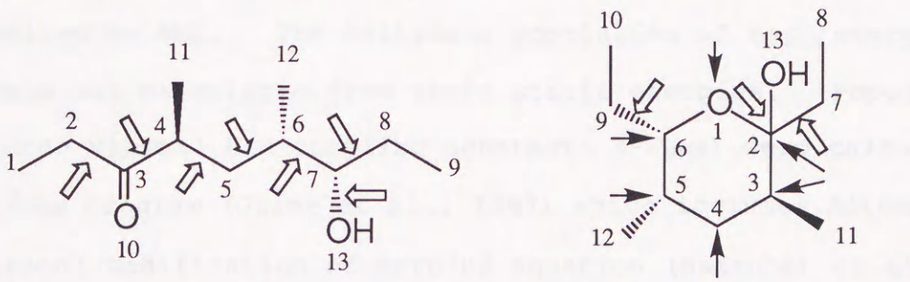

(4*S*,6*S*,7*S*)-ACYCLIC SERRICORNIN (3*S*,5*S*,6*S*)-CYCLIC SERRICORNIN

Fig. 1 Cyclic and acyclic structures of serricornin. White and black arrows point to bonds which were rotated by TREE and corners flapped by CONFLEX.

This study focused on a determination of the absolute configuration of serricornin using molecular mechanics (MM) calculations. It is revealed that MM conformational analysis is

useful for the convenient determinations of unknown stereochemistry of natural products.

Methods and Materials

Molecular Mechanics Calculation for Conformational Analysis. The MM2 (Burkert and Allinger, 1980; Version 85':Molecular Design Limited, USA) molecular mechanics program is used in structural optimization with QUANTA (Polygen Co., Waltham, Massachusetts) as a computer graphics program running on IRIS-4D/80GT (Silicon Graphics Computer Systems Inc., Mountain View, California). Introduction of the initial two-dimensional structure was performed by the CHEMNOTE option in the QUANTA program.

Exhaustive conformational analysis by generation of all possible conformations of acyclic and cyclic serricornins was performed by the TREE (Masamune et al., 1986) and CONFLEX (Gotō and Ōsawa, 1989) programs, respectively. Acyclic and cyclic candidates generated by these option programs were structurally optimized by MM2. The Boltzmann population of each energy minimum was calculated from their steric energies. Population-weighted vicinal H/H coupling constants ($^3J_{HH}$s) were calculated by the $^3J_{HH}$ program (Jaime et al., 1987) which includes Altona's empirical modification of Karplus equation (Haasnoot et al., 1980).

Procedure of Conformational Analysis of Serricornin. All possible candidates of acyclic serricornin for MM optimization were generated by the TREE program from the combination of staggered arrangements, anti, gauche(+) and gauche(-) on each backbone C2-C3, C3-C4, C4-C5, C5-C6, C6-C7, C7-C8 and C7-O13

bonds** (Figure 1). All possible candidates of the cyclic form for MM optimization also were generated by the CONFLEX program from the combinations of pyran ring conformations (chair, boat and twist), with staggered arrangements (C2-C7, C6-C9, C2-O13), and with orientations of hydroxyl group (axial and equatorial) (Figure 1).

All conformations generated were subjected to MM structural optimization to give coordinates and steric energies of each energy minimum. The Boltzmann distribution of each energy minimum were calculated from the steric energy. These conformational analyses were performed for four enantiomeric pairs of both acyclic and cyclic serricornin.

Comparison of Vicinal H/H coupling constants ($^3J_{HH}$s). Vicinal H/H coupling constants ($^3J_{HH}$s) were calculated by Altona's empirical modification of Karplus equation (Haasnoot et al., 1980). Coordinates of each energy minimum bring angle information required for the $^3J_{HH}$ calculation in the above equation. Population-weighted averaged $^3J_{HH}$ values of four enantiomeric pairs of serricornin were obtained from the calculation using $^3J_{HH}$s for each conformer and their Boltzmann distributions.

All NMR signals of naturally occurring serricornin were completely assigned to protons belonging to both the acyclic and cyclic structures independently by COSY-NMR, although the NMR spectrum was complicated because of the acyclic-cyclic equilibrium

---

** In this study, anti, gauche(+) and gauche(-) conformations were generated on two C(sp^3)-C(sp^2) bonds (C2-C3 and C3-C4 bonds) as well as other C(sp^3)-C(sp^3) bonds by TREE program.

(Mori et al., 1984). Thus, the $^3J_{HH}$s of natural occurring acyclic and cyclic serricornins can be compared to the corresponding MM calculated $^3J_{HH}$s of (*S*,S*,S**)-,[#] (*S*,S*,R**)-, (*S*,R*,S**)- and (*R*,S*,S**)-acyclic/cyclic serricornins.

Results and Discussion

Conformation analysis of the acyclic form. Two thousand one hundred eighty-seven (=3^7) candidates of acyclic serricornin for MM optimization were generated by the combination of the staggered arrangements of the seven bonds (Figure 1). MM optimization of these candidates of (*4S*,6S*,7S**)-, (*4S*,6S*,7R**)-, (*4S*,6R*,7S**)- and (*4R*,6S*,7S**)-acyclic serricornin furnished 1165, 1227, 1409 and 1164 local energy minima, respectively (Table 1). In the case of (*4S*,6S*,7S**)-serricornin, 19 conformations among these 1165 conformations have over 1% population by Boltzmann distribution calculation. The major conformer has an anti(C2-C3), anti(C3-C4), (+)-gauche(C4-C5), (+)-gauche(C5-C6), (+)-gauche(C6-C7), anti(C7-C8) and (-)-gauche(C6-O13) conformations (Figure 2). The population of the major was ca. 10%, and many local energy mimima with small population exist within Δ1.0 kcal/mol (Table 1). (*4S*,6S*,7S**)-Acyclic serricornin has no big major conformation, according to MM calculations. Fifteen majors in these 19 conformer have gauche conformations on the middle part of the molecule, C4-C5 and/or C5-C6 bonds while conformers having anti conformations in these bonds like the all-anti conformer (No.

[#] A stereochemical designation with asterisks such as (*S**, *S**, *S**) means the enantiometric pair (*S*, *S*, *S*) and (*R*, *R*, *R*).

17 conformer), are very few (Ōsawa et al., 1989). The predominant shape of the molecule is a folded type, not an extended type (Figure 2).

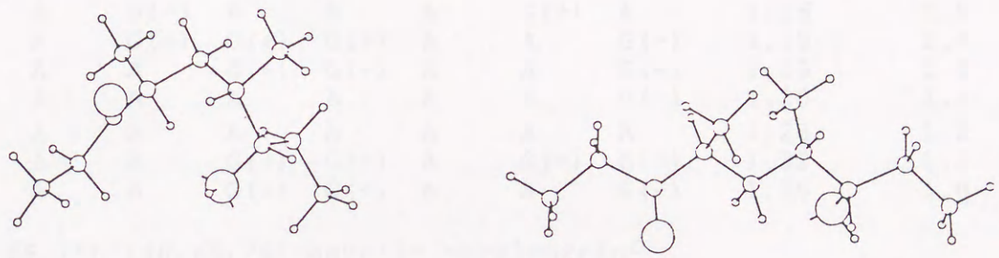

Folded Conformation
The major conformation: 10.3%

Extended Conformation
The 17th energy minimum: 1.2%

Fig. 2 Folded and extended structures of (4*S*, 6*S*, 7*S*)-acyclic serricornin. Large, medium, and small circles indicate oxygen, carbon, and hydrogrn atoms, respectively. Lone pairs of electrons are represented by lines from oxygen atoms.

The tendency is the same in the stable conformations of other acyclic serricornin isomers (Table 1). The MM2 program used in this study has no function for energy estimation of hydrogen bonding for the carbonyl and hydroxyl groups in the acyclic serricornin. By addition of this function on the MM calculation, the folded-type molecule may be estimated more positively as the stable conformation.

Table 1. Conformational analysis of acyclic serricornin

Conf.	Torsions							ΔSteric E	Population
No.	2-3	3-4	4-5	5-6	6-7	7-8	7-13	(kcal/mol)	(%)
(4S,6S,7S)/(4R,6R,7R)-acyclic serricornin[a]									
1	A	A	G(+)	G(+)	G(+)	A	G(-)	0.00	10.3
2	A	G(-)	G(-)	G(+)	A	A	A	0.23	7.0
3	A	A	G(+)	G(+)	G(+)	A	A	0.44	4.9
4	A	G(-)	G(-)	G(+)	A	G(+)	A	0.50	4.4
5	A	G(+)	G(+)	G(+)	A	A	A	0.52	4.3
6	A	G(+)	G(+)	G(+)	A	G(+)	A	0.62	3.6
7	A	A	G(+)	G(-)	A	A	A	0.78	2.7
8	A	G(-)	A	A	A	A	A	0.81	2.6
9	A	A	G(+)	G(+)	A	A	A	0.83	2.5
10	A	A	G(+)	G(+)	A	G(+)	A	0.93	2.1
11	A	A	G(+)	G(+)	A	A	G(+)	1.08	1.7
12	G(+)	A	G(+)	G(+)	G(+)	A	G(-)	1.12	1.6
13	A	G(-)	A	A	A	G(+)	A	1.16	1.5
14	A	G(+)	G(+)	G(+)	A	A	G(-)	1.19	1.4
15	A	A	G(-)	G(+)	A	A	G(-)	1.19	1.4
16	A	A	A	A	A	A	G(-)	1.20	1.4
17[b]	A	A	A	A	A	A	A	1.28	1.2
18	A	A	G(+)	G(+)	A	G(+)	G(+)	1.32	1.1
19	A	A	G(+)	G(+)	A	A	G(-)	1.36	1.0
(4S,6S,7R)/(4R,6R,7S)-acyclic serricornin[c]									
1	G(-)	A	G(+)	A	A	A	A	0.00	5.6
2	G(-)	A	G(+)	A	A	G(+)	A	0.21	3.9
3	G(+)	A	A	G(+)	G(+)	A	G(+)	0.33	3.2
4	A	A	A	G(+)	G(+)	A	G(-)	0.35	3.1
5	G(-)	A	G(-)	A	A	A	G(+)	0.36	3.1
6	G(+)	A	G(+)	G(+)	G(+)	A	A	0.39	2.9
7	G(+)	A	G(+)	G(+)	G(+)	A	G(+)	0.44	2.7
8	G(-)	A	G(-)	A	A	G(-)	G(+)	0.60	2.0
9	G(-)	A	A	A	A	A	A	0.62	2.0
b	A	A	A	A	A	A	A	1.16	0.8
(4S,6R,7S)/(4R,6S,7R)-acyclc serricornin[d]									
1	G(+)	A	A	A	G(+)	A	A	0.00	4.9
2	G(+)	G(+)	A	A	G(+)	A	A	0.14	3.9
4	G(+)	A	A	G(+)	G(+)	A	G(-)	0.21	3.5
5	A	A	A	A	G(+)	G(-)	A	0.26	3.2
6	G(+)	A	A	A	G(+)	A	G(-)	0.29	3.0
7	G(+)	G(+)	A	G(+)	G(+)	A	A	0.30	3.0
8	G(+)	G(+)	A	G(+)	G(+)	A	G(-)	0.39	2.5
9	G(-)	A	A	G(-)	A	G(-)	A	0.48	2.2
10	G(+)	G(+)	A	A	G(+)	A	G(-)	0.50	2.1
11	G(-)	A	A	G(-)	A	G(-)	G(-)	0.50	2.1
12	A	A	A	G(+)	G(+)	A	A	0.51	2.1
b	A	A	A	A	A	A	A	3.48	0.01
(4R,6S,7S)/(4S,6R,7R)-acyclic serricornin[e]									
1	A	G(+)	A	G(+)	A	A	A	0.00	5.2
2	A	A	G(-)	G(+)	A	A	G(-)	0.05	4.8

3	A	G(+)	A	G(+)	A	G(+)	A	0.13	4.2
4	A	A	G(-)	A	A	A	A	0.28	3.2
5	A	A	G(-)	A	G(+)	A	G(-)	0.30	3.1
6	A	G(-)	G(-)	A	G(+)	A	A	0.38	2.8
7	A	A	G(-)	A	A	A	G(-)	0.55	2.0
8	A	A	G(-)	G(+)	A	G(+)	G(-)	0.56	2.0
b	A	A	A	A	A	A	A	2.72	0.05

[a] The total number of local energy minima obtained:1165. Only conformers with over 1% population are represented.
[b] All-anti conformer.
[c]The total number of local energy minima obtained:1227. Only conformers with over 2% population are represented.
[d]The total number of local energy minima obtained:1409. Only conformers with over 2% population are represented.
[e]The total number of local energy minima obtained:1164. Only conformers with over 2% population are represented.

Conformational analysis of the cyclic form. The CONFLEX program for generation of all possible conformers of cyclic serricornin produced candidates for MM optimization. MM optimization of all those candidates of (*3S*,5S*,6S**)-, (*3R*,5R*,6S**)-, (*3S*,5R*,6S**)- and (*3R*,5S*,6S**)-cyclic serricornin furnished 303, 213, 277 and 260 local energy minima, respectively (Table 2). In constant to the case of acyclic serricornin, the major conformers have large populations, and the total population is composed of several energy minima, although over 200 energy minima were obtained in the conformation analysis of each enantiomeric pair of cyclic serricornin (Table 2).

Table 2. Conformational analysis of cyclic serricornin

Conf. No.	Ring Conf.	C2 Config.	Orient. of OH	Torsions 2-7	Torsions 2-13	Torsions 6-9	ΔSteric E (kcal/mol)	Population (%)
(3S,5S,6S)/(3R,5R,6R)-cyclic serricornin[a]								
1	$^4C_1$-Chair	R/S[b]	Axial	G(+)	G(-)	G(-)	0.00	47.5
2	$^4C_1$-Chair	R/S	Axial	G(-)	G(-)	G(-)	0.36	26.0
3	$^4C_1$-Chair	R/S	Axial	G(+)	G(-)	A	0.77	12.9
4	$^4C_1$-Chair	R/S	Axial	G(-)	G(-)	A	1.01	8.6
5	$^4C_1$-Chair	R/S	Axial	G(+)	G(+)	G(-)	2.09	1.4
*	$^4C_1$-Chair	R/S	Equat.	G(-)	G(-)	G(-)	3.27	0.3
(3R,5R,6S)/(3S,5S,6R)-cyclic serricornin[c]								
1	$^4C_1$-Chair	R/S[d]	Axial	G(+)	G(+)	G(-)	0.00	44.3
2	$^4C_1$-Chair	R/S	Axial	G(+)	G(+)	A	0.38	23.3
3	$^4C_1$-Chair	R/S	Axial	G(-)	G(+)	G(-)	0.72	13.1
4	$^4C_1$-Chair	R/S	Axial	G(-)	G(+)	A	1.01	8.1
5	$^4C_1$-Chair	R/S	Axial	G(+)	A	G(-)	1.84	2.0
(3S,5R,6S)/(3R,5S,6R)-cyclic serricornin[e]								
1	$^4C_1$-Chair	R/S[f]	Axial	G(+)	G(-)	G(-)	0.00	48.6
2	$^4C_1$-Chair	R/S	Axial	G(-)	G(-)	G(-)	0.41	24.3
3	$^4C_1$-Chair	R/S	Axial	G(+)	G(-)	G(+)	0.76	13.4
4	$^4C_1$-Chair	R/S	Axial	G(-)	G(-)	G(+)	1.01	8.9
(3R,5S,6S)/(3S,5R,6R)-cyclic serricornin[g]								
1	$^1C_4$-Chair	S/R[h]	Axial	G(-)	G(+)	G(-)	0.00	29.4
2	$^4C_1$-Chair	R/S	Axial	G(+)	G(-)	G(-)	0.46	13.6
3	$^1C_4$-Chair	S/R	Axial	G(+)	G(+)	G(-)	0.49	12.9
4	Twist	R/S	Axial	G(+)	G(-)	G(-)	0.49	12.8
5	$^4C_1$-Chair	R/S	Axial	A	G(-)	G(-)	1.02	5.3
6	$^4C_1$-Chair	R/S	Axial	G(+)	G(-)	A	1.23	3.7
7	Twist	R/S	Axial	G(+)	G(-)	A	1.33	3.1
8	$^1C_4$-Chair	S/R	Axial	G(-)	G(-)	G(-)	1.51	2.3

[a] The total number of local energy minima obtained: 303. Only conformers with over 2% population are represented.
[b] *R*-configuration in (*S,S,S*) and *S*-configuration in (*R,R,R*).
[c] The total number of local energy minima obtained: 213. Only conformers with over 2% population are represented.
[d] *R*-configuration in (*R,R,S*) and *S*-configuration in (*S,S,R*).
[e] The total number of local energy minima obtained: 277. Only conformers with over 2% population are represented.
[f] *R*-configuration in (*S,R,S*) and *S*-configuration in (*R,S,R*).
[g] The total number of local energy minima obtained: 260. Only conformers with over 2% population are represented.
[h] *S*-configuration in (*R,S,S*) and *S*-configuration in (*S,R,R*).

It is worth mentioning that all the major conformers of (*3S,5S,6S*)-serricornin have a common $^4C_1$ chair ring conformation

with *R*-configuration at C2, which have an axial hydroxyl group (Figure 3).

The major conformation at C2-C7, C2-O13 and C6-C9 torsions are (+)-, (-)- and (-)-gauche, respectively. The population of the major conformation having an equatorial hydroxyl at C2 is only 0.3% (Table 2). These characteristics of the stable conformation are common to those of (*3R, 5R, 6S*)- and (*3S, 5R, 6S*)-cyclic serricornins, which have the $^4C_1$ chair pyran ring with the *R*-configuration at C2 having the axial hydroxyl group (table 2, Figure 4).

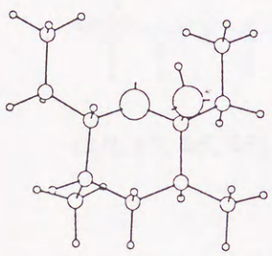

Energy Minimum-1
(48%)

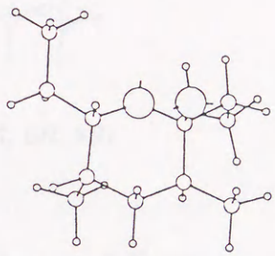

Energy Minimum-2
(26%)

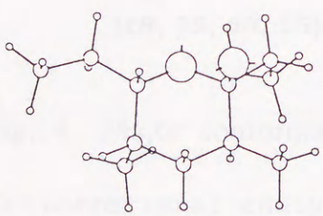

Energy Minimum-3
(13%)

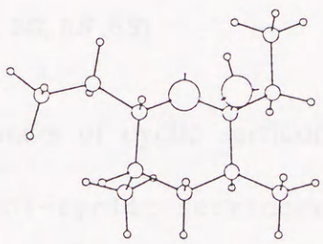

Energy Minimum-4
(9%)

Fig. 3 Major conformations of (3*S*, 5*S*, 6*S*)-cyclic serricornin.

The X-ray crystallographic analysis (Mori et al, 1984) of the (*3S, 5R, 6S*)-cyclic serricornin resulted in the same $^4C_1$ chair

conformation with *R*-configuration at C2 as that assigned by MM conformational analysis, although there are differences in the torsion of the side chain at C2-C7 and C6-C9.

The major conformations of (*3R,5R,6R*)-, (*3S,5R,6R*)- and (*3R,5S,6R*)-cyclic serricornins, enantiomers of the above *6S*-isomers, and $^4C_1$ chairs with *S*-configuration at C2 having the axial hydroxyl (Table 2).

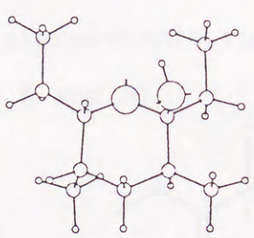

(2*R*, 3*S*, 5*S*, 6*S*)

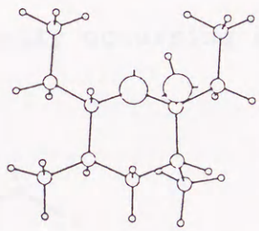

(2*R*, 3*R*, 5*R*, 6*S*)

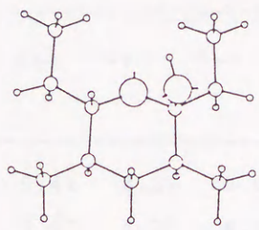

(2*R*, 3*S*, 5*R*, 6*S*)

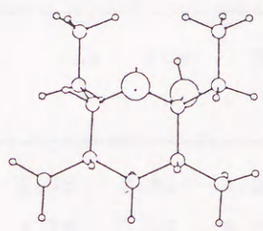

(2*S*, 3*R*, 5*S* ,6*S*)

Fig. 4 Major conformations of stereoisomers of cyclic serricornin.

Conformational analysis of (*3R,5S,6S*)-cyclic serricornin gave the major conformation having $^1C_4$ chair conformation with *S*-configuration at C2 having an axial hydroxyl (Figure 4). Two twist ring conformations also existed in the major group (Table 2). The major conformation of (*3S,5R,6R*)-cyclic serricornin, therefore, has $^4C_1$ chair conformation with *R*-configuration at C2 having an axial hydroxyl. The molecule tries to avoid 1,3-

diaxial relationship of two methyls in the $^4C_1$ or $^1C_4$ chair conformation, resulting in the 1,3-diequatorial relationship in the $^1C_4$ or $^4C_1$ chair (Table 2).

Stereochemical Assignment of Naturally Occurring Serricornin by Comparison between Calculated. and Observed $^3J_{HH}$s Values. The comparative study on vicinal H/H coupling constants ($^3J_{HH}$s) between those observed in the NMR and those calculated by Altona's modified Karplus equation was conducted for an assignment of the unknown stereochemistry of naturally occurring serricornin (Figures 5 and 6).

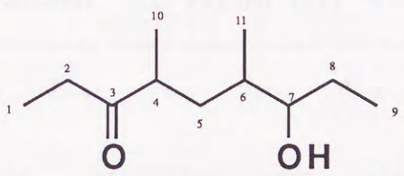

ACYCLIC SERRICORNIN

CALCULATED $^3J_{HH}$ VALUES (Hz) OF CHAIN SERRICORNIN

STEREO (4,6,7)	J_{4-5}	$J_{4-5'}$	J_{5-6}	$J_{5'-6}$	J_{6-7}	J_{7-8}	$J_{7-8'}$	RMS
SSS/RRR	5.47	8.27	8.66	6.16	2.75	8.91	4.01	0.83
SSR/RRS	7.67	6.75	6.03	8.49	4.39	3.66	8.90	2.82
SRS/RSR	9.50	4.37	5.08	9.29	4.15	3.80	8.85	3.19
RSS/SRR	8.02	6.11	7.28	7.32	2.98	8.69	4.15	1.27

OBSERVED $^3J_{HH}$ VALUES(Hz) OF NATURAL SERRICORNIN

NATURAL OCCURRING	6.20	7.60	8.10	5.40	3.80	8.50	5.00

Fig. 5 MM calculated $^3J_{HH}$s of four enatiomeric pairs of acyclic serricornin and observed $^3J_{HH}$s of naturally occuring acyclic serricornin.

As it has been shown previously (Masanune et al., 1986), this technique produces rather large errors, but simple root-mean-

square tests (the right columns of Figures 5 and 6) unambiguously shows that the observed $^3J_{HH}$s pattern of both acyclic and cyclic natural serricornin fitted best with those calculated for the *(4S*,6S*,7S*)*-acyclic serricornin and *(3S*,5S*,6S*)*-cyclic serricornin, respectively.

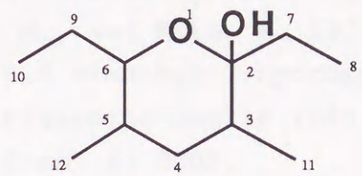

CYCLIC SERRICORNIN

CALCULATED $^3J_{HH}$ VALUES (Hz) OF CYCLIC SERRICORNIN

STEREO (3,5,6)	J_{3-4}	$J_{3-4'}$	J_{4-5}	$J_{4'-5}$	J_{5-6}	J_{6-9}	$J_{6-9'}$	RMS
SSS/RRR	3.96	12.22	1.98	4.54	2.24	9.36	3.66	1.48
SSR/RRS	2.07	4.69	3.71	12.11	10.19	9.28	2.65	5.26
SRS/RSR	3.64	12.30	3.38	12.34	10.21	9.32	2.69	5.59
RSS/SRR	9.32	4.01	8.37	5.14	4.01	3.12	10.24	5.05

OBSERVED $^3J_{HH}$ VALUES(Hz) OF NATURAL SERRICORNIN

NATURAL OCCURRING	2.50	12.50	4.10	4.30	2.60	7.80	6.10

Fig. 6 MM calculated $^3J_{HH}$s of four enatiomeric pairs of cyclic serricornin and observed $^3J_{HH}$s of naturally occuring cyclic serricornin.

If this information had been known before starting the synthetic work, it may have been unnecessary to synthesize all the stereoisomers but *(S,S,S)*- or *(R,R,R)* serricornins for determination of the absolute configuration. This work indicates that MM conformational analysis can bring effective information

for the determination of the unknown stereochemistry in natural products.

References

Burkert, U., and Allinger, N. L. 1982. Molecular Mechanics. American Chemical Society. Washington D. C.

Chuman, T., Kohno, M., and Kato, K. 1979. Synthesis of (±)-serricornin, 4,6-dimethyl-7-hydroxynonan-3-one, a sex pheromone of cigarette beetle (*Lasioderma serricorne* F.). *Agric. Biol. Chem.* 43:2005.

Chuman, T., Kohno, M., Kato, K., Noguchi, M., Nomi, H., and Mori, K. 1981. Stereoselective synthesis of erythro-serricornin, (*4R, 6R, 7S*)- and (*4S, 6R, 7S*)-4,6-dimethyl-7-hydroxynonan-3-one, stereoisomers of the sex pheromone of cigarette beetle. *Agric. Biol. Chem.* 45:2019-2023.

Chuman, T., Mochizuki, K., Mori, M., Kohno, M., Kato, K., and Noguchi, M. 1985. Lasioderma Chemistry, sex pheromone of cigarette beetle (*Lasioderma serricorne* F.). *J. Chem. Ecol.* 11:417-434.

Gotō, H., and Ōsawa, E. 1989. Corner Flapping: A simple and fast algorithm for exhaustive generation of ring conformation. *J. Am. Chem. Soc.* 111:8950-8951: Gotō, H., and Ōsawa, E. 1989. CONFLEX2, (QCPE and JCPE).

Haasnoot C. A. G., de Leeuw F. A. A. M., and Altona, C. 1980. The relationship between proton-proton NMR coupling constants and substituent electronegativities-I. *Tetrahedron.* 36: 2783-2792.

Hoffmann, R. W., Helbig, W., and Lander, W. 1982. Synthesis of *6S, 7S*-anhydro-serricornin. *Tetrahedron Lett.* 23:3479-3482.

Jaime, C., Ortuno, R. M., and Font, J. 1987. Di- and tri-substituted γ-lactones, conformational study by molecular mechanics calculations and coupling constant analysis. *J. Org. Chem.* 51:3946-3951.

Masamune,S., Ma, P., Moore, R., E., Fujiyoshi, T., Jaime, C., and Ōsawa, E. 1986. Computation of vicinal coupling constants in tetra- and hexa-aldol peracetates using molecular mechanics. A rational approach to conformational analysis in solution. *J. Chem. Soc., Chem. Commun.* 261.

A rational approach to conformational analysis in solution. *J. Chem. Soc., Chem. Commun.* 261.

Mori, K., and Watanabe, H. 1985. A new synthesis of serricornin [(*4S, 6S, 7S*)-4,6-dimethyl-7-hydroxy-3-nonanone], the sex pheromone of cigarette beetle. *Tetrahedron*. 41:3423-3428.

Mori, K., Nomi, H., Chuman, T., Kohno, M., Kato, K., and Noguchi, M. 1981. Determination of the absolute configuration at C-6 and C-7 of serricornin (4,6-dimethyl-7-hydroxynonan-3-one), the sex pheromone of cigarette beetle. *Tetrahedron Lett.* 22:1127-1130.

Mori, M., Chuman, T., Kohno, M., Kato, K., Noguchi, M., Nomi, H., and Mori, K. 1982a. Absolute stereochemistry of serricornin, the sex pheromone of cigarette beetle, as determined by the synthesis of its (*4S, 6R, 7R*)-isomer. *Tetrahedron Lett.* 23:667-670.

Mori, M., Chuman, T., Kohno, M., Kato, K., and Mori, K. 1982b. Stereoselective synthesis of "natural" (*4S, 6S, 7S*)-serricornin, the sex pheromone of cigarette beetle, from levoglucosenone. *Tetrahedron Lett.* 23:4593-4596.

Mori, M., Chuman, T., and Kato, K. 1984. Cyclic hemiacetal and acyclic chain-the two forms of serricornin. *Tetrahedron Lett.* 25:2553-2556.

Ōsawa, E., Gotō, H., Oishi, T, Outsuka, Y., and Chuman, T. 1989. Application of molecular mechanics to natural product chemistry. *Pure & Appl. Chem.* 61:597-600.

Chapter 3

X-Ray Crystallographic and NOE Studies on the Conformational of Periplanones and their Analogues.

Abstract

The structure of periplanone-A was established to be (**2**) by the X-ray crystallographic analysis. In comparison of the X-ray and ^{1}H NMR data with those of periplanone-B, it was shown that periplanone-A and -B adopt essentially the same conformation. The epoxy epimer of periplanone-A, has 10^4 times lower biological activity than periplanone-A, and NMR analysis indicated that the molecule exists in a mixture of different conformers. The conformation of the regioisomer, in which the carbonyl and epoxy groups are transposed, was analysed by the X-ray crystallography and ^{1}H NMRspectroscopy. It is highly biologically active, and the conformation of germacranoid skeleton was shown to be almost identical with that of periplanone-A. Simplified analogues and germacrene-D had relatively lower acivity. NOE Experiments on these compounds suggested the conformational resemblance of their germacranoid skeletons with those of periplanone-A and -B.

Introduction

Periplanones-A (P-A) and -B (P-B) are the extremely potent sex pheromone of American cockroach (*Periplaneta americana*. L). Since

the isolation of these pheromone components by Persoons *et al.*[1,†] in 1974, much attention has been focused on the structural determinations of the natural pheromones. Although the structure of P-B was established[2] as (**1**) earlier, the structure of P-A has long been a matter of discussion among several groups [3-6]. Very recently, through the chiral syntheses of the candidates and their X-ray crystallographic analyses[7,8,9], the structure of P-A was shown to be (**2**), a structure proposed by Hauptmann *et al.*:[4]

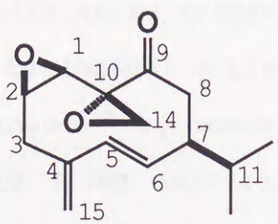

Periplanone-B (**1**)

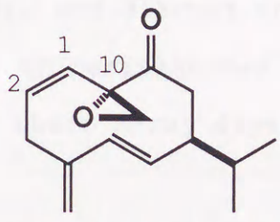

Periplanone-A (**2**)

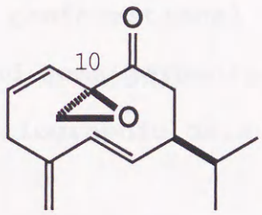

(**3**)

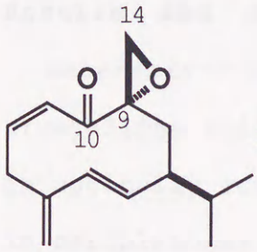

(**4**)

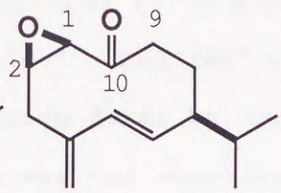

(**5**)

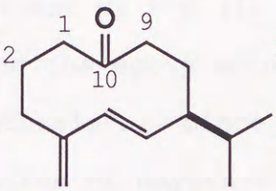

(**6**)

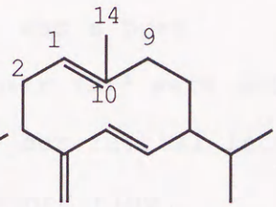

Germacrene-D (**7**)

Being interested in the unique structural features and biological activity of these pheromones, we started to investigate the molecular shapes and structural requirements for the pheromonal activity. Few

---

† Recently, new pheromone components, periplanone-D_1 and -D_2, with an activity threshold of 5×10^{-2} mg were isolated and identified from the female American cockroach (M. Biendi, H. Hauptmann, and H. Sass, *Tetrahedron Lett.*, 1989, **30**, 2367).

studies on substances pheromonally active toward the American cockroach[10,11], however, have appeared until now, and no highly active compound with an activity threshold over $>10^{-5}$ that of natural pheromones was known. Furthermore, because of the well-known flexibility of 10-membered ring systems of germacrane skeleton[12], it was important to consider the molecular shapes of the analogues compared with those of the leading natural pheromones.

In this report, we describe the structural elucidation of P-A (**2**) and its epoxy epimer (**3**), and discuss the conformational properties and biological activity of periplanones and some germacranoid analogues[††] by means of their X-ray crystallographic data and high-field ^{1}H NMR analyses.

Results and discussion

Materials---Natural (-)-enantiomer of P-B (**1**) was a pure crystalline solid.[2] P-A (**2**)[4] and the epoxy epimer (**3**)[5] were obtained in optically active forms by synthesis[8]. Since our initial interest in periplanones was the contribution of oxygen-containing functionalities on the biological activity and conformational properties, we employed the compounds (**4**)-(**7**) which were analogues altered at epoxy and carbonyl groups of periplanones (**1**) and (**2**). Compounds (**4**)-(**6**) were obtained in chemically and optically pure

---

[††] The same numbering scheme for the C atoms is employed in this paper as has been used for P-B by Persoons *et al.*[1]

forms[2,§] . The simplest molecule (**7**), (-)-germacrene-D,[10] was known as a pheromonally active natural product. All of the compounds possess a common conjugated diene and isopropyl group in their 10-membered-ring skeletons as shown by structure (**7**).

Biological Tests---For the biological evaluations of the compounds, behavioural[13] and electroantennographic (EAG) assays[14] were performed. The results are summarized in Table 1. The threshold values of (**1**), (**2**) and (**7**) in behavioural assay were in agreement with those reported in literatures.[15, 16]

Table 1 Bioassay Data of Periplanones and the Analogues.

	Behavioral test threshold (μg)	EAG response[a]
P-B (**1**)	10^{-7}	100
P-A (**2**)	10^{-5}	85
(**3**)	10^{-1}	32
(**4**)	10^{-4}	25
(**5**)	10^{-1}	18
(**6**)	1	13
(**7**)	10	11
control[b]		8

[a] Relative intensities at 10^{-1}μg doses to that of P-B (**1**) (=100).
[b] Hexane (1 μl).

Conformational Analysis ----Since the conformational properties of the compounds (**3**)-(**7**) are discussed largely on the basis of ^{1}H NMR

§ The structure of compound (**4**) was first presented at 16th International Symposium on the Chemistry of Natural Products, IUPAC, Kyoto, May, 1988, (Abstracts, p. 649).

analyses in this work, the NMR characterizations of the leading compounds (**1**) and (**2**) were prerequisite for these studies. The ^1H NMR data for (**1**) and (**2**), and the analogues (**3**)-(**5**) are listed in Table 2 and 3, respectively.

Table 2 ^1H NMR data (500 MHz) of periplanones-B (**1**) and -A (**2**) in C_6D_6.

	(**1**)			(**2**)		
	δ (ppm)	mult.	*J* (Hz)	δ (ppm)	mult.	*J* (Hz)
1	3.84	d	4.0	6.03	d	11.8
2	2.74	dt	10.2, 4.0	5.53	ddd	11.8, 11.0, 7.4
3β	2.86	dd	12.2, 10.2	3.95	br.t	11.0
3α	2.56	dd	12.2, 4.0	2.45	dd	11.0, 7.4
5	5.96	d	16.0	6.00	d	16.2
6	5.91	dd	16.0, 9.0	6.18	dd	16.2, 11.0
7	2.05	m		2.11	m	
8β	2.35	dd	11.0, 9.8	2.44	dd	11.8, 9.6
8α	1.94	dd	9.8, 5.7	1.93	dd	9.6, 5.2
11	1.30	m		1.36	m	
12	0.72	d	6.9	0.77	d	7.4
13	0.70	d	6.8	0.73	d	6.6
14	2.63	d	5.7	2.30	d	5.6
14'	2.02	d	5.7	2.16	d	5.6
15	4.81	br.s		4.84	br.s	
15'	4.78	br.s		4.75	br.s	

Periplanone-B (**1**). The conformational properties of (**1**) have been described by Still in his first synthesis of compound.[12] Recently, Hauptmann *et al.* reported X-ray crystal structure of (**1**).[16] In an examination of the 500 MHz ^1H NMR spectrum of compound (**1**) in [$^2H_6$] benzene solution, the coupling-constant data provided rather poor information on the conformational properties in solution, except that

the large couplings between 2-H/3-H$^{\beta}$ (10.2 Hz) and 7-H/8-H$^{\beta}$ (11.0 Hz) were due to their *anti* orientations. However, NOE enhancements were observed among a number of non-coupled protons on the molecule in the NOESY spectrum as depicted in Figure 1. The olefinic 6-H signal interacts with those of 3-H$^{\beta}$, 8-H$^{\beta}$ and 11-H, and, that of 5-H interacts with 7-H. As a relatively large NOE enhancement (6.0%) was observed at 3-H$^{\beta}$ on irradiation of 6-H signal, it reflects their close intramolecular distance (2.13Å from X-ray data). These results for the solution conformation of P-B (**1**) were essentially consistent with that in the solid state.

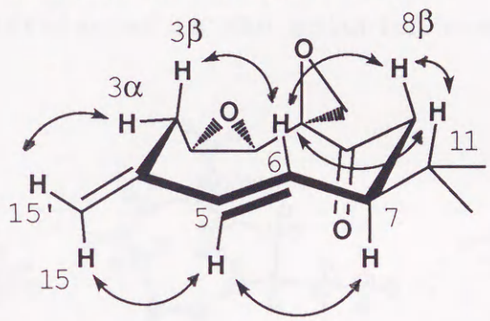

Fig. 1 Stereostructure of periplanone-B and intramolecular ^{1}H NOE interactions observed in C_6D_6 solution.

Periplanone-A (**2**) *and the epoxy epimer* (**3**) Owing to the ambiguity of the stereochemistry of the quaternary center at the spiro-epoxy group, two structures (**2**)[4] and (**3**),[5] which are epimeric at C-10 have been proposed for P-A. To clarify this point, both of these isomers were synthesized in their optically active form,[8] and subjected to precise stereochemical analyses. The biologically active epimer, of which the NMR spectrum is identical with that reported by Hauptmann *et al.*,[4] is a crystalline compound and the X-ray analysis established the structure to be (**2**). The compound (**2**) crystallized with three

molecules, the shape of which are essentially identical, in the asymmetric crystallographic unit-cell. The ORTEP stereo projections of the three molecules and unit-cell contents are shown in Figures 2 and 3, respectively. A computer-aided superimposition of the X-ray structures (Figure 4) showed that the molecular shape of P-A (**2**) (molecule A) apparently overlaps to that of P-B (**1**) except the absence of *endo* epoxy group at C-1 and -2. A ^{1}H NMR inspection of compound (**2**) also shows similar coupling and NOE patterns with those of P-B (**1**) (Figure 5). Lack of NOE interactions of 6-H to 8-H$^{\beta}$ and 11-H signals is a distinction from the situation with P-B (**1**), and indicates the differences in the solution conformation.

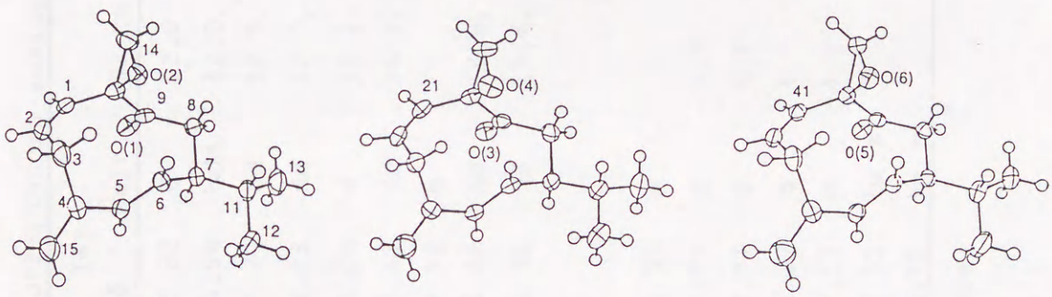

Molecule A Molecule B Molecule C

Fig. 2 ORTEP drawing of the three independent molecules of periplanone-A (**2**).

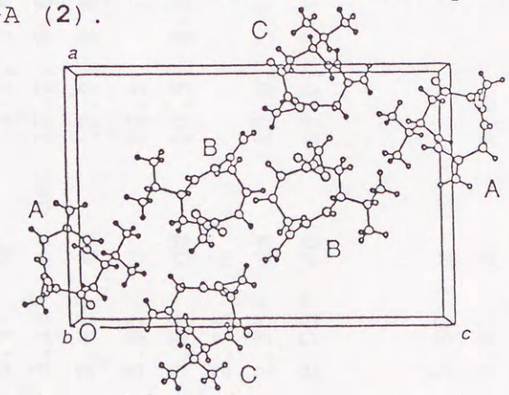

Fig. 3 Crystal-packing diagram of periplanone-A (**2**) viewed along the *b* axis.

Table 3 ^{1}H-NMR Data (500 MHz) of periplanone analogues (**3**), (**4**) and (**5**) in C_6D_6.

	(3)			(4)			(5)		
	δ	Mult.	*J* Hz	δ	Mult.	*J* Hz	δ	Mult.	*J* Hz
1	5.95	d	11.2	5.82	d	12.0	3.03	d	4.7
2	5,44	d	11.2, 8.6	5.54	ddd	12.0, 10.3, 6.6	2.79	ddd	9.9, 4.7, 3.5
3α	3.16[a]	br.dd	12.2, 8.6	3.77	dd	12.0, 10.3	2.52	dd	12.7, 3.5
3β	2.66[a]	dd	12.2, 8.6	2.48	dd	12.0, 6.6	2.35	dd	12.7, 9.9
5	5.91	d	16.5	6.04	d	16.2	5.66	d	16.2
6	5.59	dd	16.5, 8.3	5.43	dd	16.2, 10.5	5.10	dd	16.2, 10.3
7	2.06	m		2.11	m		1.29	m	
8α	2.35*	dd	10.0, 5.1	2.82	dd	13.6, 11.9	2.09	m	
8β	2.09*	dd	10.0, 7.4	1.15	dd	13.6, 4.8	1.94	br.q	-12
9							1.85	ddd	16.1, 12.5, 1.1
9'							1.64	ddd	16.1, 6.5, 1.2
11	1.50	m		1.35	m		1.29	m	
12	0.81	d	6.6	0.79	d	7.3	0.78	d	6.2
13	0.77	d	6.7	0.77	d	6.5	0.75	d	6.2
14	2.61	d	5.8	2.27	d	4.7			
14'	2.40	d	5.8	2.17	d	4.7			
15	4.80	br s		4.81	br s		4.76	br s	
15'	4.76	br s		4.72	br s		4.74	br s	

[a] Configurations were not assignable.

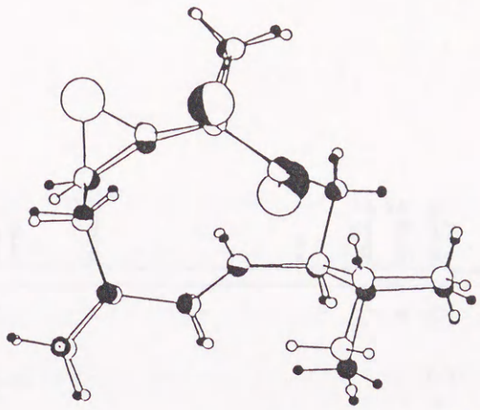

Fig. 4 Superimposition of the crystal structures of periplanone-A (**2**), (filled) and -B (**1**). Oxygen atoms are shown by large circles.

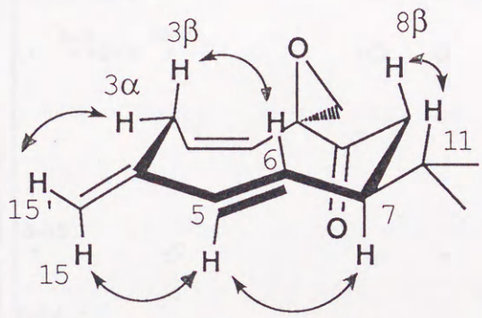

Fig. 5 Stereostructure of periplanone-A (**2**) and intramolecular ^1H NOE interactions observed in C_6D_6 solution.

On the other hand, the epoxy epimer (**3**) exhibits 10^4 -times lower activity than P-A (**2**). In contrast to compound (**2**), the NOESY spectrum (Figure 6) was so complicated that we could not define the conformation of compound (**3**). Namely, the signal of 6-H shows cross peaks to those of 2-, 3-, 3'-, 7- and 11-, and 5-H interacts with 7-H and 11-H. This spectral feature suggested that the molecule of compound (**3**) may exist in a mixture of different from those of P-A (**2**).

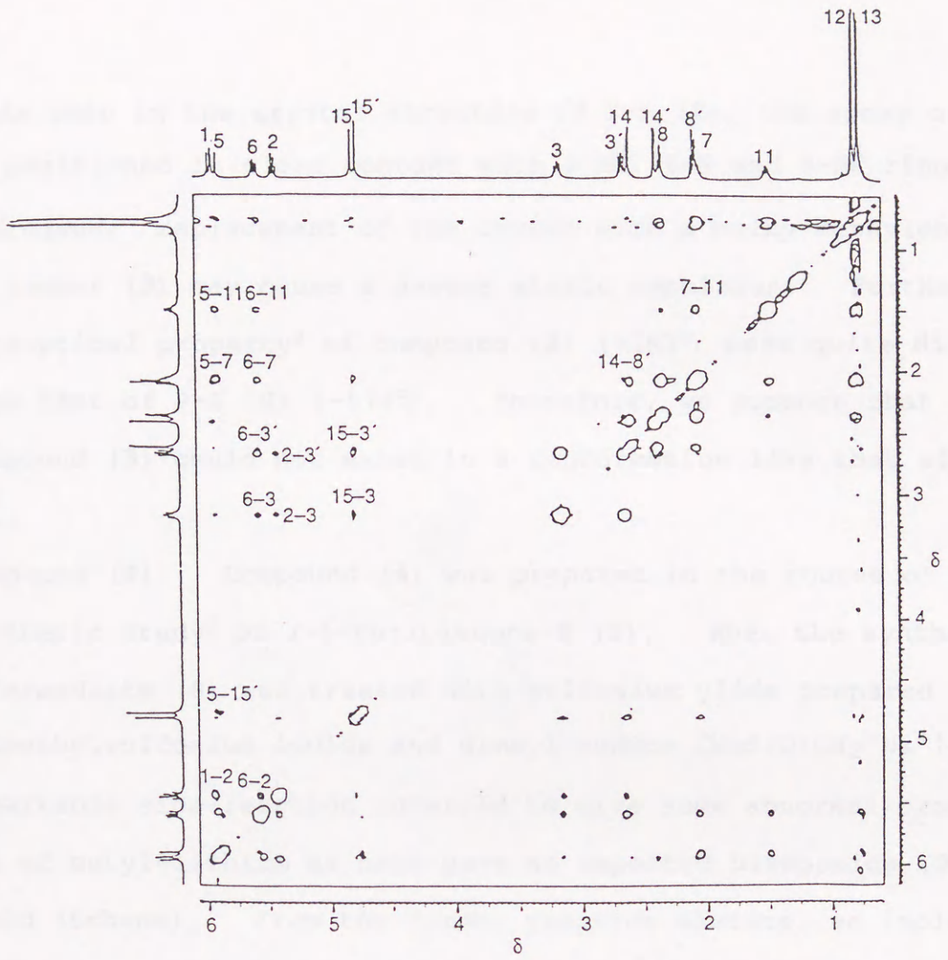

Fig. 6. Phase-sensitive 2D NOESY spectrum of compound (**3**) recorded at 500 MHz in C_6D_6 solution, and partial assignments of the cross-peaks; dispersed cross-peak between 5-H and 6-H are due to their direct coupling.

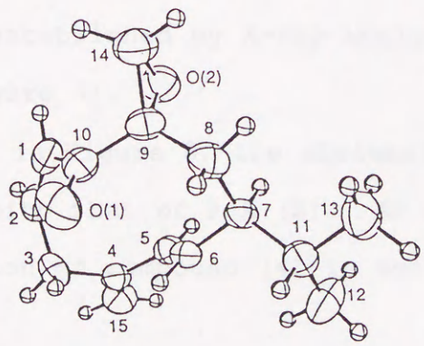

Fig. 7 ORTEP drawing of compound (**4**).

As seen in the crystal structure of P-A (**2**), the epoxy oxygen atom is positioned in close contact with 3-H$^{\beta}$, 6-H and 8-H$^{\beta}$ ring hydrogens; replacement of the oxygen with a bulky methylene group as in isomer (**3**) may cause a severe steric repulsion. Furthermore, the chiroptical property[8] of compound (**3**) (+182°) were quite different from that of P-A (**2**) (-574°). Therefore, we suppose that the compound (**3**) could not exist in a conformation like that of compound (**2**).

Compound (**4**). Compound (**4**) was prepared in the course of our synthetic study[2] of (-)-Periplanone-B (**1**). When the synthetic intermediate (**8**) was treated with sulfonium ylide prepared from trimethylsulfonium iodide and dimsyl sodium [$MeS(O)CH_2^-Na^+$], a remarkable side-reaction occurred to give some abnormal products. Use of butyl-lithium as base gave an expected bisepoxide (**9**) in good yield (Scheme). From the former reaction mixture, we isolated two products, both of which exhibited significant biological activity. Surprisingly, the minor product was spectro-scopically identical to Periplanone-A (**2**). The structure of the major product, the biological activity of which is one order of magnitude lower than P-A (**2**), was established by X-ray analysis to be (**4**), a regioisomer of P-A (**2**) (Figure 7).

As seen in Figure 8, the skeletal conformation of compound (**4**) overlaps with that of P-A (**2**). An NOE experiment indicated the conformation of compound (**4**) in solution (Figure 9).

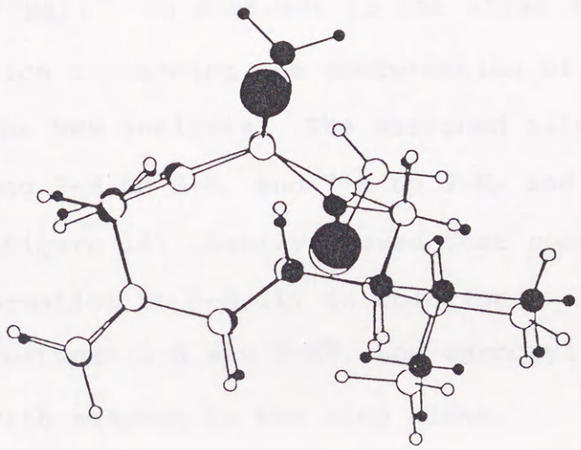

Fig. 8 Superimposition of the crystal structures of periplanone-A (**2**) (filled) and compound (**4**). Oxygen atoms are shown by large circle.

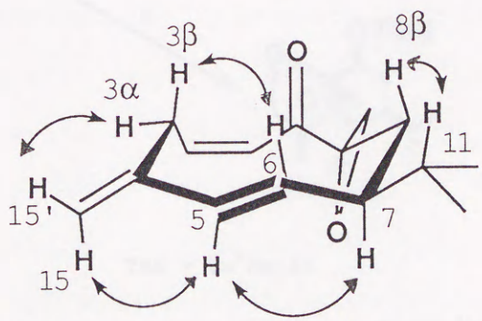

Fig. 9 Stereostructure of compound (**4**) and intramolecular ^1H NOE interactions observed in C_6D_6 solution.

It is noteworthy that a transposition of carbonyl and spiro-epoxy group did not affect the placements of each oxygen atom in the molecules.

Compound (**5**). The compound (**5**)[2,17] is a simplified analogue of P-B (**1**), which lacks carbonyl group at C-9 and possesses a carbonyl group instead of spiro-epoxy group at C-10, but still generates activity (threshold $10^{-1}\mu g$). In contrast to the above mentioned compounds, much information concerning the conformation of this compound was obtained in the NMR analysis. The assigned alignments of spin-couplings along 2-H to 3-H, and 7-H to 9-H, and the results of NOE experiments (Figure 10) clearly showed that compound (**5**) lay in a similar conformation to P-B (**1**) in solution. As an NOE interaction was observed between 1-H and 9-H^{α}, the carbonyl function at C-10 may be vertical with respect to the ring plane.

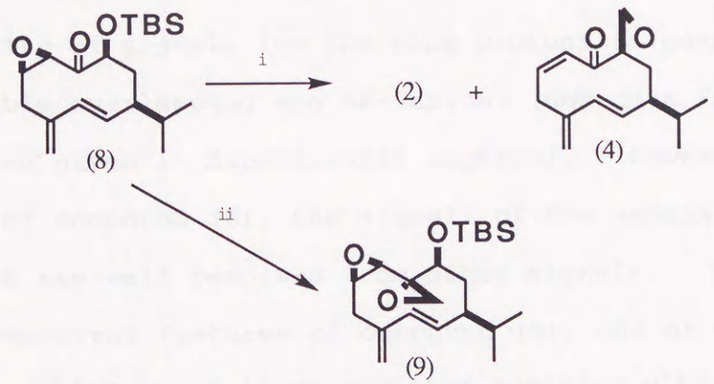

TBS = Bu^tMe_2Si

Scheme. *Reagents:* i, Me_3SI, $MeS(O)CH_2^+Na^+$, Me_2SO-THF; ii, Me_3SI, BuLi, THF.

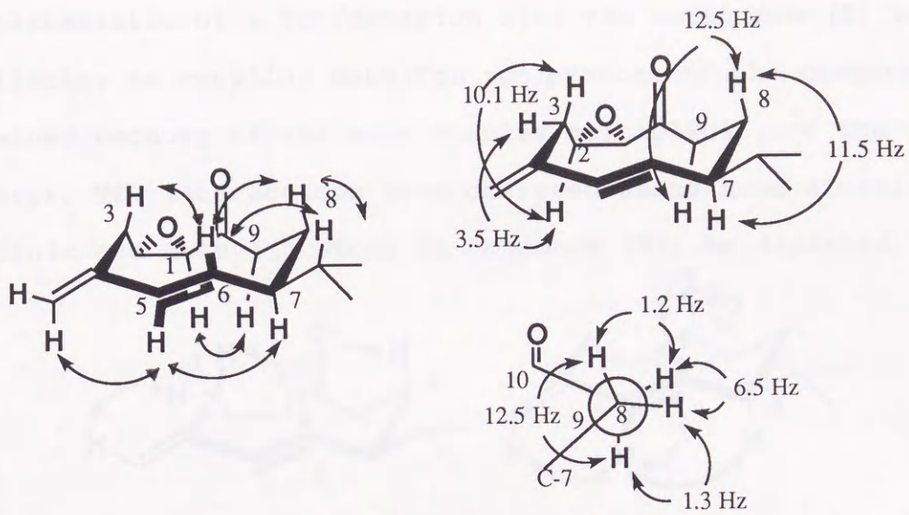

Fig. 10 Stereostructure of compound (**5**) and its ^{1}H NMR spectral properties (left: NOE interactions; right: coupling constant).

Compound (**6**)[2,17] *and Germacrene-D* (**7**).[10] Each of the more simplified analogues exhibited a lower activity than did compound (**5**). On the elucidation of the ^{1}H NMR spectra of compounds (**6**) and (**7**), the multiplicity of signals for the ring protons is complicated by considerable overlapping and AB-fusions [NMR data for compounds (**6**) and (**7**) are given in Experimental section]. However, in the spectrum of compound (**6**), the signals of the geminal methylenes at C-3 and -8 are well resolved from other signals. From the analogy with the spectral features of compound (**5**), one of the 3-H signals at δ 2.55, which has a large coupling constant with 2-H, was tentatively assigned to that of a β-orientation proton. The signal at δ 2.09 was likewise assignable to 8-H$^{\beta}$. On the irradiation of the signal due to 6-H, a significant NOE enhancement (5.8%) was observed at 3-H$^{\beta}$, along with weak interactions at 8-H$^{\beta}$ (1.4%) and 11-H (1.7%) signals (Figure 10). These spectral features are

characteristic of a conformation like the compounds (**1**) and (**5**). Similarly, no coupling data for sp^3 protons of the compound (**7**) were obtained because of the more complex multiplicity of the signals. However, NOE interactions were observed among some signals of olefinic and methyl protons of compound (**7**), as depicted in Fig. 11.

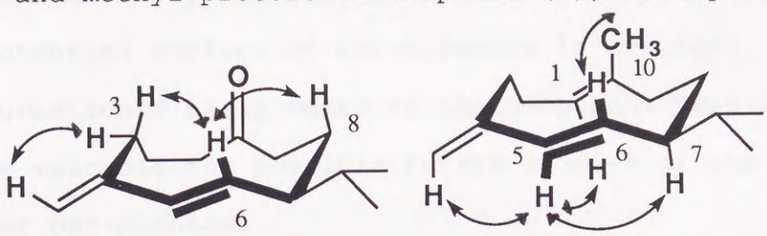

(**6**) (**7**)

Fig. 11 Proposed structures of compound (6) and germacrene-D (7), and their NOE interactions.

A transannular NOE interactions between the methyl at C-10 and 6-H proton indicated that the methyl group may be located on the β side of the ring. These evidence suggested that the molecule (**7**) may also adopt a similar conformation to that of the other compounds examined in this study.

Conclusion

On analysis of the biological activity and structural features of the periplanones and their analogues, it was seen that the conformational analogy of the germacranoid skeleton and the oxygen-containing functionalities must play an important role in the exhibition of biological activity. The characteristic three-dimentional locations of oxygen atoms in the carbonyl and spiro-epoxy groups on the ten-membered ring planes may also be necessary in order to exhibit higher activity. As seen in the case of compound (**3**), stereochemical

restrictions are essential in the conformational properties of the ten-membered ring. These findings on biological activity and structural factors could provide a guideline towards designing useful analogues for the control of cockroach insect pest. For molecular recognition not only the size but also the shape of the electropotential surface of the molecule is critical. We think that the conformational assignments of the compounds described in the study are valuable for possible future studies of the electronic aspects of periplanones.

Recent electrophysiological studies[18] suggested the presence of two distinct receptor cells for P-A and P-B on an antenna of American cockroach. Such a high specificity which can strictly distinguish these closely analogous molecular shapes may be a striking character of the receptor cells.

Experimental

General Methods.----M. p. s were measured on a Yanagimoto micro-melting-point apparatus and are uncorrected. IR spectra were recorded on a JASCO FT/IR-5000 spectrometer. GLC-MS spectra (70 eV) were run on a JEOL DX-300 spectrometer. ^{1}H-NMR (500 MHz) spectra were recorded at 27°C on a Bruker AM-500 instrument, and were measured in C_6D_6 solutions with Me_4Si as internal standard unless otherwise stated. $CDCl_3$ was not used so as to avoid decomposition of the acid-sensitive substrates during measurement of two-dimentional (2D) spectra. For the 2D-NOESY and NOE difference spectra (NOEMULT),[19] Bruker standard software was employed. The NOESY spectra were obtained in the phase-sensitive mode with 1K x 1K

data points. PLC separations were performed on JASCO 880-PU system equipped with a JASCO 875-UV detector. Computer-aided superimpositions of X-ray crystallographic data were performed using QUANTA™ program.§§ Detailed procedures of the biological test and electroantennographic assay were described in the literature.[13,14]

Materials.----Optically pure crystalline (-)-P-B (**1**) (99.95% e.e.) was obtained by our previous procedure.[2] A mixture of P-A (**2**) and the epoxy epimer (**3**) was synthesized from (*R*)-(+)-cyclohex-3-enecarboxylic acid ($[\alpha]_D^{17}$+98°) by the procedure reported by Kuwahara and Mori.[8] and were separated on preparative TLC (PLC).(twice).

Table 4 Crystallographic Data for P-A (**2**), and compound (**4**).

	(**2**)	(**4**)
Empirical formula	$C_{15}H_{20}O_2$	$C_{15}H_{20}O_2$
Formula weight	232.32	232.32
Crystal system	monoclinic	orthorhombic
Space group	$P2_1$	$P2_12_12_1$
Cell dimensions		
a (Å)	14.650(2)	12.3186(8)
b (Å)	6.469(2)	16.044(1)
c (Å)	21.361(1)	6.8292(5)
β	90.702(8)°	
Cell volume(Å^3)	2024.5(6)	1349.7(2)
Z	6	4
D_{calc} (g cm^{-3})	1.143	1.14
Number of reflections		
Measured	3459 (3313 unique)	1149
Observed ($I > 3\sigma(I)$)	3005	897
R, R_W	0.038, 0.047	0.034, 0.041

§§ Copyright Polygen Corporation, 1987, USA.

Table 5 Non-hydrogen atom co-ordinates for compound (**2**) (e.s.d.s in parentheses.).

Atom	*x*	*y*	*z*	B(eq)
	Molecule (A)			
O(1)	0.9367(2)	0.7917	0.9960(1)	3.7(1)
O(2)	0.8320(2)	0.5405(6)	1.0973(1)	3.0(1)
C(1)	0.8420(2)	0.9203(7)	1.0755(1)	2.7(1)
C(2)	0.7579(2)	0.9814(7)	1.0868(1)	2.9(1)
C(3)	0.6723(2)	0.8538(7)	1.0864(1)	3.1(2)
C(4)	0.6272(2)	0.8663(7)	1.0216(1)	2.5(1)
C(5)	0.6753(2)	0.7529(7)	0.9720(1)	2.4(1)
C(6)	0.7146(2)	0.5689(7)	0.9784(1)	2.2(1)
C(7)	0.7789(2)	0.4718(7)	0.9331(1)	2.2(1)
C(8)	0.8728(2)	0.4539(7)	0.9668(1)	2.4(1)
C(9)	0.8983(2)	0.6595(7)	0.9954(1)	2.4(1)
C(10)	0.8737(2)	0.7051(7)	1.0628(1)	2.5(1)
C(11)	0.7453(2)	0.2610(7)	0.9082(1)	2.7(1)
C(12)	0.6541(2)	0.2893(8)	0.8739(2)	3.9(2)
C(13)	0.8137(3)	0.1568(8)	0.8656(2)	4.1(2)
C(14)	0.9257(2)	0.5887(8)	1.1109(1)	3.2(2)
C(15)	0.5563(2)	0.9863(8)	1.0098(2)	3.4(2)
	Molecule (B)			
O(3)	0.6423(1)	0.9253(6)	0.6035(1)	2.8(1)
O(4)	0.5685(1)	1.4117(6)	0.6684(1)	2.8(1)
C(21)	0.5714(2)	1.3022(7)	0.5556(1)	2.4(1)
C(22)	0.4880(2)	1.3431(7)	0.6344(1)	2.6(1)
C(23)	0.4014(2)	1.3694(7)	0.5709(1)	2.5(1)
C(24)	0.3522(2)	1.1639(7)	0.5763(1)	2.4(1)
C(25)	0.3927(2)	1.0137(7)	0.6201(1)	2.3(1)
C(26)	0.4359(2)	1.0607(7)	0.6737(1)	2.2(1)
C(27)	0.4925(2)	0.9166(7)	0.7120(1)	2.5(1)
C(28)	0.5937(2)	0.9896(7)	0.7080(1)	2.6(1)
C(29)	0.6153(2)	1.0502(7)	0.6418(1)	2.1(1)
C(30)	0.6025(2)	1.2739(7)	0.6215(1)	2.2(1)
C(31)	0.4621(2)	0.9029(8)	0.7805(1)	3.5(2)
C(32)	0.5209(3)	0.752(1)	0.8181(2)	5.2(2)

C(33)	0.3625(3)	0.841(1)	0.7843(2)	5.2(2)
C(34)	0.6629(2)	1.4278(7)	0.6520(2)	3.3(2)
C(35)	0.2823(2)	1.1159(7)	0.5397(2)	3.1(2)
	Molecule (C)			
O(5)	-0.0445(1)	0.4413(6)	0.4608(1)	2.9(1)
O(6)	0.1471(1)	0.6770(5)	0.3837(1)	2.4(1)
C(41)	0.1133(2)	0.2985(7)	0.3969(1)	2.2(1)
C(42)	0.1294(2)	0.2259(7)	0.3399(1)	2.4(1)
C(43)	0.1328(2)	0.3431(7)	0.2790(1)	2.6(1)
C(44)	0.0393(2)	0.3277(7)	0.2468(1)	2.3(1)
C(45)	-0.0346(2)	0.4467(7)	0.2764(1)	2.2(1)
C(46)	-0.0249(2)	0.6297(7)	0.3036(1)	2.0(1)
C(47)	-0.0916(2)	0.7363(7)	0.3454(1)	2.0(1)
C(48)	-0.0439(2)	0.7679(7)	0.4098(1)	2.2(1)
C(49)	-0.0018(2)	0.5672(7)	0.4311(1)	2.1(1)
C(50)	0.0966(2)	0.5169(7)	0.4156(1)	2.0(1)
C(51)	-0.1275(2)	0.9411(7)	0.3177(1)	2.5(1)
C(52)	-0.1871(3)	0.8956(9)	0.2601(2)	4.5(2)
C(53)	-0.1796(2)	1.0718(7)	0.3641(2)	3.0(1)
C(54)	0.1675(2)	0.6382(7)	0.4490(1)	2.4(1)
C(55)	0.0247(2)	0.1979(7)	0.2001(2)	3.2(2)

Three recrystallizations gave pure crystalline compound (**2**). The oily compound (**3**) was further purified on HPLC [column, YMC A-024 SIL (10 x 300 mm); solvent, hexane-ethyl acetate (98:2); flow rate 4 ml/min; t_R 25.2 min for (**2**), 38.2 min for (**3**)].

Compounds (**5**) and (**6**) were the synthetic intermediates in the synthesis[2] of (-)-P-B (**1**). Compounds (**5**) and (**6**) have also been described by Schreiber and Santini[17] in their synthesis of (±)-(**1**). Each of these two samples was chromatographically pure and the optical purity was ≥ 98% e.e. However, capillary GLC-MS analysis of compound (**5**) showed contamination of a stereoisomer at the epoxy

group. A pure crystalline sample, m. p. 52-53°C, $[\alpha]_D^{25}$ -378° (*c* 0.533, hexane), was obtained on HPLC purification. [column, YMC A-012 SIL; solvent, hexane-ethyl acetate (96:4), flow rate, 1.0 ml/min; t_R 27.4 min for (**5**); t_R 32.3 min for the isomer of (**5**)]. Germacrene-D (**7**), isolated from ylang-ylang essential oil was a gift from Dr. Y. Takagi of T. Hasegawa Inc., the chemical purity was 98% as judged by GLC.

The Formations of P-A (**2**) *and of Compound* (**4**).----A solution of sodium methylsulphinyl carbanion (1.0$_M$, 0.1 ml) in dry dimethyl sulphoxide (DMSO) was added to a stirred suspension of trimethylsulphonium iodide (30 mg) in DMSO-tetrahydrofuran (THF) (1:1; 2 ml) at 0°C under Ar, and the mixture was stirred for 5 min. Then, a solution of compound (**8**) (17.0mg) in dry THF (0.3ml) was added to the mixture at -10°C. After being stirred at between -10 and 0°C for 15 min, the reaction mixture was quenched with saturated aq. NH_4Cl and extracted twice with hexane. The organic phase was washed successively with water and brine, and concentrated. The concentrate was chromatographed over silica gel (Mallinckrodt SilicAR CC-7™, 2g) to remove polar products and the fractions eluted with hexane-ethyl acetate (95:5-9:1) were combined. TLC analysis showed several components along with the unchanged compound (**8**) and traces of compound (**9**). The two major components were isolated from the crude products on HPLC [column, YMC A-012 SIL; solvent hexane-THF (99:1), flow rate 3.0 ml/min; t_R 3.6 min for (**2**) (1.4 mg); t_R 5.8 min for (**4**) (5.2 mg)]. Upon evaporation of the solvents, both of these two products crystallized readily, and the

recrystallizations from pentane-di-isopropyl ether gave pure samples.

Compound (**4**).----This showed m. p. 110-110.5°C; $[\alpha]_D^{25}$ -979° (*c* 0.034, hexane). The full assignment of 500 MHz ^1H NMR data in [$^2H_6$] benzene solution are listed in Table 3; ν_{max} (KBr, film) 3070w, 2975m, 2920m, 2869m, 1679s, 1653m, 1622s, 1612s, 1460m, 1391m, 1082m, 982s, 920s, 905s, 781s, and 761s cm^{-1}; *m/z* 232 (M^+, 0.5%),203 (0.8), 201 (1.4), 189 (7), 171 (11), 159 (16), 143 (31), 131 (32), 105 (74), and 91 (100).

^1H *NMR Data for Compound* (**6**) *and Germacrene-D* (**7**).----Compound (**6**) δ 2.28(2H, AB-m,1-H), 1.86(1H, m*, 2-H), 1.20(1H, m, 2-H'), 2.55(1H, dt, *J* 4.6, ~12.6Hz, 3-H), 2.00(1H, ddd, *J* 12.6, 5.7, 1.8Hz, 3-H'), 5.90(1H, d, *J* 15.9Hz, 5-H), 5.24(1H, dd, *J* 15.9, 10.4Hz, H-6), 1.46 (1H, m, 7-H), 2.09 (1H, m, 8-H), 1.57(1H, m, 8-H'), 1.91(1H, m*, 9-H), 1.88(1H, m*, 9-H'), 1.32(1H, m, 11-H), 0.80(3H, d, *J* 6.7Hz, 12-H_3), 0.78 (3H, d, *J* 6.7Hz, 13-H_3), 4.85(1H, br s, 15-H), and 4.82(1H, br s, 15-H') (* overlapped signals).

Compound (**7**). δ5.17(1H, m, 1-H), ~2.3(2H, m, 2-H_2), ~2.0(2H, m, 3-H_2), 5.75(1H, d, *J* 15.8Hz, 5-H), 5.25(1H, dd, *J* 15.8, 9.9Hz, 6-H), ~1.9(1H, m, 7-H), ~1.25(2H, m, 8-H_2), ~2.2(2H, m, 9-H_2), ~1.3(1H, m, 11-H), 0.88(3H, d, *J* 6.7Hz, 12-H_3), 0.84 (3H, d, *J* 6.8Hz, 13-H_3), 1.45(3H, br s, 14-H_3), 4.93(1H, br s, 15-H), and 4.79(1H, br.s, 15-H').

X-Ray Crystal Structure Analysis of Compound (**2**).---A colorless, needle-shaped crystal of compound (**2**) having dimensions of 0.60 x 0.12 x 0.05 mm was mounted on a glass fibre at a temperature of -120 ± 1°C. An experiment at room temperature resulted in sublimation of

the crystal. Data collections was made on a Rigaku AFC5R diffractometer with graphite-monochromated Cu-$K\alpha$ radiation and a 12 kW rotating anode generator. The crystallographic data for compound (**2**) are summarized in Table 4. The structure of compound (**2**) was solved by direct methods using SHELXS-86[20] and DIRDIF[21] programs. The non-hydrogen atoms were refined anisotropically. Hydrogen atoms were included in the structure factor calculation in idealized positions (d_{C-H} 0.95Å), and were assigned isotopic thermal parameters which were 20% greater than the B_{equiv}- value of the atom to which they were bonded. The final cycle of full-matrix least-squares refinement converged with unweighted and weighted agreement factors of $R = \Sigma ||F_o| - |F_c|| / \Sigma |F_o|$; $R_w = \{[\Sigma w (|F_o| - |F_c|)^2 / \Sigma w F_o^2]\}^{1/2}$. The standard deviation of unit weight was 1.48. The weighting scheme was based on counting statistics and included a factor (p = 0.03) to downweight the intense reflections.

Table 6 Bond lengths (Å) involving the non-hydrogen atoms for Compound (**2**) (e.s.d.s in parentheses).

Bond	Distance	Bond	Distance
O(1)-C(9)	1.205(4)	C(26)-C(27)	1.486(5)
O(2)-C(10)	1.437(4)	C(27)-C(28)	1.559(4)
O(2)-C(14)	1.435(4)	C(27)-C(31)	1.538(4)
C(1)-C(2)	1.319(5)	C(28)-C(29)	1.506(4)
C(2)-C(3)	1.501(5)	C(29)-C(30)	1.522(5)
C(3)-C(4)	1.529(4)	C(30)-C(21)	1.485(4)
C(4)-C(5)	1.475(4)	C(30)-C(34)	1.479(5)
C(4)-C(15)	1.319(5)	C(31)-C(32)	1.527(6)
C(5)-C(6)	1.329(5)	C(31)-C(33)	1.517(5)
C(6)-C(7)	1.497(4)	O(5)-C(49)	1.211(4)
C(7)-C(8)	1.550(4)	O(6)-C(50)	1.435(4)
C(7)-C(11)	1.541(5)	O(6)-C(54)	1.445(4)
C(8)-C(9)	1.509(5)	C(41)-C(42)	1.329(4)
C(9)-C(10)	1.516(4)	C(42)-C(43)	1.506(4)
C(10)-C(1)	1.494(5)	C(43)-C(44)	1.529(4)
C(10)-C(14)	1.479(5)	C(44)-C(45)	1.478(4)
C(11)-C(12)	1.528(5)	C(44)-C(55)	1.318(5)
C(11)-C(13)	1.520(5)	C(45)-C(46)	1.325(5)
O(3)-C(29)	1.218(4)	C(46)-C(47)	1.500(4)
O(4)-C(30)	1.435(4)	C(47)-C(48)	1.548(4)
O(4)-C(34)	1.436(4)	C(47)-C(51)	1.541(5)
C(21)-C(22)	1.325(4)	C(48)-C(49)	1.506(5)
C(22)-C(23)	1.507(4)	C(49)-C(50)	1.519(4)
C(23)-C(24)	1.517(5)	C(50)-C(41)	1.490(5)
C(24)-C(25)	1.470(5)	C(50)-C(54)	1.478(4)
C(24)-C(35)	1.318(5)	C(51)-C(52)	1.529(5)
C(25)-C(26)	1.336(4)	C(51)-C(53)	1.516(5)

Table 7. Bond Angles (°) involving the non-hydrogen Atoms for Compound (2) (e.s.d.'s in parentheses)

Angle		Angle	
C(10)-O(2)-C(14)	62.0(2)	C(30)-C(4)-C(34)	62.0(2)
O(2)-C(10)-C(14)	58.9(2)	O(4)-C(30)-C(34)	59.0(2)
O(2)-C(14)-C(10)	59.0(2)	O(4)-C(34)-C(30)	59.0(2)
O(1)-C(9)-C(8)	122.0(3)	O(3)-C(29)-C(28)	122.1(3)
O(1)-C(9)-C(10)	118.3(3)	O(3)-C(39)-C(30)	118.7(3)
C(2)-C(1)-C(10)	127.3(3)	C(22)-C(21)-C(30)	128.3(3)
C(1)-C(2)-C(3)	128.1(3)	C(21)-C(22)-C(23)	128.6(3)
C(2)-C(3)-C(4)	109.1(3)	C(22)-C(23)-C(24)	110.1(3)
C(3)-C(4)-C(15)	122.3(3)	C(23)-C(24)-C(35)	121.9(3)
C(5)-C(4)-C(15)	122.5(3)	C(25)-C(24)-C(35)	121.8(3)
C(3)-C(4)-C(5)	114.9(3)	C(23)-C(24)-C(25)	116.1(3)
C(4)-C(5)-C(6)	125.5(3)	C(24)-C(25)-C(26)	125.4(3)
C(5)-C(6)-C(7)	125.8(3)	C(25)-C(26)-C(27)	125.7(3)
C(6)-C(7)-C(11)	113.2(3)	C(26)-C(27)-C(31)	113.2(3)
C(8)-C(7)-C(11)	111.8(3)	C(28)-C(27)-C(31)	110.8(3)
C(6)-C(7)-C(8)	107.0(2)	C(26)-C(27)-C(28)	107.8(3)
C(7)-C(8)-C(9)	109.6(3)	C(27)-C(28)-C(29)	109.9(2)
C(8)-C(9)-C(10)	119.7(3)	C(28)-C(29)-C(30)	119.2(3)
O(2)-C(10)-C(1)	117.6(3)	O(4)-C(30)-C(21)	118.7(3)
O(2)-C(10)-C(9)	116.8(3)	C(4)-C(30)-C(29)	115.8(3)
C(1)-C(10)-C(9)	115.6(3)	C(21)-C(30)-C(29)	115.0(3)
C(1)-C(10)-C(14)	120.5(3)	C(21)-C(30)-C(34)	120.7(3)
C(9)-C(10)-C(14)	115.8(3)	C(29)-C(30)-C(34)	116.3(3)
C(7)-C(11)-C(12)	109.4(3)	C(27)-C(31)-C(32)	111.7(3)
C(7)-C(11)-C(13)	112.9(3)	C(27)-C(31)-C(33)	110.9(3)
C(12)-C(11)-C(13)	110.2(3)	C(32)-C(31)-C(33)	109.8(4)
C(50)-O(6)-C(54)	61.4(2)	C(46)-C(47)-C(51)	112.9(2)
O(6)-C(50)-C(54)	59.2(2)	C(48)-C(47)-C(51)	112.0(3)
O(6)-C(54)-C(50)	59.4(2)	C(46)-C(47)-C(48)	107.4(2)
O(5)-C(49)-C(48)	121.8(3)	C(47)-C(48)-C(49)	109.5(3)
O(5)-C(49)-C(50)	117.9(3)	C(48)-C(49)-C(50)	120.3(3)
C(42)-C(41)-C(50)	127.8(3)	O(6)-C(50)-C(41)	117.7(2)
C(41)-C(42)-C(43)	128.4(3)	O(6)-C(50)-C(49)	116.2(3)

C(42)-C(43)-C(44)	108.5(3)	C(41)-C(50)-C(49)	114.9(3)
C(43)-C(44)-C(55)	121.2(3)	C(41)-C(50)-C(54)	121.1(3)
C(45)-C(44)-C(55)	122.9(3)	C(49)-C(50)-C(54)	116.4(3)
C(43)-C(44)-C(45)	115.5(3)	C(47)-C(51)-C(52)	109.4(3)
C(44)-C(45)-C(46)	125.3(3)	C(47)-C(51)-C(53)	113.6(3)
C(45)-C(46)-C(47)	127.2(3)	C(52)-C(51)-C(53)	110.3(3)

Non-hydrogen atomic co-ordinates are listed in Table 5, and bond lengths and angles of the non-hydrogen atoms in Table 6 and 7,* respectively.

X-Ray Crystal Structure Analysis of Compound (**4**).----A colorless parallelepiped crystal of compound (**4**) having dimensions of 0.15 x 0.20 x 0.40 mm was mounted on a glass fibre. The data was collected at 23 ± 1°C on a Rigaku AFC5R diffractometer with graphite-monochromated Cu-$K\alpha$ radiation and a 12kW rotating anode generator. The crystallographic data for compound (**4**) are summarized in Table 4. The structure of compound (**4**) was solved by direct methods using DIRDIF and MITHRIL[22] programs. The non-hydrogen atoms were refined anisotropically. Hydrogen atoms were refined with assigned isotropic thermal parameters which were greater than the B_{equiv}- value of the atom to which they were bonded. The final cycle of full-matrix least-squares refinement converged with unweighted and weighted agreement factors of $R = \Sigma ||F_o| - |F_c|| / \Sigma |F_o|$; $R_w = \{[\Sigma w (|F_o| - |F_c|)^2 / \Sigma w F_o^2]\}^{1/2}$. The

* Non-hydrogen atomic thermal parameters and hydrogen atomic co-ordinates calculated assuming ideal geometries have deposited at the Cambridge Crystallographic Data Centre. For details see section 5. 6. 3 of the Instructions for Authors, *J. Chem. Soc., Perkin Trans. 1*, in the January issue.

standard deviation of unit weight was 1.18. The weighting scheme was based on counting statistics and included a factor (p = 0.05) to downweight the intense reflections. Non-hydrogen atomic co-ordinates were given in Table 8, and bond lengths and angles of the non-hydrogen atoms are in Table 9.**

Table 8. Non-hydrogen atom co-ordinates for compound (**4**) (e.s.d.'s in parentheses).

atom	*x*	*y*	*z*	B(eq)
O(1)	0.7120(2)	0.5950(2)	0.7544(5)	5.7(1)
O(2)	0.5009(2)	0.4741(1)	0.5261(4)	5.0(1)
C(1)	0.6438(2)	0.5871(2)	0.4178(6)	4.7(2)
C(2)	0.6424(3)	0.6636(2)	0.3475(7)	4.6(2)
C(3)	0.4396(3)	0.7411(2)	0.4627(7)	4.4(2)
C(4)	0.5185(3)	0.7577(2)	0.4637(5)	3.5(1)
C(5)	0.4529(3)	0.6976(2)	0.5757(5)	3.4(1)
C(6)	0.4762(3)	0.6680(2)	0.7513(5)	3.2(1)
C(7)	0.4208(3)	0.5959(2)	0.8506(5)	3.4(1)
C(8)	0.5039(3)	0.5237(2)	0.8715(6)	4.3(2)
C(9)	0.5653(3)	0.5057(2)	0.6869(5)	3.9(2)
C(10)	0.6530(3)	0.5658(2)	0.6282(6)	4.2(2)
C(11)	0.3709(3)	0.6199(2)	1.0489(5)	4.1(2)
C(12)	0.3215(4)	0.5467(3)	1.1568(7)	5.8(2)
C(13)	0.2878(4)	0.6892(3)	1.0204(8)	6.5(3)
C(14)	0.5798(4)	0.4191(2)	0.6148(7)	5.5(2)
C(15)	0.4746(4)	0.8178(2)	0.3579(6)	5.1(2)

** Non-hydrogen atom thermal parameters and hydrogen atomic co-ordinates have been deposited at the Cambridge Crystallographic Data Centre.

Table 9. Bond length (Å) and angles (°) involving the non-hydrogen atoms for compound (**4**) (e.s.d.s in parentheses).

Bond length			
O(1)-C(10)	1.221(4)	C(5)-C(6)	1.322(5)
O(2)-C(14)	1.445(5)	C(6)-C(7)	1.505(4)
O(2)-C(9)	1.446(4)	C(7)-C(11)	1.537(5)
C(1)-C(2)	1.317(5)	C(7)-C(8)	1.551(5)
C(1)-C(10)	1.483(5)	C(8)-C(9)	1.498(5)
C(2)-C(3)	1.498(5)	C(9)-C(14)	1.485(5)
C(3)-C(4)	1.516(5)	C(9)-C(10)	1.503(5)
C(4)-C(15)	1.320(5)	C(11)-C(12)	1.513(5)
C(4)-C(5)	1.473(4)	C(11)-C(13)	1.524(6)
Bond angle			
C(14)-O(2)-C(9)	61.8(2)	C(11)-C(7)-C(8)	111.7(3)
O(2)-C(9)-C(14)	59.1(2)	C(7)-C(8)-C(9)	113.5(3)
O(2)-C(14)-C(9)	59.1(2)	O(2)-C(9)-C(8)	115.5(3)
C(2)-C(1)-C(10)	124.5(4)	O(2)-C(9)-C(10)	114.6(3)
C(1)-C(2)-C(3)	125.7(4)	C(14)-C(9)-C(8)	121.4(3)
C(2)-C(3)-C(4)	109.5(3)	C(14)-C(9)-C(10)	115.2(3)
C(15)-C(4)-C(5)	122.5(3)	C(8)-C(9)-C(10)	117.6(3)
C(15)-C(4)-C(3)	122.0(4)	O(1)-C(10)-C(1)	122.8(4)
C(3)-C(4)-C(5)	115.3(3)	O(1)-C(10)-C(9)	119.0(3)
C(4)-C(5)-C(6)	126.0(3)	C(1)-C(10)-C(9)	118.1(4)
C(5)-C(6)-C(7)	125.9(3)	C(12)-C(11)-C(13)	111.0(4)
C(6)-C(7)-C(11)	112.7(3)	C(12)-C(11)-C(7)	113.3(3)
C(6)-C(7)-C(8)	108.4(3)	C(13)-C(11)-C(7)	109.8(3)

Acknowledgements We are grateful to Professor H. Hauptmann of the University of Regensburg for sending X-ray crystallographic data of (±)-periplanone-B (**1**). We thank Dr. Y. Takagi of T. Hasegawa Co. Ltd. for the gift of germacrene-D (**7**). We also thank Mr. T. Tobita of Tobacco Science Research Laboratory, Japan Tobacco Inc. (JT) for recording NMR spectra. Special thanks are due to Dr. Y.

Kitano of Toray Research Centre for the X-ray crystallography measurement.

References

1 C. J. Persoons, F. J. Ritter, and W. J. Lichtendonk, *Proc. Kon. Ned. Akad. Wetensch. Amsterdam*, 1974, **C77**, 201.

2 T. Kitahara, M. Mori, and K. Mori, *Tetrahedron*, 1987, **43**, 2689, and references cited therein. For recent progress on the synthesis of (**1**), see: S. Kuwahara and K. Mori, *Heterocycles*, 1989, **28**, 167, and references cited therein.

3 C. J. Persoons, P. E. J. Verwiel, F. J. Ritter and W. J. Nooyjen, *J. Chem. Ecol., 1982, 8*, 439, and references cited therein.

4 H. Hauptmann, G. Mühlbauer, and H. Sass, *Tetrahedron Lett.*, 1986, **27**, 6189.

5 T. L. Macdonald, C. M. Delahunty, and J. S. Sawyer, *Heterocycles*, 1987, **25**, 305.

6 Y. Shizuri, K. Matsunaga and S. Yamaura, *Tetrahedron Lett.*, 1989, **30**, 3693.

7 K. Mori and Y. Igarashi, *Tetrahedron Lett.*, 1989, **30**, 5145.

8 S. Kuwahara and K. Mori, *Tetrahedron Lett.*, submitted.

9 S. Kuwahara and K. Mori, *Tetrahedron Lett.*, 1989, **52**, 7447.

10 S. Tahara, M. Yoshida, J. Mizutani, C. Kitamura, and S. Takahashi, *Agric. Biol. Chem.*, 1975, **39**, 1517; S. Takahashi, C. Kitamura and I. Horibe, *ibid.*, 1978, **42**, 79.

11 W. S. Bowers anW. G. Bodensteinin, *Nature*, 1971, **232**, 259; C. Nishino, K. Kobayashi, S. Manabe and A. Mori, *Comp. Biochem. Physiol.*, 1989, **92A**, 129, and references cited therein.

12 W. C. Still, L. J. MacPherson, T. Harada, and J. F.Callahan, *Tetrahedron*, 1984, **40**, 2275. W. C. Still, *J. Am. Chem. Soc.*, 1979, **101**, 2493.

13 K. Okada, M. Mori, K. Shimazaki, and T. Chuman, *J. Chem. Ecol.*, 1991, **17**, 695.

14 K. Okada, M. Mori, S. Kuwahara, T. Kitahara, K. Mori, K. Shimazaki, and T. Chuman, *Agric. Biol. Chem.*, 1990, **54**, 575.

15 C. Nishino and K. Kuwabara, *Comp. Biochem. Physiol.*, 1989, **74A**, 909; S, Takahashi, H. Takegawa, T. Takahashi, and T. Doi, *J. Pesticide Sci.*, 1998, **13**, 501.
16 H. Hauptmann, G. Mühlbauer, and N. P. C. Walker, *Terahedron Lett.*, 1986, **27**, 1315.
17 S. L. Schreiber and C. Santini, *J. Am. Chem. Soc.*, 1984, **106**,4038.
18 For a recent reviews, see; J. Boeckh and K. -D. Ernst, *J. Comp. Physiol.*, 1987, **A161**, 549.
19 D. Neuhaus, *J. Magn. Res.*, 198, **53**, 199; M. Kimms and J. K. M. Sanders, *ibid.*, 1984, **56**, 518.
20 G. M. Sheldrick, SHELX-86, A Program for the solution of Crystal Structure from Diffraction data, Institute für Anorganische Chemie der Universität, Tammannstrasse 4, Göttingen, Germany.
22 P.T.Beursken, DIRDIF, Direct Methods for Difference Structures - an Automatic Procedure for Phase Extension and Refinement of Difference Structure Factors, Technical Report 1984/1, Crystallography Laboratory, Toernooiveld, 6525 Ed Nijmegen, Netherland.
23 C.J.Gilmore; MITHRIL, An Integrated Direct Methods Computer Program, University of Glasgow, Scotland; *J. Appl. Crystallogr.*, 1984, **17**, 42.

Chapter 4

Conformational Analyses of Periplanone Analogues by Molecular Mechanics Calculations.

Abstract

Conformational parameters of pheromonally active analogues (**1** and **2**) of periplanones, the sex pheromones of american cockroach, were investigated by molecular mechanics calculations. They existed in several conformers with small energy differences. These results were supported by NMR analysis. The structural features of the conformers of the analogues were compared with X-ray structures of periplanones.

Introduction

The utilization of molecular mechanics (MM) calculations on the conformational analysis of organic molecules has become an active area of research. We have already reported the application of MM analysis on the conformational property of insect pheromone serricornin (Chuman et al., 1990).

Periplanones-A (**P-A**) (**3**) (Hauptmann et al., 1986a) and -B (**P-B**) (**4**) (Persoons et al., 1974) are the major sex pheromone components produced by female American cockroach (*Periplaneta americana L.*). Their activity is extremely high: threshold 10^{-5} μg for **3** and 10^{-7} μg for **4**. The X-ray crystallographic analyses of them (**P-A**; Kuwahara and Mori, 1989, Mori et al., 1990, **P-B**;

Hauptmann et al., 1986b) have established that their ten-membered rings adopt similar twist-chair (**TC**) conformations.

Recently, we reported the conformational analyses of periplanones and their analogues by the use of NMR and X-ray crystallographic analyses, and pointed out the conformational resemblances among the bioactive analogues. (Mori et al., 1990). However, the structurally simplified analogue (**1**) [(4S,5E)-7-Methylene-4-(1-methylethyl)-5-cyclodecen-1-one] and germacrene-D (**2**) (Tahara et al., 1975) (activity thresholds: 1 μg for **1** and 10 μg for **2**) did not yield crystalline samples suitable for X-ray analysis, and their complicated NMR spectra did not provide insufficient information (NOEs and $^3J_{HH}$'s) for the conformational analyses. Thus, we attempted to investigate the conformational properties of these compounds by MM calculations to overcome the difficulty on the structural assignments by conventional methods.

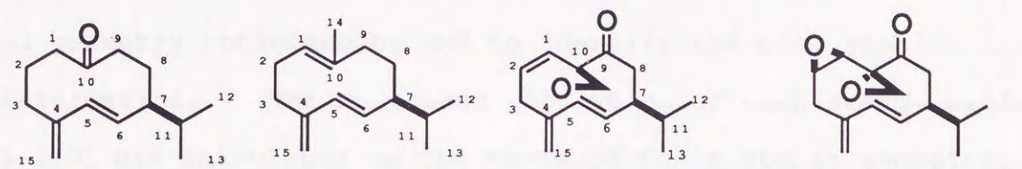

Fig. 1 Structures of analogue **1**, germacrene-D (**2**), periplanone-A (**3**) and -B (**4**).The same numbering scheme for the C atoms is employed in this paper as has been used for **P-B** by Persoons et al. (1974).

Methods and Materials

The details of the preparations and purity determinations of the compounds **1-4** have been described in our previous paper (Mori

et al., 1990). Their bioassay data have also been reported (Okada et al., 1990). The synthesis of racemic compound (**1**) was first reported by Schreiber and Santini (1984). [^{1}H]NMR (500 MHz) spectra were recorded at 27°C in C_6D_6 solution with Me_4Si as internal standard.

Molecular mechanics calculations. MM2 molecular mechanics program (Burkert and Allinger, 1982; version '87: Molecular Design Ltd., Farallon Drive, San Leandro, California, U.S.A.) was employed to the structural optimizations. The three-dimentional structures were visualized and superimposed using QUANTA program (Polygen Co., Waltham, Massachusetts, U.S.A.) run on an IRIS-4D/80GT computer system (Silicon Graphics Inc., Mountain View, California, U.S.A.).

The initial geometries of the ring conformations, including the rotamers regarding isopropyl group were exhaustively generated by CONFLEX2 program (Gotō and Ōsawa, 1989: QCPE #592). They were all geometry optimized by MM2 to identify the most stable conformations. The Boltzmann population of each energy minimum at 25°C was calculated on the basis of their steric energies.

The conformers of 10-membered ring conformation on the aspect of dihedral angles were defined using a new nomenclature (in CONFLEX2, Gotō, 1992).[1]

---

[1] A note on the ring nomenclature. In view of inconveniences inherent to the current ring nomenclatures, we devised the following new definition in CONFLEX2. Details will be described elsewhere. 1. Classify all the endocyclic bonds in a ring structure as g^+, g^- and anti. 2. When two contiguous gauches of the same sign exist, the midpoint in a corner. 3.When two contiguous gauches of the opposite sign exist, the midpoint is a pseudo-

Calculations of vicinal coupling constants ($^3J_{HH}$). Averaged vicinal H/H coupling constants ($^3J_{HH}$) were calculated on MM2 geometry-optimized structures of **1** and **2** using Altona's empirical modification of Karplus equation (Haasnoot et al., 1980). These calculation were based on 93 energy minima of **1** and 47 of **2** which were found by MM2 calculation.

Results and Discussion

Conformational analysis by molecular mechanics calculation

*Analogue **1**.* CONFLEX2 generated 577 initial geometries for **1**, which were structurally optimized by MM2, to identify 93 energy minima. The number of major conformers over 5% Boltzmann population at 25°C (ΔSE<1.1 kcal/mol) was five and those over 1% population (ΔSE<2.1 kcal/mol) was 12. The conformational parameters of the major five conformers are summarized in Table 1. The perspective drawings of these structures are reproduced in Figure 2. Regarding the ring conformation, the major five conformers can be classified into three types. For example, both of **1A** and **1D** (the rotamer of **1A** regarding isopropyl group) possess [1'324'] type ring conformations. Similarly, both of **1B** and **1E** (the rotamer of **1B**) possess [1'4'1'4'] type ring conformations. The relative ratio of ring conformations of the stable conformers of **1** at 25°C

---

corner, if at least one side is connected to anti. 4. Number of bonds between corners and/or pseudocorners are entered in sequence between brackets, in such a way that the small possible integer results. 5. When a pseudocorner appears, the number of bonds is primed. When more than two possibilities exist, corner is preferred to pseudocorner.

is [1'324']: [1'4'1'4']: [132'4'] = 56: 30: 14. As shown in Table 1, the dihedral angles along C6-C7-C8-C9-C10-C1 and C7-C11 atoms are practically coincident in **1A-1E** structures. Therefore, the ring conformation involving C7 isopropyl and C10 carbonyl groups are well conserved in the major conformers, in contrast to the flexible C2-C5 region of the ring.

The most stable conformer **1A** has similar conformational feature to that of the X-ray structure of periplanones. The superimposition (Figure 3) clearly showed the overlapping of **1A** and the X-ray structure of P-B (**4**). A significant match on the location of C10 carbonyl oxygen of **1A** with that of the spiro-epoxy group in **4** was also noteworthy.

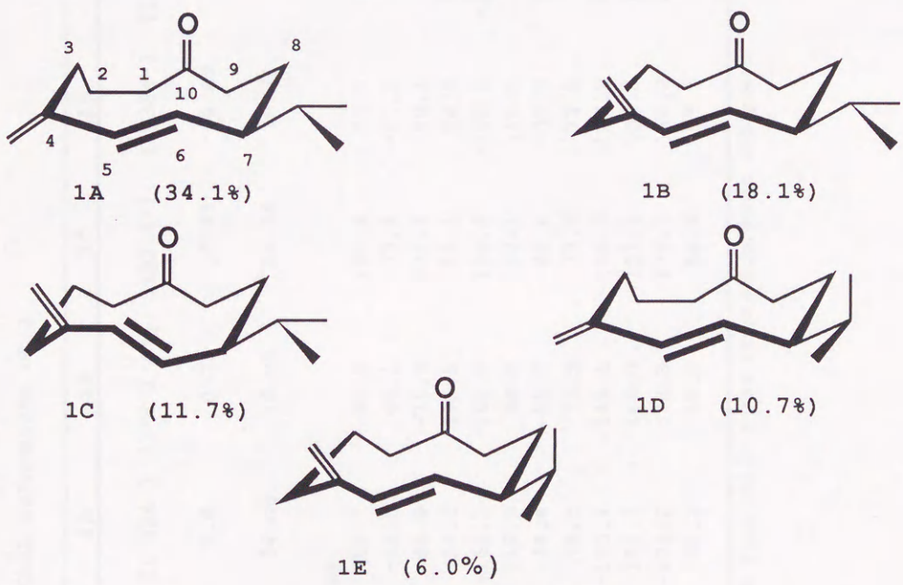

Fig. 2 Major conformers of analogue **1**.

Table 1. CONFORMATIONAL PARAMETERS OF **1**

	1A	**1B**	**1C**	**1D**	**1E**	**P-A**[a] (3)	**P-B**[a] (4)
Ring conformation	[1'324']	[1'4'1'4']	[132'4']	[1'324']	[1'4'1'4']	[123'1'3']	[123'1'3']
ΔSE (kcal/mol)	0.0	0.38	0.63	0.69	1.03		
Boltzmann dist. (%) at 25°C	34.08	18.08	11.74	10.71	5.98		
Dihedral angle (degree)							
C10-C1-C2-C3	-58.7	-80.9	-75.8	-59.9	-81.6	-3.5	-1.5
C1-C2-C3-C4	-49.5	66.1	73.8	-51.1	65.3	-93.3	-90.0
C2-C3-C4-C5	82.0	-76.3	-78.4	80.1	-75.4	72.0	80.0
C3-C4-C5-C6	24.6	140.5	-15.1	24.8	141.3	39.9	29.5
C4-C5-C6-C7	-166.7	-165.8	166.4	-165.2	-164.4	-167.0	-166.4
C5-C6-C7-C8	113.9	92.2	-68.1	119.4	92.7	114.4	110.1
C6-C7-C8-C9	-48.4	-55.7	-46.8	-52.3	-58.4	-50.0	-40.8
C7-C8-C9-C10	74.5	73.9	75.4	73.5	73.5	92.5	95.6
C8-C9-C10-C1	-133.7	-149.1	-126.8	-129.2	-147.4	140.4	-148.9
C9-C10-C1-C2	151.2	149.0	151.4	153.3	150.9	106.4	97.3
C9-C8-C7-C11	-171.2	-178.8	-173.1	-178.7	174.5	-174.6	-166.4
C8-C7-C11-H11	60.3	60.0	58.4	-53.7	-59.4	64.2	57.7

[a]The data of **P-A** and **P-B** from their X-ray crystallographic analyses.

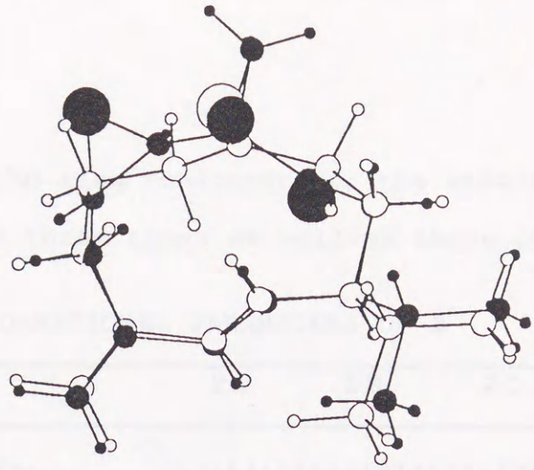

Fig. 3 Superimposition of analogue **1** (conformer **1A**) and **P-B** (filled).

Germacrene-D (**2**). CONFLEX2 generated 626 initial geometries for **2**, and their structural minimization by MM2 identified 47 energy minima. There is no predominant conformer and five conformers are found within ΔSE 0.5 kcal/mole; 11 over 1% population (ΔSE <1.6 kcal/mole). The conformational parameters of the major five conformers are summarized in Table 2. The perspective drawings of these structures are shown in Figure 4.

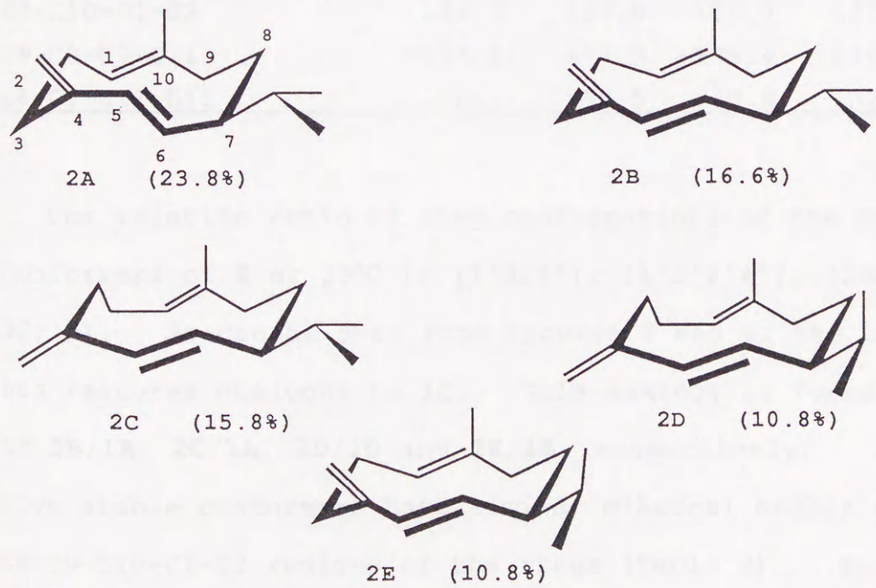

Fig. 4 Major conformers of germacrene-D (**2**).

As regards the ring conformation, the stable conformers can be classified into three types as well as those of **1**.

Table 2. CONFORMATIONAL PARAMETERS OF **2**

	2A	**2B**	**2C**	**2D**	**2E**
Ring conformation	[232'3']	[1'3'2'4']	[1'324']	[1'324']	[1'3'2'4']
ΔSE (kcal/mol)	0.00	0.21	0.24	0.47	0.47
Boltzmann dist.(%)	23.76	16.60	15.83	10.82	10.79
Dihedral angle (degree)					
C10-C1-C2-C3	-99.0	-114.4	-79.3	-79.2	-115.5
C1-C2-C3-C4	65.3	56.7	-53.5	-54.7	56.7
C2-C3-C4-C5	-69.8	-69.4	69.8	68.7	-69.6
C3-C4-C5-C6	-20.3	128.7	27.1	27.6	127.7
C4-C5-C6-C7	167.5	-166.3	-167.5	-165.6	-164.3
C5-C6-C7-C8	-65.3	106.7	126.5	129.3	108.6
C6-C7-C8-C9	-48.8	-59.9	-52.5	-55.8	-62.5
C7-C8-C9-C10	71.0	67.7	65.8	65.8	67.8
C8-C9-C10-C1	-104.1	-115.1	-106.0	-104.0	-113.5
C9-C10-C1-C2	164.7	167.0	166.7	167.2	167.5
C9-C8-C7-C11	-175.2	177.5	-175.4	178.0	171.1
C8-C7-C11-H11	60.1	59.5	60.9	-52.1	-57.2

The relative ratio of ring conformations of the major five conformers of **2** at 25°C is [1'324']: [1'3'2'4']: [232'3'] = 34: 35: 31. As can be seen from Figures 2 and 4, the conformer **2A** has features analogus to **1C**. This analogy is found in the cases of **2B**/**1B**, **2C**/**1A**, **2D**/**1D** and **2E**/**1E**, respectively. All of the five stable conformers have similar dihedral angles along C6-C7-C8-C9-C10-C1-C2 regions of the rings (Table 2). Among the conformers, the orientations of methyl group at C10, which extends

vertically above the ring plane, are well retained. The third conformer **2C** is most superimposable to P-B (**4**) (Figure 5).

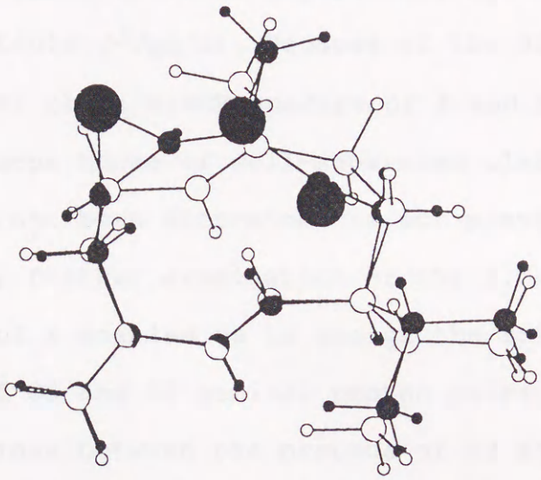

Fig. 5 Superimposition of germacrene-D **2** (conformer **2C**) and P-B (filled).

Shizuri et al. (1986) proposed the most stable conformations of **2** by MM-calculations, and reported that **2** adopted two main conformations **2E** (CC) and **2C** (TC) in the relative ratio at 25°C of CC: TC: others = 82: 17: 1. The most stable conformation, **2A**, identified in our work was not found by them. Our result was more reliable in terms of the exhaustive generation of initial geometries by CONFLEX2 and the use of more improved version of MM2 program for the calculations.

Comparisons of Calculated and Observed NMR data

To verify the conformational properties of **1** and **2** predicted by MM calculation, their calculated NMR parameters ($^3J_{HH}$'s) were compared with those observed experimentally.

Coupling constants ($^3J_{HH}$'s). Because of the high multiplicity and overlappings of the [^{1}H]NMR spectra of **1** and **2**, their coupling constants, except those of well-separated olefinic and methyl signals, have not been determined in our previous work. In the present study, further examination of the 1.0-2.7 ppm region of the spectrum of **1** enabled us to assign the splitting patterns of the signals of C3 and C8 geminal proton pairs. For the four vicinal couplings between the protons of H2 and H3, as well as for H8 and H9, the population-weighted coupling constants were calculated on the basis of the MM2 structures and their Boltzmann populations. As shown in Table 3, the calculated values essentially agreed with those observed, while the values were not accurately coincident (Masamune, et al., 1986).

Table 3. Comparison between observed and calculated values of vicinal NMR coupling constants for **1**

	J values (H_Z) between protons							
	2α-3α	2β-3α	2α-3β	2β-3β	8α-9α	8β-9α	8α-9β	8β-9β
calcd.	3.76	9.29	6.87	3.60	1.65	5.94	13.10	1.60
obsd.	~1.0	12.5	5.9	1.5	2.9	4.4	11.8	2.2

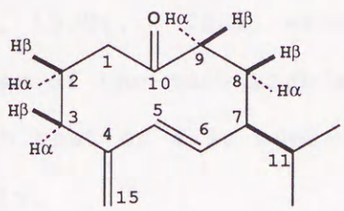

Conclusion

The MM calculations on the periplanone analogues **1** and **2** revealed that they exist in several conformers with small energy differences. These results were well coincident with those of NMR-analysis. Regarding the ring conformation, the conformational parameters of **1** and **2** resemble each other. In the case of **2**, the substitution of the C10 carbonyl group of **1** into the methyl group and the presence of C1-C10 *trans* double bond do not cause any drastic change on the conformation, although they must contribute to make the difference of the relative ratio and the order of the conformers between **1** and **2**.

The conformers **1A** and **2C** adopt ring conformations very similar to those of natural pheromones established by X-ray analyses, and the other stable conformers can be regarded as the partially altered ("flapped") ones. The similarity of structure is not a sufficient condition for activity. For instance, there are many examples from enzyme-substrate binding studies in which the X-ray structures of enzymes do not necessarily represent the active conformers. However, we have already mentioned that the X-ray structures of the periplanones were well explained by their NMR analyses, and the close conformational resemblance between natural pheromones and the bioactive analogues was shown by X-ray and NMR analyses (Mori et al., 1990). Thus, examination of the structural resemblances of the most stable conformers of the analogues **1** and **2** with that of **4** is useful in correlating structure with activity.

The activity thresholds for the natural periplanones are 10^{-7}-10^{-5} μg, while they are 1 and 10 μg for **1** and **2**, respectively. Since the removal and substitution of the oxygen-containing functionalities on **3** and **4** greatly reduce the activity (Mori et al., 1990), these significant decrease in activity are attributed to the lacks of electrostatic effects of the functionalities, which can strongly interact to pheromonereceptor. As each of the analogues exits in a mixture of conformers, it may also contribute to the low activity.

The present work showed that the results obtained by MM analysis should be of great value for the understanding of structure-activity relationships for the type of compounds studied.

References

Burkert, U., and Allinger, N. L. 1982. Molecular mechanics. ACS Monograph 177. American Chemical Society. Washington, DC.

Chuman, T., Shimazaki, K., Mori, M., Okada, K., Goto, H., Osawa, E., Sakakibara, K., and Hirota, M. 1990. Conformational analysis of serricornin application of molecular mechanics calculations to stereochemical assignment of serricornin, the sex pheromone of cigarette beetle (*Lasioderma serricorne* F.). *J. Chem. Ecol.* 16:2877-2888.

Gotō, H., and Ōsawa, E. 1989. Corner flapping: A simple and fast algorithm for exhaustive generation of ring conformations. *J. Am. Chem. Soc.* 111:8950-8951.

Gotō, H. 1992. A revised nomenclature for the ring conformation and a note on the conformational distance in cyclodecane. *Tetrahedron* 48:7131-7144.

Haasnoot, C.A.G., de Leeuw, F.A.A.M., and Altona, C. 1980. The relationship between proton-proton NMR coupling constants and substituent electronegativities-I. *Tetrahedron* 36:2783-2792.

Hauptmann, H., Mühlbauer, G., and Sass, H. 1986a. Identifizierung und Synthese von Periplanon A. *Tetrahedron Lett.* 27:6189-6192.

Hauptmann, H., Mühlbauer, G., and Walker, N.P.C. 1986b. Synthese und Kristallstruktur von (±)-Periplanone B. *Tetrahedron Lett.* 27:1315-1318.

Kuwahara , S., and Mori, K. 1989. Clarification of structure of Persoons's periplanone-A, an artifact derived from Hauptmann's periplanone-A. *Tetrahedron Lett.* 30:7447-7450.

Masamune, S., Ma, P., Moore, R.E., Fujiyoshi, T., Jaime, C., and Ōsawa, E. 1986. Computation of vicinal coupling constants in tetra- and hexa-alditol peracetates using molecular mechanics. A rational approach to conformational analysis in solution. *J. Chem. Soc., Chem. Commun.*, 261-263.

Mori, M., Okada, K., Shimazaki, K., Chuman, T., Kuwahara, S., Kitahara, T., and Mori, K. 1990. X-ray crystallographic and NOE studies on the conformation of periplanones and their analogues. *J. Chem. Soc. Perkin Trans.*1, 1769-1777.

Okada, K., Mori, M., Kuwahara, S., Kitahara, T., Mori, K., Shimazaki, K., and Chuman, T. 1990. Behavioral and electro-antennogram responses of male American cockroaches to periplanones and their analogs. *Agric. Biol. Chem.* 54:575-576.

Persoons, C.J., Ritter, F.J., and Lichtendonk, W.J. 1974. Sex pheromones of american cockroach periplaneta americana. Isolation and partial identification of two excitants. *Proc. Kon. Ned. Akad. Wetensch. Amsterdam.* C77:201.(*Chem.abstr.*81:88 209f)

Schreiber, S.L., and Santini, C. 1984. Cyclobutene bridgehead olefin route to the american cockroach sex pheromone, periplanone-B. *J. Am. Chem. Soc.* 106:4038-4039.

Shizuri, Y. Yamaguchi, S. Terada, Y. and Yamamura, S. 1986. Biomimetic syntheses of oppositol, oplopanone, and aphanamol II from germacrene-D. *Tetrahedron Lett.* 27:57-60.

Tahara, S., Yoshida, M., Mizutani, J., Kitamura, C., and Takahashi, S. 1975. A sex stimulant to the male american cockroach in the compositae plants. *Agric. Biol. Chem.* 39: 1517-1518.

Chapter 5

Combined Molecular Mechanics (MM2) and Molecular Orbital (AM1) Study of Periplanone-B and Analogues. Evaluation of Biological Activity from Electronic Properties and Geometries. Part 1

Abstract

Combined molecular mechanics (MM) and semiempirical molecular-orbital (MO) calculations have been applied to the investigation on the conformational and electronic properties of periplanone-B (**1**), a major component of the sex pheromone of American cockroach, and structurally related analogues **2**, **3**, **4** and **5**. In the first step, the geometries of conformers of **1-5** were obtained by MM2 combined a new algorithm for exhaustive generation of ring conformations, CONFLEX2, and an additional set MM2 force-field parameters. The global minimum (**1A**) of the natural pheromone populates predominantly and is superimposable on the X-ray structure. Minor conformers **1B** and **1C** correspond to the rotamers at the isopropyl group of **1A**. The global minimum of the analogue **2** was identified to have a structure **2A**, which agrees well with the X-ray data. The structural comparison of the stable conformers of the analogues **2-5** with **1A** revealed similar ring conformations in the most stable conformers of **2**, **3** and **4**, and the third one of **5**. These results suggest that the ring structure characteristic of the conformer **1A** and the conformer populations must be a significant

factor in the biological activity of these analogues. In the next step, the electronic properties were calculated by the semiempirical MO (AM1) method. A significant correlation is found between the biological activity and one of the unoccupied frontier orbitals which is localized around C1-C10-C9 including the carbonyl and spiro-epoxy groups. A newly defined effective frontier parameter: $EF^{(N)}{}_{(S)}$, which regards the orbital electron density, orbital energy, and ring conformation is found to correlate well with the biological activity of these analogues.

Introduction

The development of computational chemical method for the treatment of the geometrical and electronic indices of biologically active molecules has provided widely used techniques for evaluation of the structure-activity relationships and for designing new analogues.[1-6] By the use of this new method, we have attempted to investigate the conformational properties of some insect pheromones with verification by conventional NMR and X-ray analyses.[7,8]

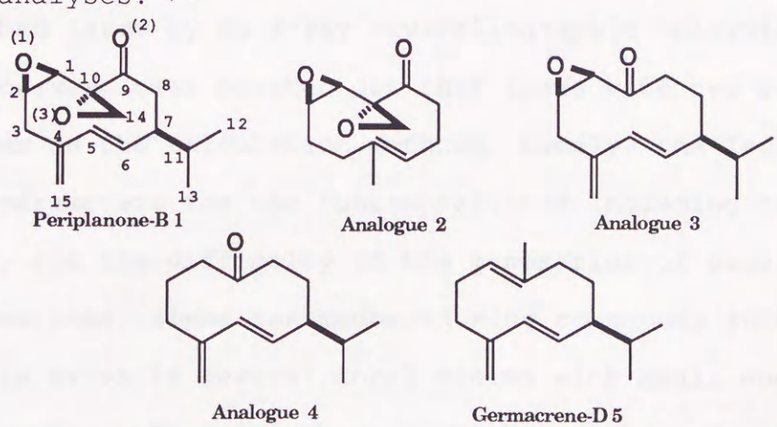

Fig. 1 Structures of periplanone-B (**1**) and analogues **2-5**. The same numbering scheme for the C atoms is employed in this paper as has been used for P-B by Persoons *et al.* (1974).[9]

Periplanone-B (**1**)[9] is the major sex pheromone component produced by female American cockroach (*Periplaneta americana* L.), and has a unique germacrane structure bearing two epoxy functional groups (Fig. 1). The extremely potent activity (threshold 10^{-13}g),[10] was expected to serve as effective controlling agent for this insect pest. However, because of the complexity of the structure, known synthetic procedures are not suitable for industrial production of **1**. We have been investigating the conformational and electronic features of periplanone-B and their analogues in order to obtain useful information for the design of new analogues. A structurally simpler analogue (**2**),[11] provided possibilities of creating more useful analogues. Recent conformational analysis of periplanone-B and its analogues by the use of the X-ray crystallographic and NMR methods suggested a conformational resemblance.[12] Following Still's pioneering work,[13] several applications of MM calculations on periplanones have appeared.[14-16] The predicted static structure of **1**[13] was confirmed later by an X-ray crystallographic analysis.[17] It has, however, been pointed out that there were two serious problems on the calculation methods, namely, the lack of force-field parameters for the functionalities including the epoxy groups, and the difficulty of the generation of possible conformations, since ten-membered ring compounds such as **1**, normally exist in several local minima with small energy differences. To solve these problems, we have developed the new force-field parameters for epoxy group,[18] and employed a

newly developed program, CONFLEX2,[19*] for the exhaustive generation of geometries for ring systems. The conformational analysis of the analogues **4** and **5** by use of CONFLEX2 has been reported.[8]

Furthermore, we have pointed out that the oxygen-containing functionalities of the analogues may play an important role in their biological processes, because their activities decreased with the removal or substitution of these functionalities.[12] Therefore, the relationship between the electronic effects of these functionalities and the observed activity must be noted.

In this study, we carried out complete molecular mechanics analysis of periplanone-B and several analogues by CONFLEX/MM2. The electronic properties of the stable conformers were calculated by means of a semiempirical AM1 method. On the basis of these calculated results, we discussed the correlation of some geometrical and electronic indices with the biological activities of the compounds examined.

---

* CONFLEX2 is based on one of the latest and most effective algorithms, called 'corner flapping', developed for the search of conformational space of cyclic molecules. The program has been carefully tested for a number of cycloalkanes[19] and confirmed, for example, to generate 68 conformers of cycloheptadecane known to exist (in the framework of MM2) within 2 kcal/mol from its global minimum conformation.[20b] Since we consider throughout this work only those conformers having populations higher than 2%, our search in this range is considered to be complete.

Methods and Materials

The preparation and characterization of the compound **1-5** have been described previously.[11,12,20] Their biological activities have been assessed by behavioral tests: the threshold dosages for **1** 10^{-13}g; **2** 10^{-9}g; **3** 10^{-7}g; **4** 10^{-6}g; and **5** 10^{-5}g, and the experimental details have been also reported.[10]

Computational Details.——MM2 program, version '87, was obtained from Molecular Design Ltd.[21] and used for geometry optimization. The new force-field parameters for epoxy functional groups were determined by using the results of *ab initio* calculations on model compounds of periplanone-B and the reported structural data of epoxy compounds.[18] All possible geometries of the ring conformations were generated by CONFLEX2 and optimized by MM2.[19] The Boltzmann population of each energy minimum at 25°C was calculated on the basis of their steric energy.

Average vicinal H-H coupling constants ($^3J_{HH}$) were calculated from 38 energy minima of **1** and 70 of **3** using Altona's empirical modification of the Karplus equation.[22]

The optimized geometries obtained by CONFLEX/MM2 calculations were used as the input data for AM1 (AMPAC version 2.1)[23] calculations for stable conformers, having populations above 1.0%. The total number of the stable conformers calculated are **1**, 7; **2**, 4; **3**, 6; **4**, 12; **5**, 11. Computations were carried out on an IRIS 4D/320GTX workstation (Silicon Graphics). The three-dimentional structures, the frontier orbital extension and superposition of the target molecules were visualized by the use of the QUANTA program (Polygen Co., U.S.A.).

Ultraviolet spectroscopy.--- λ_{max} was evaluated from the population-weighted energy differences between the first excited and the ground state of conformers by taking the configuration interaction (CI) into account.

X-Ray Crystal Structure Analysis of **2**.——A colourless prism crystal of **2** having approximate dimensions of 0.50 x 0.20 x 0.30 mm was mounted on a glass fibre at a temperature of -120 ± 1°C. An experiment at room temperature resulted in sublimation of the crystal. All measurements were made on a Rigaku AFC6R diffractometer with graphite monochromated Mo-$K\alpha$ radiation and a 12 kW rotating anode generator. The crystallographic data for **2**: $C_{12}H_{16}O_3$, formula weight 206.28, monoclinic, $P2_1/c$ (#14); a=12.014(2), b=7.086(2), c=13.586(2)Å, β=112.151(9)°, V=1071.3(4)Å^3, Z=4, D_{calc}=1.291 g/cm^3, $F(000)$=448, $\mu_{(Mo\text{-}K\alpha)}$=0.86 cm^{-1}, $r_{(Mo\text{-}K\alpha)}$=0.71069Å. The structure of **2** was solved by direct methods using DIRDIF[24] and MITHRIL[25] programs. Non-hydrogen atoms were refined anisotropically. Hydrogen atoms were refined isotropically. The final cycle of full-matrix least-squares refinement was based on 1482 observed reflections ($I > 3.00\sigma(I)$) and 201 variable parameters and converged (largest parameters shift was 0.06 times its esd) with unweighted and weighted agreement factors of:

$R = \Sigma||F_o|-|F_c||/\Sigma|F_o| = 0.034$,

$R_w = [(\Sigma w(|F_o| - |F_c|)^2/\Sigma wF_o^2)]^{1/2} = 0.043$.

The standard deviation of an observation of unit weight was 1.81. The weighting scheme was based on counting statistics

and included a factor (p=0.03) to downweight the intense reflections. Fractional non-hydrogen atomic co-ordinates are listed in Table 1, and bond lengths and valence angles of the non-hydrogen atoms in Table 2, respectively. Full lists of bond lengths and bond angles for **2**, together with hydrogen atom coordinated, thermal parameters and tables of least-squares planes, have been deposited at the Cambridge Crystallographic Data Centre.†

Table 1 Fractional non-hydrogen atomic co-ordinates for **2**

Atom	*x*	*y*	*z*
C(1)	0.368 0(2)	0.515 3(3)	0.348 0(1)
C(2)	0.264 4(2)	0.636 1(3)	0.336 5(1)
C(3)	0.136 5(2)	0.573 2(3)	0.296 4(2)
C(4)	0.073 4(2)	0.606 4(3)	0.176 1(2)
C(5)	0.131 3(1)	0.496 1(3)	0.112 5(1)
C(6)	0.126 3(1)	0.308 4(3)	0.111 2(1)
C(7)	0.191 7(2)	0.176 0(3)	0.065 6(1)
C(8)	0.304 9(2)	0.095 7(2)	0.155 3(1)
C(9)	0.376 3(1)	0.258 2(2)	0.219 8(1)
C(10)	0.362 0(1)	0.308 7(2)	0.322 8(1)
C(Me)[a]	0.195 6(2)	0.609 7(3)	0.057 7(2)
O(1)	0.344 8(1)	0.569 6(2)	0.439 88(9)
O(2)	0.443 8(1)	0.352 2(2)	0.192 1(1)
O(3)	0.280 7(1)	0.194 3(2)	0.351 49(9)

[a] Methyl group attached to C(5) position of the ten-membered ring.

† For details of the CCDC deposition scheme, see 'Instructions for Authors.' *J. Chem. Soc., Perkin Trans. 2*, 1992, issue 1.

Table 2 Bond lengths /Å and angles/° involving the non-hydrogen atoms for **2** (esds in parentheses)

Bond length			
C(1)-C(2)	1.470(3)	C(10)-C(1)	1.500(2)
C(2)-C(3)	1.492(3)	C(5)-C(Me)*	1.494(3)
C(3)-C(4)	1.538(3)	C(10)-C(14)	1.468(2)
C(4)-C(5)	1.515(3)	C(1)-O(1)	1.431(2)
C(5)-C(6)	1.332(3)	C(2)-O(1)	1.451(2)
C(6)-C(7)	1.500(3)	C(9)-O(2)	1.214(2)
C(7)-C(8)	1.552(2)	C(10)-O(3)	1.432(2)
C(8)-C(9)	1.504(2)	C(14)-O(3)	1.437(2)
C(9)-C(10)	1.515(2)		
Bond angle			
C(1)-C(2)-C(3)	125.4(2)	C(4)-C(5)-C(Me)[a]	116.2(2)
C(2)-C(3)-C(4)	111.7(2)	C(6)-C(5)-C(Me)[a]	124.2(2)
C(3)-C(4)-C(5)	112.3(2)	O(1)-C(2)-C(3)	118.3(2)
C(4)-C(5)-C(6)	119.6(2)	O(1)-C(2)-C(1)	58.7(1)
C(5)-C(6)-C(7)	127.0(2)	O(1)-C(1)-C(2)	60.0(1)
C(6)-C(7)-C(8)	110.2(1)	O(1)-C(1)-C(10)	116.9(1)
C(7)-C(8)-C(9)	108.4(1)	C(10)-O(3)-C(14)	61.5(2)
C(8)-C(9)-C(10)	118.7(1)	O(3)-C(10)-C(1)	118.0(1)
C(9)-C(10)-C(1)	115.4(1)	O(3)-C(10)-C(9)	116.4(1)
C(10)-C(1)-C(2)	125.3(2)	O(3)-C(10)-C(14)	59.4(1)
C(1)-O(1)-C(2)	61.3(1)	O(3)-C(14)-C(10)	59.1(1)
C(8)-C(9)-O(2)	122.7(1)	C(9)-C(10)-C(14)	116.6(1)
C(10)-C(9)-O(2)	118.6(1)	C(1)-C(10)-C(14)	119.6(2)

[a] Methyl group attached to C(5) position of the ten-membered ring.

Results and discussion

Molecular-mechanics Calculations.——The conformational properties of major conformers over 2% Boltzmann populations at 25°C of **1**, **2** and **3** are summarized in Tables 3, 4 and 5, respectively. The results of **4** and **5** had already been reported.[8]

Table 3 Conformational properties and X-ray data of **1**

	1A	**1B**	**1C**	**1D**	**X-ray**[a]
Ring conformation[b]	[1'333']	[1'333']	[1'333']	[1'333']	[123'1'3']
ΔE_S/kcal mol^{-1}	0.0	0.99	1.35	1.69	
Boltzmann dist.(%) at 25°C	67.90	12.80	7.01	3.95	
Dihedral angle/°					
C(10)-C(1)-C(2)-C(3)	2.4	2.2	2.4	4.7	-1.5
C(1)-C(2)-C(3)-C(4)	-90.1	-91.1	-90.7	-68.3	-90.0
C(2)-C(3)-C(4)-C(5)	74.9	73.2	74.4	20.2	80.0
C(3)-C(4)-C(5)-C(6)	35.1	34.9	33.9	114.6	29.5
C(4)-C(5)-C(6)-C(7)	-167.5	-166.7	-166.6	-169.2	-166.4
C(5)-C(6)-C(7)-C(8)	109.0	113.3	111.6	89.0	110.1
C(6)-C(7)-C(8)-C(9)	-40.4	-43.5	-41.6	-59.7	-40.8
C(7)-C(8)-C(9)-C(10)	92.4	91.1	91.6	87.4	95.6
C(8)-C(9)-C(10)-C(1)	-147.2	-144.2	-145.8	-140.0	-148.9
C(9)-C(10)-C(1)-C(2)	96.4	98.7	97.4	114.9	97.3
C(8)-C(7)-C(11)-H(11)	60.3	-51.6	-177.4	60.4	57.7
C(9)-C(8)-C(7)-C(11)	-163.8	-170.4	-168.2	177.1	-166.4

[a] Data from their X-ray crystallographic analysis of **1**. [b] Modified Dale nomenclature. Primes indicate a pseudo-corner (*g*+ *g*-), ref. 8. 38 energy minima were obtained from 250 initial geometries which were generated by CONFLEX2.

Periplanone-B (**1**). MM analysis on **1** identified four dominant conformers. As can be seen in Figure 2 and Table 3, the three most stable conformers, (**1A, 1B, 1C**), have almost identical twist-chair (TC) ring conformation; they differ only in the rotation of the isopropyl group. The spiro-epoxy carbon (C10) and the transannular alkenic carbon (C5) are closely located. The combined population for **1A-1C** amounts to 88% and in this regard the ten-membered ring of periplanone-B is rather 'rigid'. The calculated ring structure common to these three conformers (**1A, 1B** and **1C**) is superimposable on the experimental X-ray structure[17] (Figure 3).

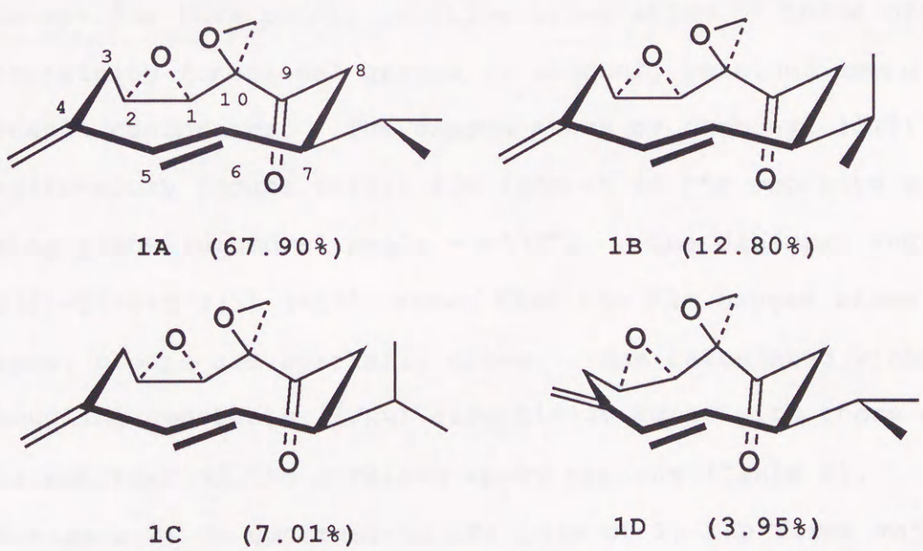

1A (67.90%) **1B (12.80%)**

1C (7.01%) **1D (3.95%)**

Fig. 2 Major conformers of periplanone-B **1**.

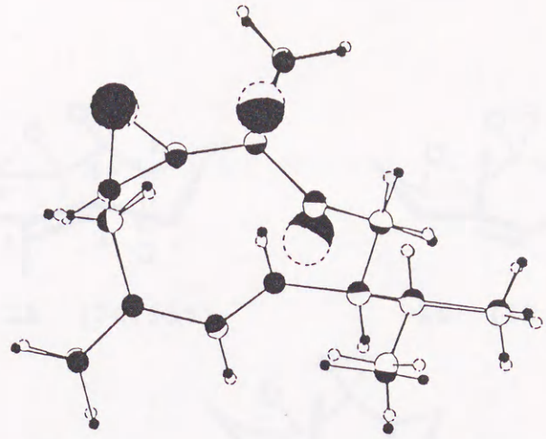

Fig. 3 Superimposition of the global minimum of **1** (**1A**) (filled) and the X-ray structure of **1**

The fourth conformer (**1D**) is given the same ring nomenclatures but has slightly different dihedral angles around C1-C2-C3-C4-C5 from those of the major isomers, as the result of flipping in the exomethylene double bond (Table 3). The dihedral angle of C15-C4-C5-C6 in **1D** (=-61.22°) is about 90° different from those of the three major conformers (*ca.* -154°). Except for this point, relative orientation of three oxygen-containing functional groups is uniquely retained among the stable conformers. The oxygen atoms of carbonyl [O(2)] and of spiro-epoxy groups [O(3)] are located in the opposite sides of ring plane (dihedral angle = -179°). The dihedral angle around O(1)-C1-C10-O(3) (=19°) shows that the two oxygen atoms of the epoxy groups are spatially close. The calculated vicinal H-H coupling constants ($^3J_{HH}$) essentially agree with those observed, except that of the strained epoxy protons (Table 6).

Analogue **2**. In contrast to the case of **1**, the three major conformers have rather different structural features from each other (Figure 4 and Table 4).

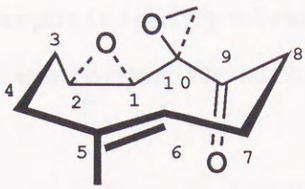

2A (74.91%)

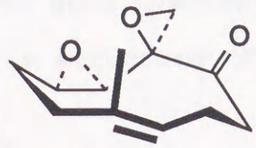

2B (12.46%)

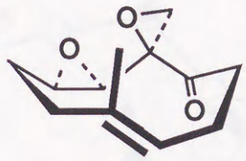

2C (10.76%)

Fig. 4 Major conformers of analogue **2**

Table 4 Conformational properties of **2**

	2A	**2B**	**2C**	**2D**	**X-ray**[a]
Ring conformation[b] [123'1'3']	[1'333']	[232'3']	[3'34]	[2323]	
ΔE_S/kcal mol^{-1}	0.0	1.06	1.15	2.19	
Boltzmann dist.(%) at 25°C	74.91	12.46	10.76	1.84	
Dihedral angle/°					
C(10)-C(1)-C(2)-C(3)	1.2	-0.2	1.1	-2.5	-0.9
C(1)-C(2)-C(3)-C(4)	-90.3	-88.0	-86.3	-98.9	-93.5
C(2)-C(3)-C(4)-C(5)	56.0	60.8	69.9	46.9	61.6
C(3)-C(4)-C(5)-C(6)	72.4	-85.5	-85.6	60.6	66.2
C(4)-C(5)-C(6)-C(7)	-174.6	172.2	174.7	-168.8	171.1
C(5)-C(6)-C(7)-C(8)	95.2	-107.0	-76.1	73.7	99.7
C(6)-C(7)-C(8)-C(9)	-46.1	68.7	-46.1	66.5	-51.3
C(7)-C(8)-C(9)-C(10)	89.8	-77.5	84.1	-74.4	98.0
C(8)-C(9)-C(10)-C(1)	-142.5	-20.1	-116.7	-41.7	-144.2
C(9)-C(10)-C(1)-C(2)	104.8	118.7	119.5	117.8	103.9

[a] Data from the X-ray crystallographic analysis of **2**. [b] Modified Dale nomenclature. Prime sign means a pseudo-corner (*g*+ *g*-), ref. 8. Nine energy minima were obtained from 60 initial geometries which were generated by CONFLEX2.

Superpositioning clearly showed good overlap of the most stable conformer **2A** with the X-ray structure (Figure 5).

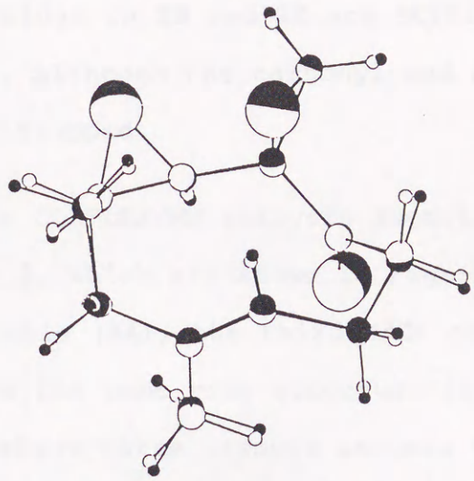

Fig. 5 Superimposition of the global minimum of **2** (**2A**) and the X-ray structure of **2**

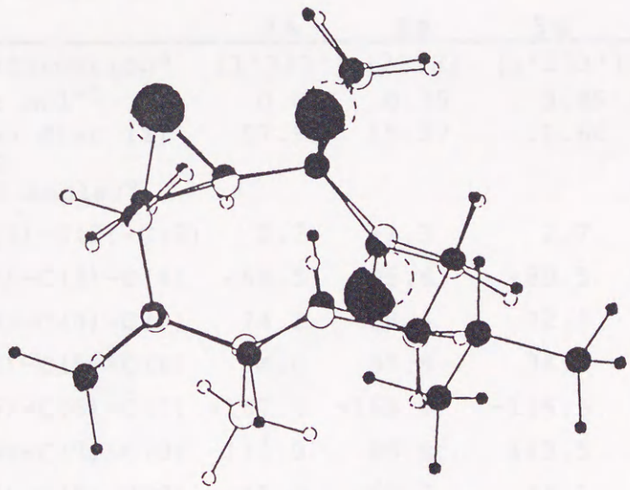

Fig. 6 Superimposition of the global minimum of **2** (**2A**) and of **1** (filled)

The conformer **2A** with 74.91% population has a ring conformation very similar to that of **1A** as shown in Figure 6. Hence it is shown that the removal of isopropyl and exomethylene groups from **1** does not change on the ring conformational behaviour, as far as the global energy-minimum structure is

concerned. The ring conformations of other conformers are significantly different. However, the relative orientations of the two epoxy rings in **2B** and **2C** are still conserved as in the best conformer, although the carbonyl and methyl groups in these conformers are flipped.

Analogue **3**. The CONFLEX/MM analysis identified five stable conformers for **3**, which are shown in Figure 7 and Table 5.

The most stable (**3A**), the third (**3C**) and the fourth (**3D**) conformers have the same ring structure as **1A**. The combined population of these three isomers amounts to 75%.

Table 5 Conformational properties of **3**

	3A	**3B**	**3C**	**3D**	**3E**
Ring conformation[a]	[1'333']	[2323]	[1'333']	[1'333']	[1'3'2'4']
ΔE_S/kcal mol^{-1}	0.0	0.79	0.95	1.36	1.93
Boltzmann dist.(%) at 25°C	57.98	15.37	11.66	5.83	2.23
Dihedral angle/°					
C(10)-C(1)-C(2)-C(3)	2.7	-1.3	2.7	2.8	-0.1
C(1)-C(2)-C(3)-C(4)	-88.5	-95.6	-89.5	-89.2	9.8
C(2)-C(3)-C(4)-C(5)	74.2	58.4	72.9	73.6	-68.2
C(3)-C(4)-C(5)-C(6)	34.0	37.9	34.3	33.3	146.4
C(4)-C(5)-C(6)-C(7)	-167.4	-165.5	-166.5	-166.5	-161.3
C(5)-C(6)-C(7)-C(8)	110.0	86.0	113.5	112.7	87.7
C(6)-C(7)-C(8)-C(9)	-41.0	63.7	-44.1	-42.7	-49.4
C(7)-C(8)-C(9)-C(10)	80.5	-64.0	80.5	80.6	76.8
C(8)-C(9)-C(10)-C(1)	-152.7	-62.0	-150.7	-151.4	-162.2
C(9)-C(10)-C(1)-C(2)	111.6	127.7	113.0	112.3	102.7
C(8)-C(7)-C(11v-H(11)	61.1	63.4	-51.3	-177.5	60.8
C(9)-C(8)-C(7)-C(11)	-164.8	-60.5	-171.5	-169.7	-172.8

[a] Modified Dale nomenclature. Prime sign means a pseudo-corner (*g*+ *g*-), ref. 8. 73 energy minima were obtained from 527 initial geometries which were generated by CONFLEX2.

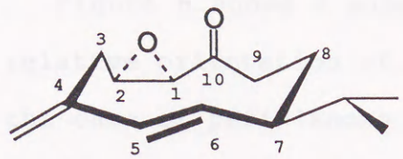

3A (57.98%)

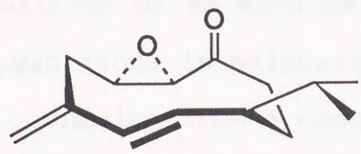

3B (15.37%)

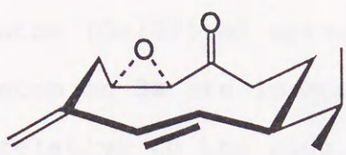

3C (11.66%)

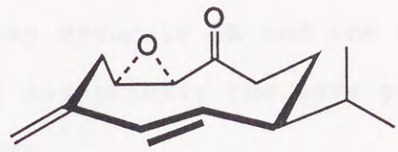

3D (5.83%)

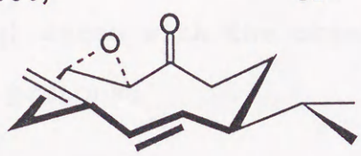

3E (2.23%)

Fig. 7 Major conformers of analogue **3**

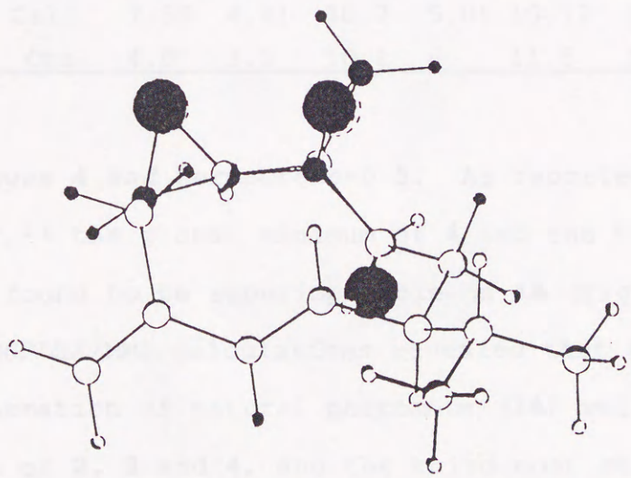

Fig. 8 Superimposition of the global minimum of **3** (**3A**) and of **1** (**1A**) (filled)

Figure 8 shows a superposition of **3A** with **1A**. Again, the relative orientation of oxygen atoms is maintained as found in the case of periplanone-B. Judging from a comparison of dihedral angles along the C7-C8-C9-C10-C1 region of the ring in **3A** with those in **1A**, it should be pointed out that the oxygen atom [O-(3)] of spiro-epoxy group in **1A** and the carbonyl oxygen atom in **3A** are located at essentially the same positions relative to the ring planes.

As shown in Table 6, the calculated vicinal H-H coupling constants ($^3J_{HH}$) agree with the observed, except those of the strained epoxy protons.

Table 6 Comparison of the observed vicinal NMR coupling constants with calculated values for proton on **1** and **3**

		J/Hz							
compound	1-2	2-3α	2-3β	7-8α	7-8β	8α-9α	8β-9α	8α-9β	8β-9β
1 Calc.	7.75	4.83	10.78	5.15	11.48				
Obs.	4.0	4.0	10.2	5.7	11.0				
3 Calc.	7.59	4.41	10.7	5.05	10.12	1.00	11.32	8.54	0.97
Obs.	4.0	3.5	10.1	-	11.5	1.1	12.5	6.5	1.2

Analogue **4** *and Germacrene-D* **5**. As reported in our previous paper,[11] the global minimum of **4** and the third conformer of **5** were found to be superimposable on **1A** (Figures 9 and 10).

CONFLEX/MM2 calculations revealed that the global minimum conformation of natural pheromone (**1A**) well overlapped with those of **2**, **3** and **4**, and the third most stable conformation of **5**. One attractive hypothesis would be to assume that activity of a periplanone-B analogue is related to the total population

of the conformers having the ring conformation superimposable on that of the global minimum of **1**. CONFLEX/MM2 study suggests that the ring conformation of **1A** is the biologically important structure.

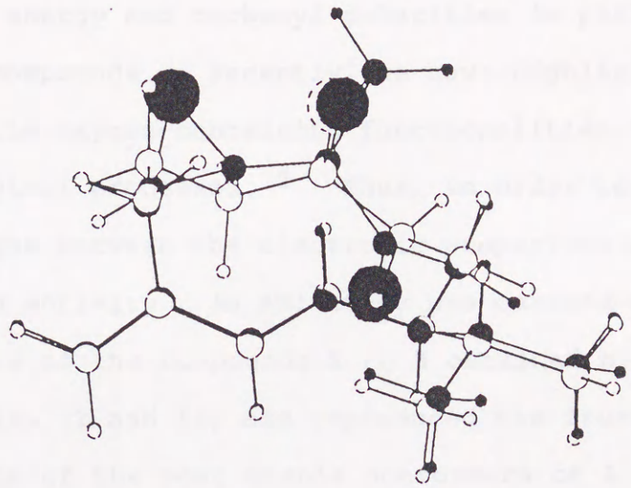

Fig. 9 Superimposition of the global minimum of **4** and of **1** (**1A**) (filled)

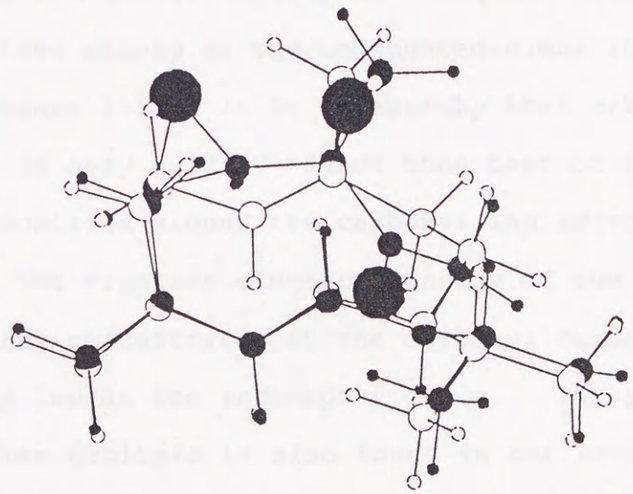

Fig. 10 Superimposition of the third conformer of **5** and the global minimum of **1**(**1A**)(filled)

Molecular-orbital calculations.——Several studies, which have attempted to correlate the electronic structure, especially frontier orbitals, with biological activity, have been reported.[2-4] M. N. Ramos and B. B. Neto[3] reported least-squares fits show a correlation between hypolipidemic activities and LUMO energy and carbonyl polarities in phthalimide and related compounds. Recently, we have highlighted an important role of the oxygen-containing functionalities of the analogues in biological processes.[12] Thus, in order to investigate the correlation between the electronic properties and their pheromone activity , an AM1 study was carried out on the stable conformers of the compounds **1** to **5** obtained by CONFLEX/MM2. In Figures 11, 12 and 13, are reproduced the frontier-orbital extensions of the most stable conformers of **1**, **2** and **3**, respectively.

Periplanone-B (**1**). Both the highest occupied molecular orbital (HOMO) and the lowest unoccupied molecular orbital (LUMO) of **1A** are localized mainly at the conjugated-diene (C15-C4-C5-C6) moiety (Figure 11). It is noteworthy that orbital energy of next-LUMO is only 0.12 eV higher than that of LUMO. The next-LUMO is localized around the carbonyl and adjacent spiro-epoxy groups. The frontier electron density of the next-LUMO is particularly concentrated at the carbonyl carbon atom, but relatively low at the *endo*-epoxy group. The same feature of the frontier orbitals is also found in the second (**1B**) and the third (**1C**) stable conformers. In the forth conformer (**1D**), whose ring structure is slightly different from those of the

three most stable conformers as the result of flipping of exo-methylene group, the LUMO is localized at the carbonyl and spiro-epoxy moiety, and the next-LUMO exists at the conjugated diene moiety (C15-C4-C5-C6).

Analogue **2**. As shown in Figure 12, the HOMO and next-LUMO of the most stable conformer of **2** are localized around the double-bond moiety at C5-C6. In this case, LUMO is localized at the carbonyl and spiro-epoxy moiety, whose extension resembles that of the next-LUMO of **1A**. The orbital-energy gap between the LUMO and next-LUMO is larger than that found in **1A**. In other conformers of **2**, the features of frontier orbitals are essentially the same as those in the most stable conformer.

Analogue **3**. In Figure 13, it can be seen that the HOMO and LUMO of the global minimum of **3** are distributed around the diene moiety as are those of **1A**. The next-LUMO is localized mainly around the carbonyl functional group [C(10)-O(3)]. The energy difference between the two unoccupied frontier orbitals is about 0.4 eV in the global minimum of **3**.

Analogue **4**. In all stable conformers of **4**, the extension of the HOMO and LUMO essentially resembles that of the global minimum of **3**. The frontier electron density of next-LUMO is concentrated at the carbonyl carbon atom. A rather large energy difference (0.7 eV) between the two unoccupied frontier orbitals (LUMO; 0.441 eV, next-LUMO; 1.171 eV) is found in the global minimum of **4**.

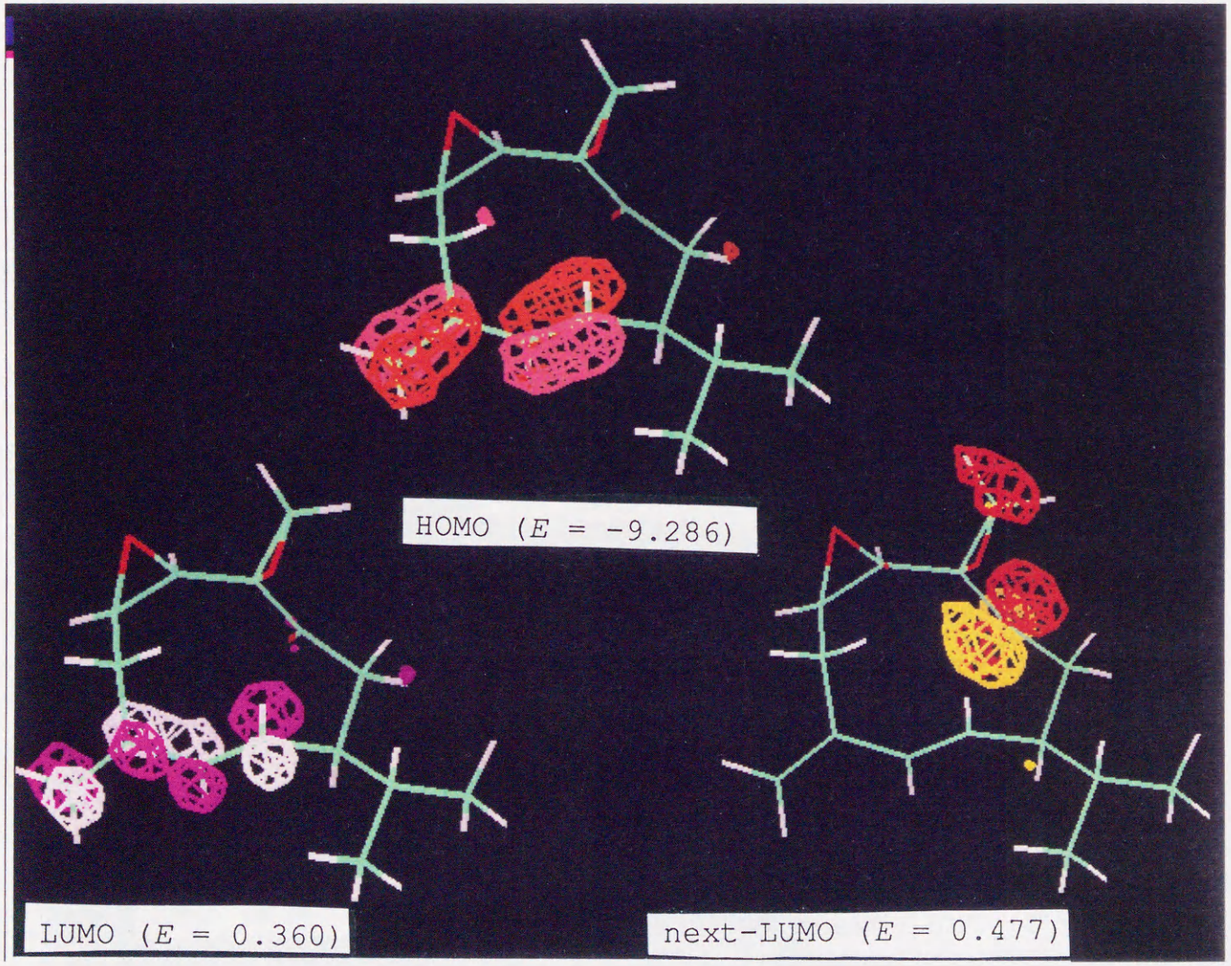

Fig. 11 Frontier orbital of the global minimum of **1**; the value of each frontier orbital energy (*E*/eV) is shown in each parethesis

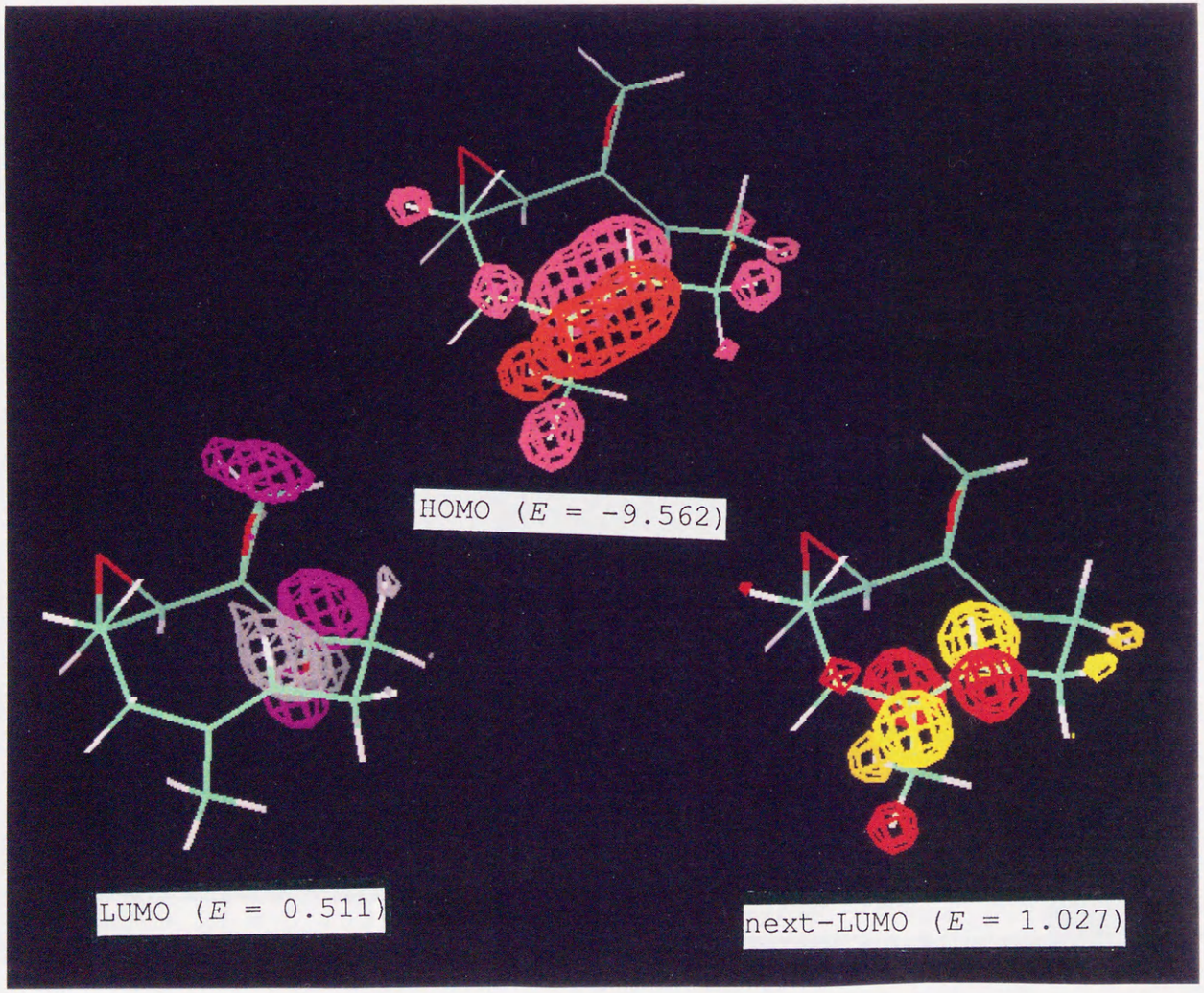

Fig. 12 Frontier orbital of the global minimum of **2**; the value of each frontier orbital energy (*E*/eV) is shown in each parethesis

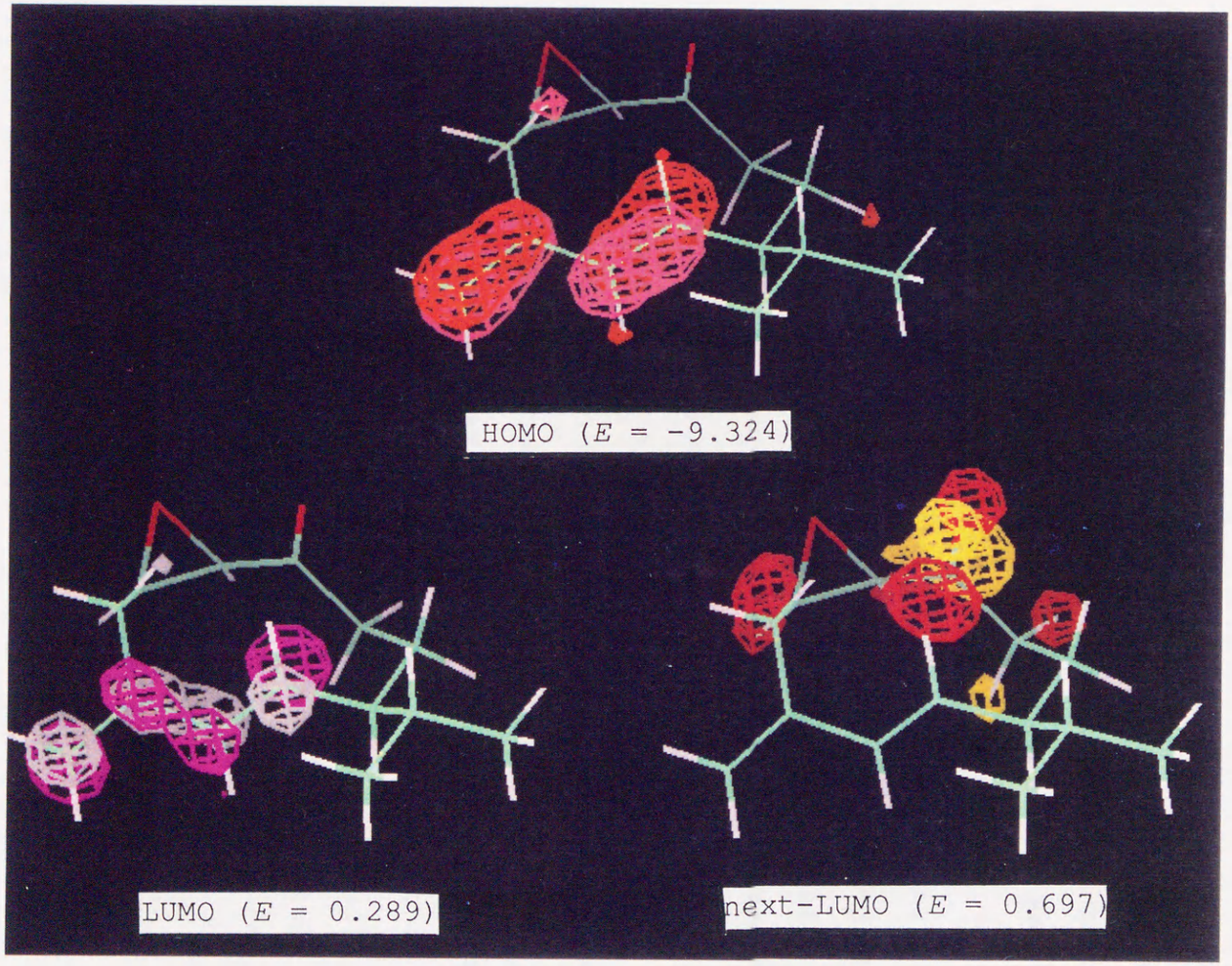

Fig. 13 Frontier orbital of the global minimum of **3**; the value of each frontier orbital energy (E/eV) is shown in each parethesis

Germacrene-D **5**. In all stable conformers of **5**, the extension of the HOMO and LUMO is similar to that of **1A**. The next-LUMO is localized at the double bond [C(10)-C(1)].

The distribution of the LUMO and next-LUMO on the ten-membered ring systems in compounds **1-5**, can be classified into two groups. In the first group, unoccupied frontier orbitals are localized mainly at the C9-C10-C1 region of the ten-membered ring, extending to the carbonyl and spiro-epoxy groups of **1**, **2**, **3** and **4**, and to the double bond of **5**. In the second group, they are localized at the C15-C4-C5-C6 region of ten-membered ring, which covers the diene part of **1**, **3**, **4** and **5**, and the double bond of **2**. As the former unoccupied frontier orbital is localized around the 'upper' part of ten-membered ring in the structural formula, we call it the frontier unoccupied orbital around upper part of ten-membered ring (abbreviated as $FUMO_{upper}$). In the same manner, the latter unoccupied frontier orbital is called the frontier unoccupied orbital around lower part of ten-membered ring (abbreviated as $FUMO_{lower}$).

Theoretical Aspect.——In order to take into account of the contribution of every stable conformer whose Boltzmann population is larger than 1% at 25°C, total energy and orbital energy are both population-weighted for the discussion. The reliability of the AM1 calculations on periplanone-B (**1**) and analogues was confirmed by comparison of the calculated (=224.4nm) and observed (=225.4nm) λ_{max} value of **1**. The population-weighted frontier-orbital energies of HOMO, $FUMO_{lower}$ and $FUMO_{upper}$ of **1-5** are shown in Table 7.

Table 7 Population-weighted frontier orbital energy (eV), $EF^{(N)}$, $EF^{(N)}{}_{(s)}$, and biological activity of compounds

compound	HOMO (eV)	$FUMO_{lower}$[a] (eV)	$FUMO_{upper}$[b] (eV)	$EF^{(N)}$	$EF^{(N)}{}_{(s)}$	Biological activity[c]
(1)	-9.290	0.386	0.470	4.225	3.634	-13
(2)	-9.555	1.022	0.511	3.994	3.011	-9
(3)	-9.330	0.311	0.693	2.792	2.069	-7
(4)	-9.014	0.522	1.077	1.549	0.789	-6
(5)	-8.632	0.688	1.261	1.413	0.376	-5

[a]frontier unoccupied orbital around upper part of ten-membered ring. [b]frontier unoccupied orbital around lower part of ten-membered ring. [c]effective frontier parameter. [d]$\log_{10}$[threshold(g)]

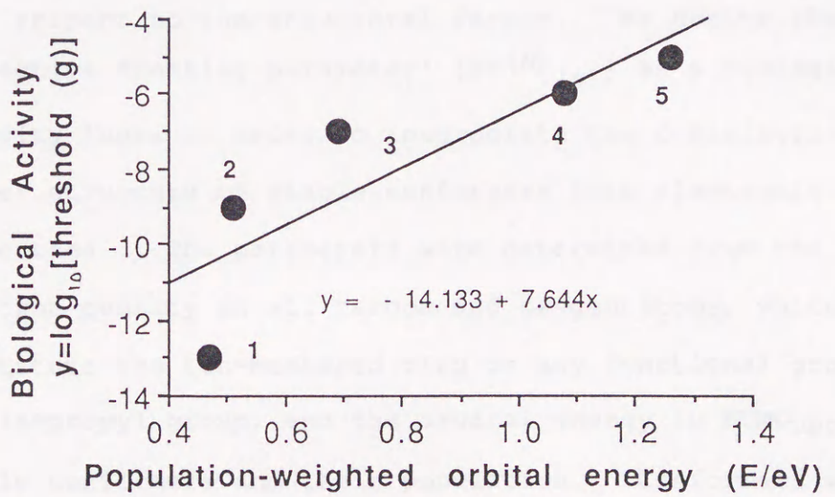

Fig. 14 Relation between biological activities and population-weighted orbital energy of $FUMO_{upper}$. (R = 0.849, σ = 1.93, t statistic = 2.78 and n = 5) The number of compounds shows the acitvity level of them.

In general, population-weighted orbital energy of $FUMO_{lower}$ (localized at diene moiety) is lower than that of $FUMO_{upper}$ (localized at spiro-epoxy and carbonyl groups) except for the case of **2**. The small energy gap between $FUMO_{lower}$ and $FUMO_{upper}$ of **1** is noteworthy. In the frontier orbitals, only the population-weighted energy of $FUMO_{upper}$ shows good correlation with the biological activity (R = 0.849, Figure 14), those of HOMO and $FUMO_{lower}$ do not show linear relationship.

Effective Frontier Parameter $[EF^{(N)}{}_{(s)}]$.——Since the MM study indicated that the ring conformation is important for biological activity of periplanone analogues, the correlation between biological activity and electronic indices was further examined with respect to the structural factor. We derive the 'effective frontier parameter' $[EF^{(N)}{}_{(s)}]$ as a biological activity index in order to incorporate the contribution of the proper structure of stable conformers into electronic properties. The parameters were determined from the frontier electron density on all carbon and oxygen atoms, which constitute the ten-membered ring or any functional groups except the isopropyl group, and the orbital energy in $FUMO_{upper}$ of stable conformers and their population. Conformers whose population at 25°C is above 1.0% were taken into account for the calculation of 'effective frontier parameter'. It is defined as shown in eqns. (1)-(3)

$$f_r{}^{(N)} = 2C^2{}_{r(FUMOupper)} \qquad (1)$$

$$Ef_r(N) = \Sigma \{ f_r(N)\mu / E(\text{FUMOupper})\mu \} \times \text{Pop}\mu \qquad \mu = 1 \text{ to } M \quad (2)$$

$$EF(N) = \Sigma \{ Ef_r(N) \} \qquad r = 1 \text{ to } R \quad (3)$$

where,

$f_r(N)$ is the frontier electron density in $FUMO_{upper}$ of atom r, r is the atom number (excepting protons), R is the total number of atoms considered, μ is the number of local minima, M is the total number of local minima, $E_{FUMOupper}$ is the frontier orbital energy of $FUMO_{upper}$ (eV), and Pop is the population of each local minimum at 25°C.

First, the frontier electron density of atom r on $FUMO_{upper}$ is calculated [$f_r(N)$]. Then, $f_r(N)$ is divided by its own orbital energy ($E_{FUMOupper}$), and averaged by Boltzmann population (Pop) ($Ef_r(N)$). $EF(N)$ is the sum of $Ef_r(N)$ of all non-hydrogen atoms considered. The correlation between activities and $EF(N)$ of all **1-5** compounds was examined. $EF(N)$ is supposed to reflect population-weighted total contribution of electronic effects. In Figure 15, biological activity *vs.* $EF(N)$ is plotted. A better linear correlation (R = 0.899) than that of the plot of biological activity *vs.* population-weighted frontier orbital energy of $FUMO_{upper}$ (Figure 14) was found.

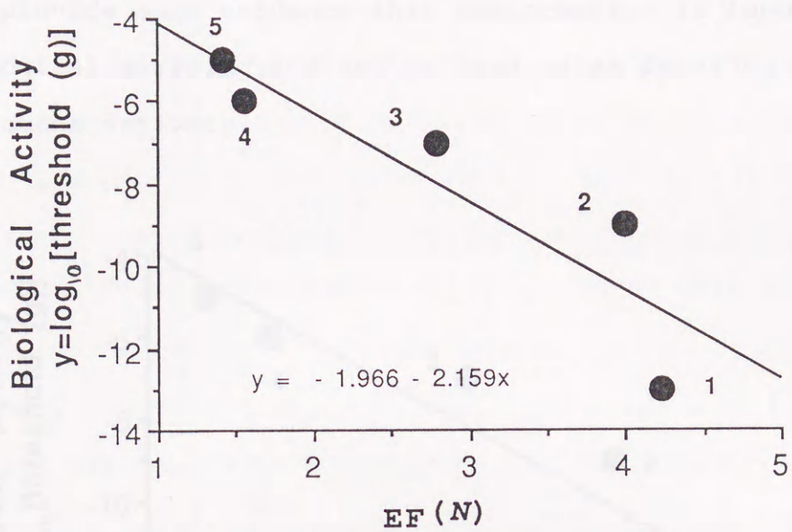

Fig. 15 Relation between biological activities and value of $EF^{(N)}$ of compounds. (R= 0.899, σ = 1.60, t statistic = 3.56 and n = 5)

Next, we calculate the effective frontier parameter $EF^{(N)}{}_{(s)}$ by taking into account of the contribution of the ring structure. The effective frontier parameter $EF^{(N)}{}_{(s)}$ is hence defined as eqns. (4)and (5) where, A is the structure factor;1 , the ring conformation is well superimposable on that of X-ray structure of **1**; 0, the conformation is not superimposable.

$$Ef_r{}^{(N)}{}_{(s)}=\Sigma\{f_r{}^{(N)}\mu/E(\mathrm{FUMOupper})\mu\} \times \mathrm{Pop}\mu \times A \qquad \mu=1-M \qquad (4)$$

$$EF^{(N)}{}_{(s)}=\Sigma\{Ef_r{}^{(N)}{}_{(s)}\} \qquad r=1-R \qquad (5)$$

The effective frontier parameter $EF^{(N)}{}_{(s)}$ correlates with biological activity (R = 0.929) as shown in Figure 16. This correlation indicates that the ring conformation, which is found in the global minimum of **1-4** and the third most stable conformer

of **5**, should be better maintained in order to improve the biological activity. The effective frontier parameter $EF^{(N)}_{(S)}$ may provide some evidence that conformation is important to biological activity and can be used as an index to evaluate pheromone activity.

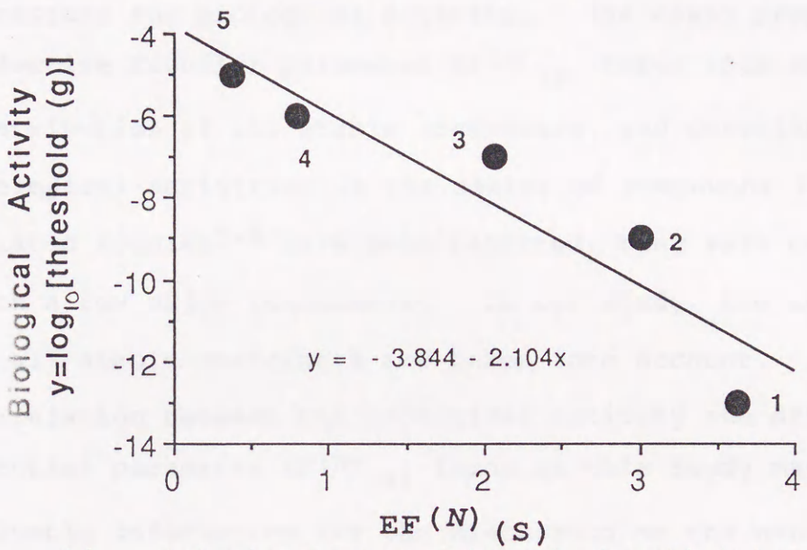

Fig. 16 Relation between biological activities and value of $EF^{(N)}_{(S)}$ of compounds. (R=0.929, σ = 1.35, t statistic = 4.35 and n = 5)

Conclusion

Detailed structural information of stable conformers of periplanone-B (**1**) and their analogues **2**-**5** obtained by CONFLEX/MM2 are compared. The validity of the calculated results was confirmed by comparison with X-ray crystallographic and NMR results.

The biological activity of **1** and analogues **2**-**5** can be explained as the combined effect of electronic properties and

geometries of stable conformers. In the present case, the unoccupied frontier orbital localized mainly around C9-C10-C1-C2 including carbonyl and spiro-epoxy groups ($FUMO_{upper}$) is important for biological activity. It seems that the proper ring structure and the relative orientation of carbonyl and epoxy groups, which are observed in X-ray studies of **1**, are necessary for biological activity. The newly proposed effective frontier parameter $EF^{(N)}{}_{(S)}$ takes into account of the contribution of all stable conformers, and correlates well with biological activities in the series of compounds **1-5**. Although related studies[1-6] have been reported, they were concerned only with a few major conformers. In our study, the contributions of all stable conformers are taken into account. This correlation between the biological activity and effective frontier parameter $EF^{(N)}{}_{(S)}$ found in this study may provide valuable information for the discussion on the nature of pheromone recognition system of insects.

References

1 T. Liljefors, B. Thelin, J. N. C. Pers and C. Löfstedt, *J. Chem. Soc., Perkin Trans. 2,* 1985, 1957.

2 A. T. Maynard, L. G. Pedersen, H. S. Posner, and J D. McKinney, *Molecular Pharmacology,* 1986, **29**, 629.

3 M. N. Ramos, and B. B. Neto, *J. Comp. Chem.*, 1990, **11**, 569.

4 A. K. Debnath, R. L. L. Compadre, G. Debnath, A. J. Shusterman, and C. Hansch, *J. Med. Chem.*, 1991, **34**, 786.

5 B. Waszkowycz, I. H. Hiller, N. Gensmantel, and D. W. Payling, *J. Chem. Soc., Perkin Trans. 2*, 1991, 225.

6 M. Froimowitz, and S. Rämsby, *J. Med. Chem.*, 1991, **34**, 1707.

7 T. Chuman, K. Shimazaki, M. Mori, K. Okada, H. Gotō, E. Ōsawa, K. Sakakibara, and M. Hirota, *J. Chemical Ecology*, 1990, **16**, 2877.
8 (*a*) K. Shimazaki, M. Mori, K. Okada, T. Chuman, H. Gotō, E. Ōsawa, K. Sakakibara, and M. Hirota, *J. Chemical Ecology*, 1991, **17**, 779.
8 (*b*) H. Gotō, *Tetrahedron*, 1992, **48**, 7131.
9 C. J. Persoons, F. J. Ritter, and W. J. Lichtendonk, *Proc. Kon. Ned. Akad. Wetensch. Amsterdam*, 1974, **C77**, 201 (*Chem. Abstr.* **81**, 88-209f); for a review on American cockroach sex pheromone, see: C. J. Persoons, F. J. Ritter, P. E. J. Verwiel, H. Hauptmann, and K. Mori, *Tetrahedron Lett.*, 1990, **31**, 1747, and references cited therein.
10 K. Okada, M. Mori, K. Shimazaki, and T. Chuman, *J. Chemical Ecology*, 1991, **17**, 695.
11 M. Mori, K.Okada, K. Shimazaki, and T. Chuman, *Tetrahedron Lett.*, 1990, **31**, 4037.
12 M. Mori, K. Okada, K. Shimazaki, T. Chuman, S. Kuwahara, T. Kitahara, and k. Mori, *J. Chem. Soc., Perkin Trans. 1*, 1990, 1769.
13 W. C. Still, *J. Am. Chem. Soc.*, 1979, **101**, 2493.
14 Y. Shizuri, S. Yamaguchi, Y. Terada, and S. Yamamura, *Tetrahedron Lett.*, 1987, **28**, 1791.
15 T. Takahashi, Y. Kanda, H. Nemoto, K. Kitahara, J. Tsuji, and Y. Fukazawa, *J. Org. Chem.*, 1986, **51**, 3394.
16 T. Takahashi, T. Doi, and H. Nemoto, *J. Synthetic Organic Chemistry, Japan*, 1989, **47**, 135.
17 H. Hauptmann, G. Mühlbauer, and N. P. C. Walker, *Tetrahedron Lett.*, 1986, **27**, 1315.
18 K. Sakakibara, M. Hirota, K. Shimazaki, and T. Chuman, in preparation for *J. Chem. Soc., Perkin Trans. 2.*
19 H. Gotō, and E. Ōsawa, *J. Am. Chem. Soc.*, 1989, **111**, 8950.
20 (*a*) T. Kitahara, M. Mori, K. Koseki, and K. Mori, *Tetrahedron Lett.*, 1986, **27**, 1343; (*b*) T. Kitahara, M. Mori, and K. Mori, *Tetrahedron* 1987, **12**, 2689.

21 U. Burkert, and N. L. Allinger, *Molecular mechanics*, ACS Monograph 177, American Chemical Society, Washington, DC, 1982.
22 (*a*) C. A. G. Haasnoot, F. A. A. M. de Leeuw, and C. Altona, *Tetrahedron*, 1980, **36**, 2783; (*b*) S. Masamune, P. Ma, R. E. Moore, T. Fujiyoshi, C. Jaime, and E. Ōsawa, *J. Chem. Soc., Chem. Commun.* 1986, 261.
23 *QCPE* Program No. 506, AMPAC version 2.1
24 P. T. Beursken, DIRDIF, *Direct Methods for Difference Structures - an Automatic Procedure for Phase Extension and Refinement of Difference Structure Factors*, Technical Report 1984/1, Crystallography Laboratory, Toernooiveld, 6525 Ed Nijmegen, Netherlands.
25 C. J. Gilmore, MITHRIL, *An Integrated Direct Methods Computer Program*, University of Glasgow, Scotland; see also *J. Appl. Crystallogr.*, 1984, **17**, 42.

Chapter 6

Combined Molecular Mechanics (MM2) and Molecular Orbital (AM1) Study of Periplanone-A and Analogues. Evaluation of Biological Activity from Electronic Properties and Geometries part 2

Abstract

Combined molecular mechanics (MM) and semiempirical molecular orbital (MO) calculations have been applied on periplanone-A (**1**), the epoxy epimer (**2**) and a structurally-related analogue (**3**). Conformational properties of these compounds have been obtained by the use of MM2 with an additional set of force-field parameters in conjunction with an automatic conformation generating program. The global minimum **1A** has the same type of ring conformation as that found in periplanone-B (**4**). The remarkable contrast between **1** and **4** is the presence in **1** of significant amounts of conformers having different ring conformations such as **1B**. In both **2** and **3**, which are far less biologically active than **1**, **1A** ring type conformers exist only in low populations. The conformer distribution of **2** obtained by MM2 well explains the highly complex NMR (2D-NOESY) spectrum. The MM-predicted geometries of the stable conformers of **3** show good agreements with that observed in dynamic NMR spectroscopy. When the **1B** ring type conformers are taken into account, the accuracy of the previously proposed index for the

evaluation of the pheromone activity of analogues, effective frontier parameter $EF^{(N)}{}_{(S)}$, is improved.

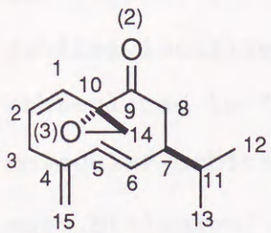

Periplanone-A 1

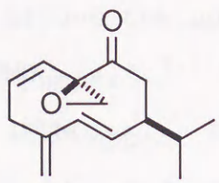
epoxy epimer 2

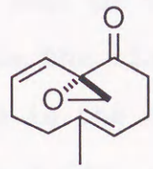
Analogue 3

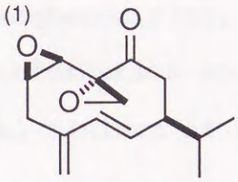

Periplanone-B 4

Introduction

Periplanones-A (**P-A, 1**)[##,1,2] and -B (**P-B, 4**)[3,4] are the sex pheromone components of the American cockroach (*Periplaneta americana* L.). Their unique structural features and potent biological activity (threshold: 10^{-11}g for **1**; 10^{-13}g for **4**, assessed by behavioral tests)[5] have attracted much attention from many organic chemists. To reveal the structural requirements for the biological activity of periplanones, we have been studying the conformational and electronic properties of these pheromones by a combination of X-ray analyses, NMR measurements, MM and MO-calculations[6,7] and bioassay.[5] MM analysis on the periplanone-type compounds was made possible by the development of additional force field parameters and by the new program CONFLEX2 which exhaustively generates low energy conformers. In our previous paper, we described how the biological activities of **P-B** (**4**) and

---

[##] The same numbering scheme for the carbon atoms as has been used for **1** by Persoons *et al.*[3] is employed in this paper.

some structurally-related analogues (**5-8**) depended closely on the total population of conformers having the same ring conformation as the global minimum of **4** and on their frontier unoccupied molecular orbital localized around the upper part of ten-membered ring, abbreviated to '$FUMO_{upper}$'.[7] Since the ring conformation and molecular orbital ($FUMO_{upper}$) found in the global minimum of the most biologically active **P-B** (**4**) could be regarded as the biologically relevant ones, we proposed a new index for the prediction of biological activity of periplanone-analogues, called effective frontier parameter $EF^{(N)}{}_{(S)}$. It includes the contribution of the electron density and orbital energy in $FUMO_{upper}$ of all of the stable conformers and the ring structure of biologically important conformers. $EF^{(N)}{}_{(S)}$ is defined as shown in eqns. (1)-(3).

$$f_r{}^{(N)} = 2C^2{}_{r(FUMOupper)} \tag{1}$$

$$Ef_r{}^{(N)}{}_{(S)} = \Sigma\{f_r{}^{(N)}\mu / E_{(FUMOupper)\mu}\} \times Pop\mu \times A \qquad \mu = 1 \sim M \tag{2}$$

$$EF^{(N)}{}_{(S)} = \Sigma\{Ef_r{}^{(N)}{}_{(S)}\} \qquad r = 1 \sim R \tag{3}$$

where, $f_r{}^{(N)}$ is the frontier electron density in $FUMO_{upper}$ of atom r, r is the atom number (excepting protons), R is the total number of atoms considered, μ is the number of local minima, M is the total number of local minima, $E_{FUMOupper}$ is the frontier orbital energy of $FUMO_{upper}$ (eV), Pop is the population of each local minimum at 25°C, and A is the structure factor: 1, the ring conformation is well superimposable on that of global minimum of **4**; 0, the conformation is not superimposable. The biological activity

and $EF^{(N)}_{(S)}$ of **P-B** (**4**) and compounds **5-8** showed a good linear relation as in eqns. (4),

$$\log_{10}[\text{Activity threshold(g)}] = -3.844 - 2.104 \times EF^{(N)}_{(S)} \quad (4)$$

(R = 0.929, σ= 1.35, F = 18.89, SE = 0.48, t_{static} = 4.35 and n = 5).[7]

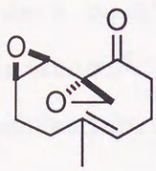

5

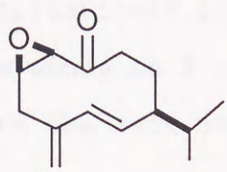

6

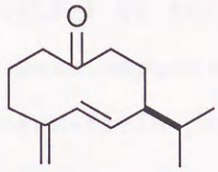

7

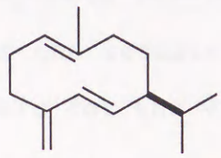

Germacrene D8

Another natural pheromone **P-A** was first isolated and characterized along with **P-B** by Persoons *et al.* in 1974.[3] However, because of the very minute amount and instability of the isolated sample, the structural elucidation remained unsettled for a long time. In 1986, Hauptmann *et al.* independently isolated **P-A** from female American cockroach and proved synthetic **1** to have high pheromone activity.[1] The epoxy epimer (**2**) has also been proposed to be the structure of **P-A** by Macdonald.[8] Recently, the structure of **P-A** has been established to be **1** by the synthesis of both **1** and **2**, coupled with the X-ray crystallographic analysis of **1**.[2] The bioassy of **2** shows a drastic reduction of the biological activity (threshold: 10^{-7}g).[5,6] In the meantime, a structurally-simplified analogue (**3**) was synthesized with the expectation of strong biological activity by the analogy with the highly active analogue **5** (threshold: 10^{-9} g), but **3** showed no significant biological activity even at a dose of 10^{-5} g.[5]

The reduction of the biological activities of **1**, **2** and **3** from that of **4** is considered to be due to the changes in the steric and electronic factors. Thus, it was deemed valuable to reveal these properties of **1**, **2** and **3** for the improvement of structure-activity relationship. Although the X-ray and NMR data had been reported, data on the conformational properties of these compounds remained scarce.[6] An MM study on **1** has been reported, but the results are unreliable due to the lack of force-field parameters for the vinyl-epoxy group.[9]

In this study, the quantitative evaluation of the conformer distribution of **1**, **2** and **3** has been performed by the MM calculations with newly developed force-field parameters, and the electronic properties of the stable conformers calculated with a semiempirical molecular orbital (AM1) method.[10] On the basis of this information, we discuss structural characteristics of **1**, **2**, and **3** by comparison with those of **P-B** and analogues, and examine the validity of $EF^{(N)}{}_{(S)}$ as an index to evaluate their pheromone activity in comparison with their experimental bioassay.

Experimental

Preparation and characterization of compounds **1-3** have been described previously.[6,11] Their biological activities were assessed by behavioural tests.[5]

Computational Details.——Force-field parameters. New parameters for vinyl-epoxy functional group were estimated by fitting to the results of *ab initio* calculations using GAUSSIAN 90[12] on model

compounds 2-vinyloxirane (**A**), 2-allyoxirane (**B**) and 2-acetyl-2-vinyloxirane (**C**) at MP2/6-31G*//HF/6-31G* level on an IBM power station R6000/550.[13] A new parameter set is summarized in Table 1.

Table 1 newly developed force-field parameters for vinyl-epoxy compounds

(*a*) Bending Parameters

Angle type	kb/mdyn Å rad^{-2}	θ_0/deg
<2-73[a]-49[b]	0.883	117.167
<2-73-3	0.499	117.300

(*b*) Torsional Parameters

Dihedral angle type	V1	V2	V3
2-2-73-49	0.088	3.044	-1.392
5-2-73-49	0.000	0.000	0.010
2-73-49-73	-0.160	-0.260	0.140
2-73-73-49	-0.186	-0.180	0.432
2-73-49-20	0.000	0.000	0.000
1-2-2-73	-0.740	12.812	0.736
2-2-73-3	-0.602	1.170	0.286
5-2-73-3	0.604	1.148	-0.296
2-73-3-7	-1.460	0.436	0.188
2-73-3-1	1.494	0.450	-0.282

[a]The atom type of epoxide carbon atom for MM calculation
[b]The atom type of epoxide oxygen atom for MM calculation

The relative energies of stable conformers obtained by *ab initio* and by MM2 methods are shown in Fig. 1.

MM2 program, version '87, was obtained from Molecular Design Ltd.[14] All possible ring conformations were generated by CONFLEX2[15,16] and optimized by MM2. The Boltzmann population of each energy minimum at 25°C was calculated on the basis of its

steric energy. Average vicinal H/H coupling constants (J_{HH}'s) were calculated from 60 energy minima of **1** and 64 of **2** using Altona's empirical modification of the Karplus equation.[17-19] The optimized geometries of conformers having populations above

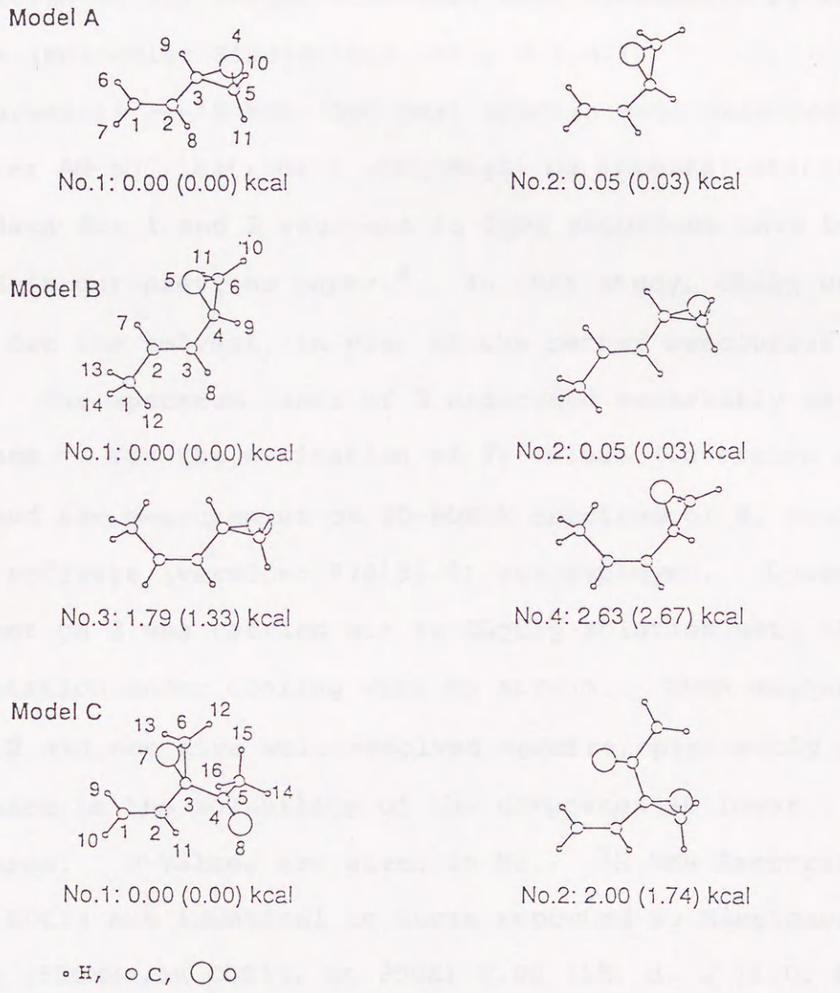

Fig. 1 Stable conformers of model compounds calculated by *ab initio* (MP2/6-31G*//HF/6-31G*) and their relative energies (MM2 values in parentheses)

1.0% obtained by CONFLEX/MM2 calculations were used as the input for AM1 (AMPAC version 2.1)[10] calculations. The total number of the stable conformers calculated are seven for **1**, 12 for **2**, and three for **3**. These MM and MO calculations were carried out on an IRIS 4D/320GTX workstation (Silicon Graphics). Three-dimentional structures, frontier orbital extension and superposition of the target molecules were visualized by the use of QUANTA (Molecular Simulations Inc., U.S.A.).

NMR measurements.——^{1}H NMR (500 MHz) spectra were measured at 27°C on a Bruker AM-500 instrument with Me_4Si as internal standard. The NMR data for **1** and **2** recorded in C_6D_6 solutions have been described in our previous paper.[6] In this study, $CDCl_3$ was employed for the solvent, in view of the better resolution of signals. The spectrum lines of **3** broadened remarkably at normal temperature. For the estimation of T_1 values (inversion recovery method) and the measurement of 2D-NOESY spectrum of **2**, Bruker standard software (version: 870101.0) was employed. Dynamic NMR measurement on **3** was carried out in CD_2Cl_2 solution with the same instrumentation under cooling with N_2 stream. DNMR measurements on **1** and **2** did not give well-resolved spectra, presumably due to the decrease in the solubility of the compounds at lower temperatures. *J*-Values are given in Hz. ^{1}H NMR Spectral data for **1** in $CDCl_3$ are identical to those reported by Hauptmann *et al.*[1] For **2**: δ_H (500MHz,in $CDCl_3$, at 300K) 6.00 (1H, d, *J* 11.0, H-1,T_1=3.13 s), 5.86 (1H, d, *J* 16.2, H-5, T_1=2.78), 5.67 (1H, dt, *J* 11.0, 8.1, H-2, T_1=2.66), 5.62 (1H, dd, *J* 9.6, 16.2, H-6, T_1=2.25),

4.94 (1H, br.s, H-15, T_1=1.52), 4.81 (1H, t, J 1.5H-15', T_1=1.63), 3.13 (1H, dd, J 12.5, 8.8, H-3α, T_1=1.24), 3.08 (1H, d, J 6.6, H-14,T_1=1.52), 2.90 (1H, dd, J 12.5, 8.1, H-3β, T_1=1.59), 2.89 (1H, d, J 6.6, H-14',T_1=1.08), 2.56 (1H, dd, J 11.0,5.9, H-8α, T_1=1.08), 2.51 (1H, dd, J 11.0, 8.1, H-8β, T_1=1.01), 2.27 (1H, m, H-7, T_1=1.81), 1.68 (1H, m, H-11, T_1=1.80), 0.96 (3H, d, J 6.6, H-12, T_1=1.01), 0.91 (3H, d, J 6.6, H-13, T_1=1.01). For **3**: δ_H (500MHz, in $CDCl_3$, at 300K) 6.06 (1H, d, J 11.0, H-1), 5.79 (1H, dt, J 7.1, 11.0, H-2), 5.43 (1H, br, H-6), 2.85 (1H, d, J 6.0, spiroepoxy), 2.8 (1H, m, H-3), 2.79 (1H, d, J 6.0, spiroepoxy), 2.78 (1H, m, H-8), 2.48 (1H, br,H-7), 2.35 (1H, br, H-7'), 2.28 (1H, br, H-4), 2.1 (1H, br, H-8'), 2.03 (1H, m, H-3'), 1.74 (1H, dt, J 3.1, 12.7, H-4'), 1.57 (3H, s, methyl group at C-5).

Results and discussion

Molecular mechanics calculations.——The conformational properties of major conformers having over 4% Boltzmann populations at 25°C of **1**, **2** and **3** are summarized in Tables 2, 3 and 4, respectively. *Periplanone-A* (**1**). CONFLEX2 generated 60 energy minima. Among them, six major conformers of **1** (**1A** to **1F**) within 1.2 kcal mol^{-1} from the global energy minimum are considered significant, and they are shown in Fig. 2.[†††] Only two types of ring conformations appears in these major conformers, each containing three rotamers at the isopropyl groups in addition to those depicted in Fig. 2. **1A**, **1D**, and **1F** have almost identical twist-chair (TC) ring con-

[†††] 1 cal = 4.184J.

formation, in spite of the distinction of their nomenclatures.[20] The structure of global minimum **1A** can be considered identical with the X-ray structure (Table 2).[6] It should be noted that the ring conformation **1A**, and also **1D** and **1F**, is the same as the global minimum of **4**. The combined population of these conformers, **1A**, **1D** and **1F** amounts to 48.7%.

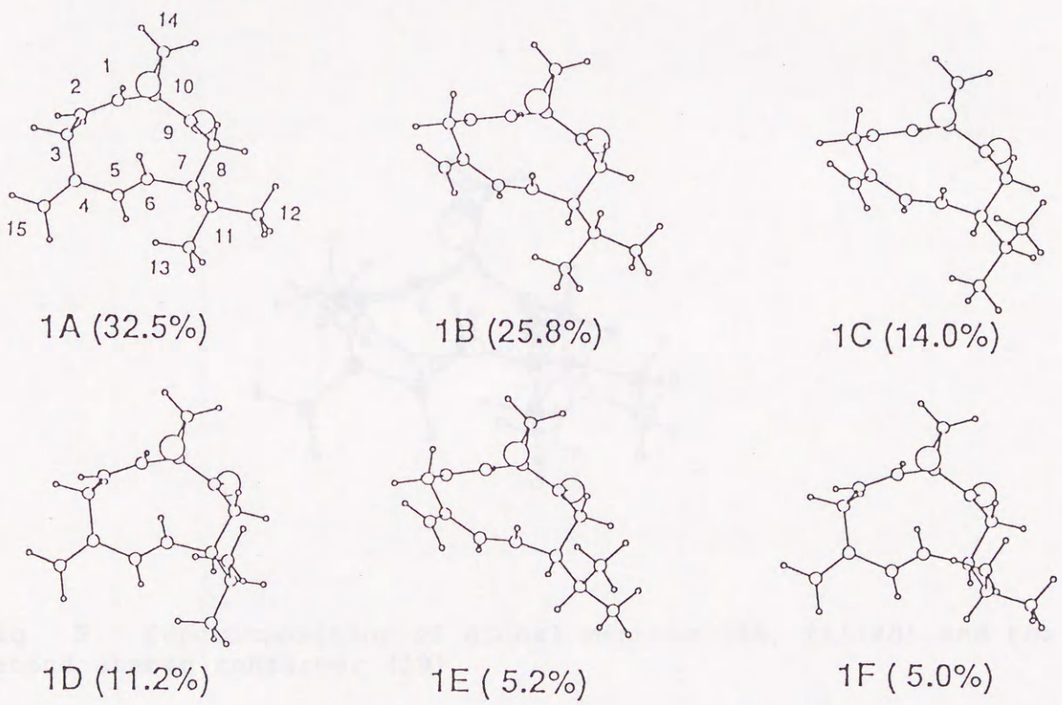

Fig. 2 Major conformers of periplanone-A **1** (the estimated Boltzmann populations at 298K in parentheses)

On the other hand, the second stable conformer **1B**, as well as the rotamers **1C** and **1E**, have a ring structure in which the C(2)-C(3)-C(4)-C(5) portion including C(4) exomethylene group flap upward. The dihedral angle of C(15)-C(4)-C(5)-C(6) in **1B** (-55.5°) is about 100° different from that of **1A** (*ca.* -151.5°). As can be seen in Fig. 3, **1A** and **1B** are almost superimposable except for the exomethylene moiety. Flapping of exomethylene group brings epoxy-oxygen [O(3)] close to the C(5)-C(6) moiety in **1B** [O(3)-C(5) =3.00Å, O(3)-C(6) =2.86Å], in comparison with **1A** [O(3)-C(5) =3.82Å, O3-C6 =3.05Å].

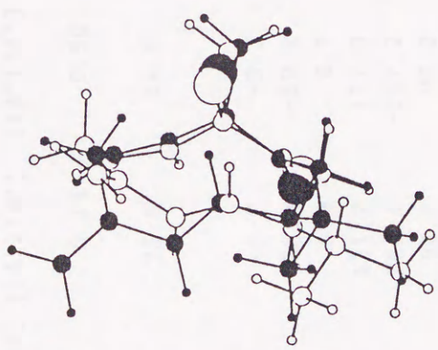

Fig. 3 Superimposition of global minimum (**1A**, filled) and the second stable conformer (**1B**)

The calculated vicinal H/H coupling constants ($^3J_{HH}$'s) essentially agree with those observed [7-8α:obs. 11.8(*J*/Hz), calc. 12.08(*J*/Hz); 7-8β:obs. 5.2(*J*/Hz), calc. 3.27(*J*/Hz)].

Table 2 Conformational properties of **1** and X-ray data of **1**.

	1A	1B	1C	1D	1E	1F	X-ray[a]
Ring conformation[b]	[123'1'3']	[14'1'4']	[14'1'4']	[124'3']	[14'1'4']	[124'3']	[123'1'3']
ΔE_S/kcal mol^{-1}	0.0	0.14	0.50	0.63	1.09	1.11	
Boltzmann dist.(%) at 25°C	32.5	25.8	14.0	11.2	5.2	5.0	
Dihedral angle/°							
C(10)-C(1)-C(2)-C(3)	-7.5	-3.2	-3.3	-7.7	-3.2	-7.6	-3.5
C(1)-C(2)-C(3)-C(4)	-89.9	-58.4	-59.2	-92.1	-58.6	-91.9	-93.4
C(2)-C(3)-C(4)-C(5)	69.1	6.9	6.7	65.7	6.7	66.6	71.9
C(3)-C(4)-C(5)-C(6)	38.1	121.2	121.0	38.5	121.8	37.4	39.9
C(4)-C(5)-C(6)-C(7)	-167.8	-164.1	-162.2	-166.3	-162.6	-166.6	-167.0
C(5)-C(6)-C(7)-C(8)	116.8	94.8	96.2	123.7	94.8	123.4	114.4
C(6)-C(7)-C(8)-C(9)	-46.8	-62.4	-64.5	-51.8	-64.0	-50.6	-50.0
C(7)-C(8)-C(9)-C(10)	82.8	75.2	74.1	80.5	75.0	81.0	92.5
C(8)-C(9)-C(10)-C(1)	-133.3	-130.4	-128.6	-127.7	-129.6	-128.6	-140.5
C(9)-C(10)-C(1)-C(2)	113.9	131.2	132.5	117.5	131.9	116.7	106.5
C(8)-C(7)-C(11)-H(11)	60.4	58.2	-60.4	-52.9	169.3	-179.9	64.2
C(9)-C(8)-C(7)-C(11)	-169.7	175.2	169.2	-178.1	171.1	-176.2	-174.6

[a]Ref. 6. [b]Modified Dale nomenclature. Primes indicate a pseudo-corner(g^+ g^-).[20]

Epoxy epimer (**2**). Four conformers of **2** are considered significant (Fig. 4). The ring conformation of global minimum **2A** has never appeared in our previous studies, while those of **2B** and **2D** are similar to that of **1A** (Table 3).

Table 3 Conformational properties of **2**.

	2A	**2B**	**2C**	**2D**
Ring conformation[a]	[14'1'4']	[1'333']	[1324]	[1'333']
ΔE_S/kcal mol^{-1}	0.0	0.1	0.80	1.12
Boltzmann dist.(%) at 25°C	34.2	29.0	8.8	5.1
Dihedral angle/°				
C(10)-C(1)-C(2)-C(3)	3.4	1.2	4.4	1.3
C(1)-C(2)-C(3)-C(4)	56.7	-90.5	57.6	-92.4
C(2)-C(3)-C(4)-C(5)	-5.7	77.5	2.7	75.4
C(3)-C(4)-C(5)-C(6)	-126.5	31.2	-120.9	30.9
C(4)-C(5)-C(6)-C(7)	162.2	-165.2	162.0	-164.5
C(5)-C(6)-C(7)-C(8)	-89.4	105.6	-57.7	111.5
C(6)-C(7)-C(8)-C(9)	64.2	-36.1	-51.7	-40.0
C(7)-C(8)-C(9)-C(10)	-78.2	90.2	76.1	89.4
C(8)-C(9)-C(10)-C(1)	131.3	-149.1	48.6	-145.6
C(9)-C(10)-C(1)-C(2)	-130.7	98.3	-135.5	100.9
C(8)-C(7)-C(11)-H(11)	59.7	59.6	59.2	-51.4
C(9)-C(8)-C(7)-C(11)	-64.2	-159.5	-176.5	-166.8

[a]Modified Dale nomenclature. Primes indicate a pseudo-corner(g^+ g^-).[20]
64 Energy minima were obtained from 456 initial geometries which were generated by CONFLEX2.

The difference of the ring conformation between **2A** and **2C** can be seen along C(7)-C(8)-C(9)-C(10) moiety, where the flap around the carbonyl group causes H-1 to approach H-8β (2.68 Å). These

results are consistent with the NMR data. The complex 2D-NOESY spectrum[6] of **2** (Fig. 5) indicates the coexistence of two or more conformers. This spectrum contrasts with that of **1** where only three NOE contacts (H-5/H-7, H-5/H-15, H-6/H-3) involving H-5 and H-6 could be measured.[6] The observed NOE contacts can be explained in terms of the three major conformers. The assignments of the NOESY cross peaks and proximate proton pairs in each conformers of **2** are shown in Fig. 6. The calculated vicinal H/H coupling constants ($^3J_{HH}$'s) essentially agree with those observed [7-8α:obs. 5.9(*J*/Hz), calc. 4.62(*J*/Hz); 7-8β:obs. 8.1(*J*/Hz), calc. 7.87(*J*/Hz)].

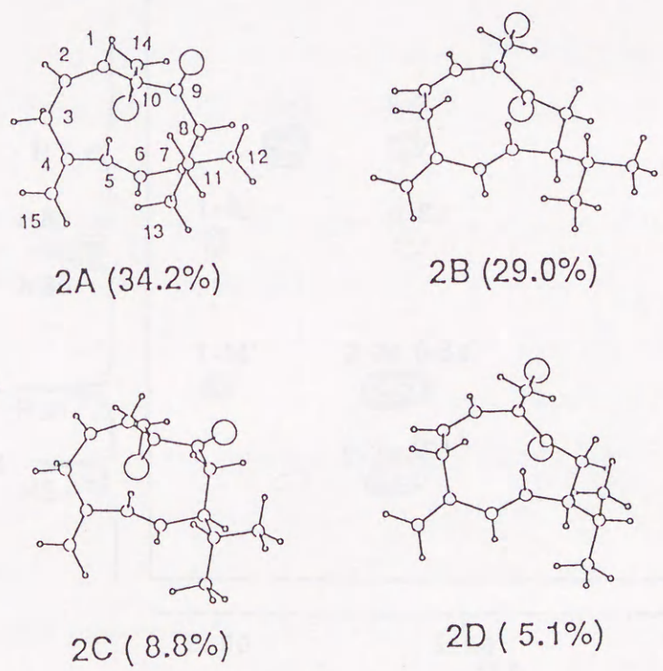

Fig. 4 Major conformers of the epimer **2** (the estimated Boltzmann populations at 298K in parentheses)

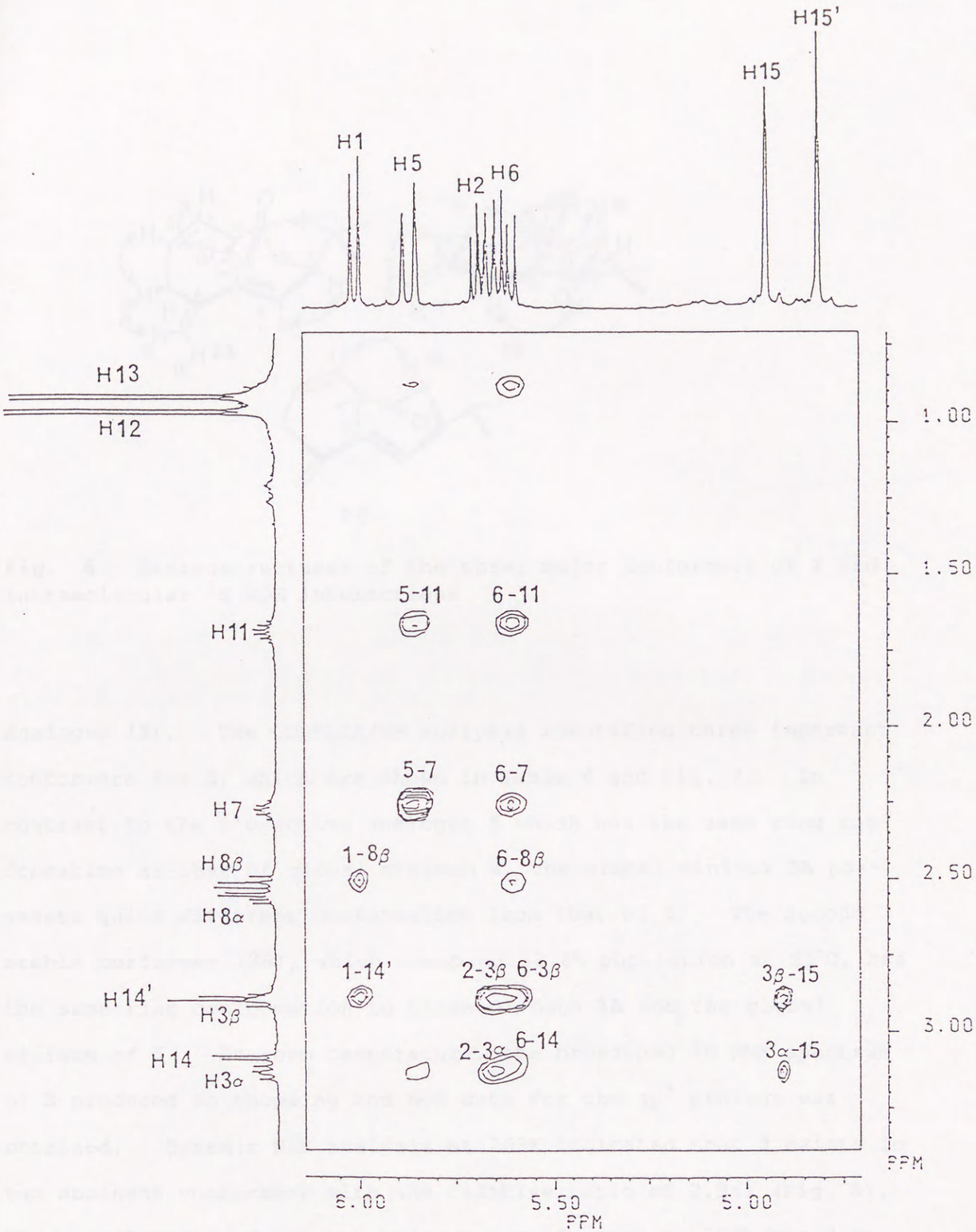

Fig. 5 Partial 2D NOESY spectrum of **2** (mixing time 3 s) in $CDCl_3$ at 300K

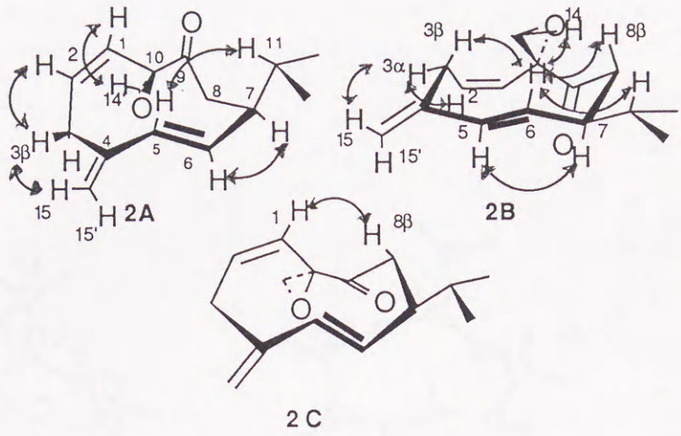

Fig. 6 Stereostructures of the three major conformers of **2** and intramolecular ^{1}H NOE interactions

Analogue (**3**). The CONFLEX/MM analysis identified three important conformers for **3**, which are shown in Table 4 and Fig. 7. In contrast to the bio-active analogue **5** which has the same ring conformation as that of global minimum **4**, the global minimum **3A** possesses quite different conformation from that of **1**. The second stable conformer (**3B**), which occupied 32.6% population at 25°C, has the same ring conformation to those of both **1A** and the global minimum of **5**. At room temperature, the broadened ^{1}H NMR spectrum of **3** produced no coupling and NOE data for the sp^{3} protons was obtained. Dynamic NMR analysis at 203K indicated that **3** exists in two dominant conformers with the relative ratio of 2.3:1 (Fig. 8). The calculated ratio of the major two conformers at 203K based on the relative energies of conformers (2.6:1) is in good agreement with the observed data.

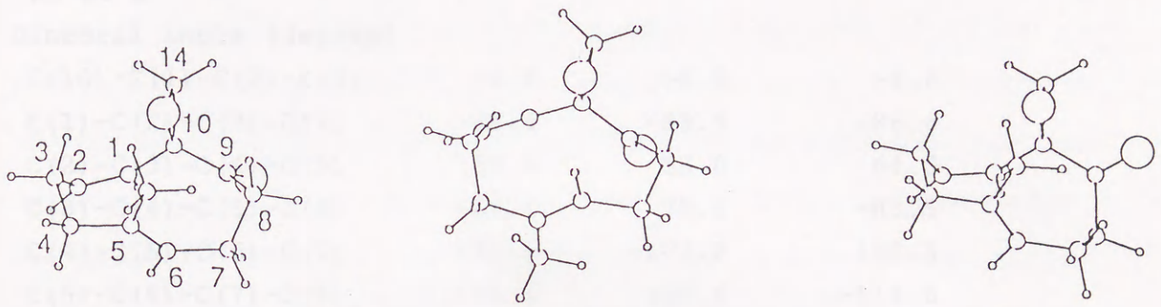

3A (62.7%) **3B (32.6%)** **3C (4.2%)**

Fig. 7 Major conformers of analogue **3** (the estimated Boltzmann populations at 298K in parentheses)

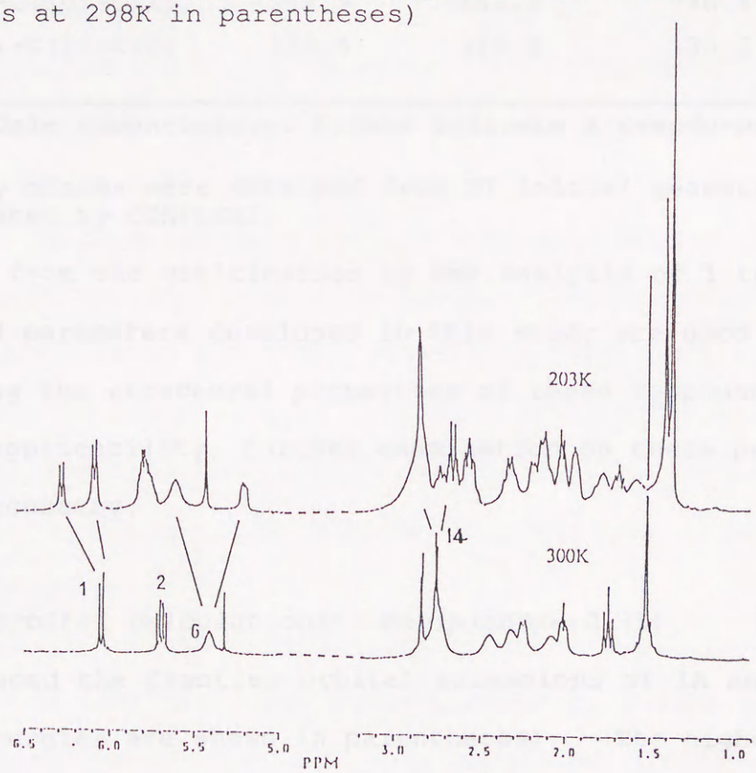

Fig. 8 Dynamic NMR spectra of **3** in CD_2Cl_2 solution at 300K and 203K

Table 4 Conformational properties of **3**.

	3A	**3B**	**3C**
Ring conformation[a]	[23'23']	[123'1'3']	[232'3']
ΔE_S/kcal mol^{-1}	0.0	0.39	1.60
Boltzmann dist.(%) at 25°C	62.7	32.6	4.23
Dihedral angle (degree)			
C(10)-C(1)-C(2)-C(3)	-4.4	-6.0	-4.6
C(1)-C(2)-C(3)-C(4)	-84.4	-89.9	-86.6
C(2)-C(3)-C(4)-C(5)	69.9	53.8	64.0
C(3)-C(4)-C(5)-C(6)	-86.1	70.5	-83.5
C(4)-C(5)-C(6)-C(7)	172.9	-173.2	168.3
C(5)-C(6)-C(7)-C(8)	-75.4	100.6	-116.6
C(6)-C(7)-C(8)-C(9)	-44.1	-49.3	71.0
C(7)-C(8)-C(9)-C(10)	79.2	82.9	-61.8
C(8)-C(9)-C(10)-C(1)	-114.9	-133.3	-40.4
C(9)-C(10)-C(1)-C(2)	129.5	116.9	135.2

[a]Modified Dale nomenclature. Primes indicate a pseudo-corner (g^+ g^-).[20]
Four Energy minima were obtained from 27 initial geometries which were generated by CONFLEX2.

Judging from the verification by NMR analysis of **1** to **3**, our force-field parameters developed in this study are good enough for representing the structural properties of these compounds. For the wider applicability, further examination on these parameters would be necessary.

Molecular orbital calculations——Periplanone-A (**1**). In Fig. 9, are reproduced the frontier orbital extensions of **1A** and **1B** (orbital energies are shown in parentheses). The highest occupied molecular orbital (HOMO) of both **1A** and **1B** are localized mainly at the conjugated-diene [C(15)-C(4)-C(5)-C(6)]

moiety. Both LUMO and next-LUMO of **1A** are widely distributed over all π-type orbitals of many atoms in the molecule. It may be recalled here that LUMO and next-LUMO of the global minimum of **P-B** (**4**) are relatively localized. However, a closer analysis revealed that the frontier electron density of LUMO of **1A** is particularly concentrated at the conjugated-diene; the densities in conjugated-diene, epoxy-carbonyl and double bond moieties are calculated to 1.2316, 0.3018 and 0.3791 ($e^- Å^{-3}$), respectively. The frontier electron density of next-LUMO is more concentrated at epoxy-carbonyl moiety (1.1027 $e^- Å^{-3}$) than at the conjugated-diene moiety (0.6116 $e^- Å^{-3}$). The same tendency is found in the isopropyl rotamers **1D** and **1F**.

In contrast to **1A**, the LUMO of **1B** (and of the isopropyl rotamers **1C** and **1E**) is mainly localized around the epoxy-carbonyl moiety and the next-LUMO at the conjugated diene moiety (Fig. 9). It is noteworthy that in conformer **1B** the LUMO atomic orbital of the carbonyl carbon is delocalized with that of C(1) olefinic carbon atom, and forms relatively high electron density region along the inner side of C(9)-C(10)-C(1)-C(2) sequence. A good overlapping between the high density regions around the epoxy-carbonyl moiety of **1A** (next-LUMO) and those of **1B** (LUMO) can be pointed out.

Epoxy epimer (**2**). The extension of frontier orbitals of the global minimum (**2A**) and other major conformers except the second and forth ones (**2B** and **2D**) are quite different from that of **1A**. In the case of **2B**, which possesses essentially the same conform-

ational feature as **1A**, the distribution of frontier orbitals resembles that of **1A**. However, the transposition of the oxygen atom in the epoxy group resulted in the reduction of the delocalization of the π-electrons between the epoxy and carbonyl groups.

Analogue (**3**). Among the two major conformers of **3**, the feature of the frontier orbital in the global minimum (**3A**) seems to be similar to that of **5**,[7] while the ring conformation itself is drastically different. On the other hand, the second stable conformer (**3B**) has a **1A** type ring conformation and the LUMO is localized around the epoxy-carbonyl moiety as in the case of the global minimum of **5**. The next-LUMO in **3B** exists mainly at C(1)-C(2) double bond, but the orbital is delocalized around the carbonyl group.

The Contribution of New Ring Structure as seen in **1B** *toward the Biological Activity.*---From the results of the MM and MO calculations, the resemblance between the conformational and electronic characteristics of the stable conformers of **P-A** (**1**) and **P-B** (**4**)[7] are now apparent. The ring structure and molecular orbital of the global minimum **1A** are superimposable to that of **4**. However, the remarkable difference is the presence of the partially-flapped conformers having the ring type **1B**, of which the combined population (45.0%) is as large as that of **1A** (48.7%). In the case of **4**, the combined population of the conformers having the

ring type **1A** is predominant (87.8%), and that of type **1B** is relatively small (6.5%).

In our previous study on the structure-activity relationships on **4** and its analogues, only the ring type of the global minimum of **4** had been taken into account as being biologically important. However, good overlapping of frontier unoccupied orbital around upper part of ten-membered ring ($FUMO_{upper}$) are indicated as well as the conservation of their molecular shapes around the biologically important epoxy-carbonyl moiety between **1A** and **1B**, in this study. In the light of the similarity of **1B** to **1A**, it was anticipated that both the ring type of **1A** and **1B** must be biologically relevant ring structure. Therefore, effective frontier parameters [$EF^{(N)}{}_{(S)}$] were re-calculated for **4-8** with regard to these two ring types (Table 5).

Table 5 Improved $EF^{(N)}{}_{(S)}$ obtained by considering two ring types and observed biological activity of compounds

compound	improved $EF^{(N)}{}_{(S)}$[a]	Biological activity[b]
4	3.925	-13
5	3.011	-9
6	2.116	-7
7	1.183	-6
8	0.865	-5

[a]Effective frontier parameter.
[b]$\log_{10}$[threshold(g)], assessed by behavioural test.

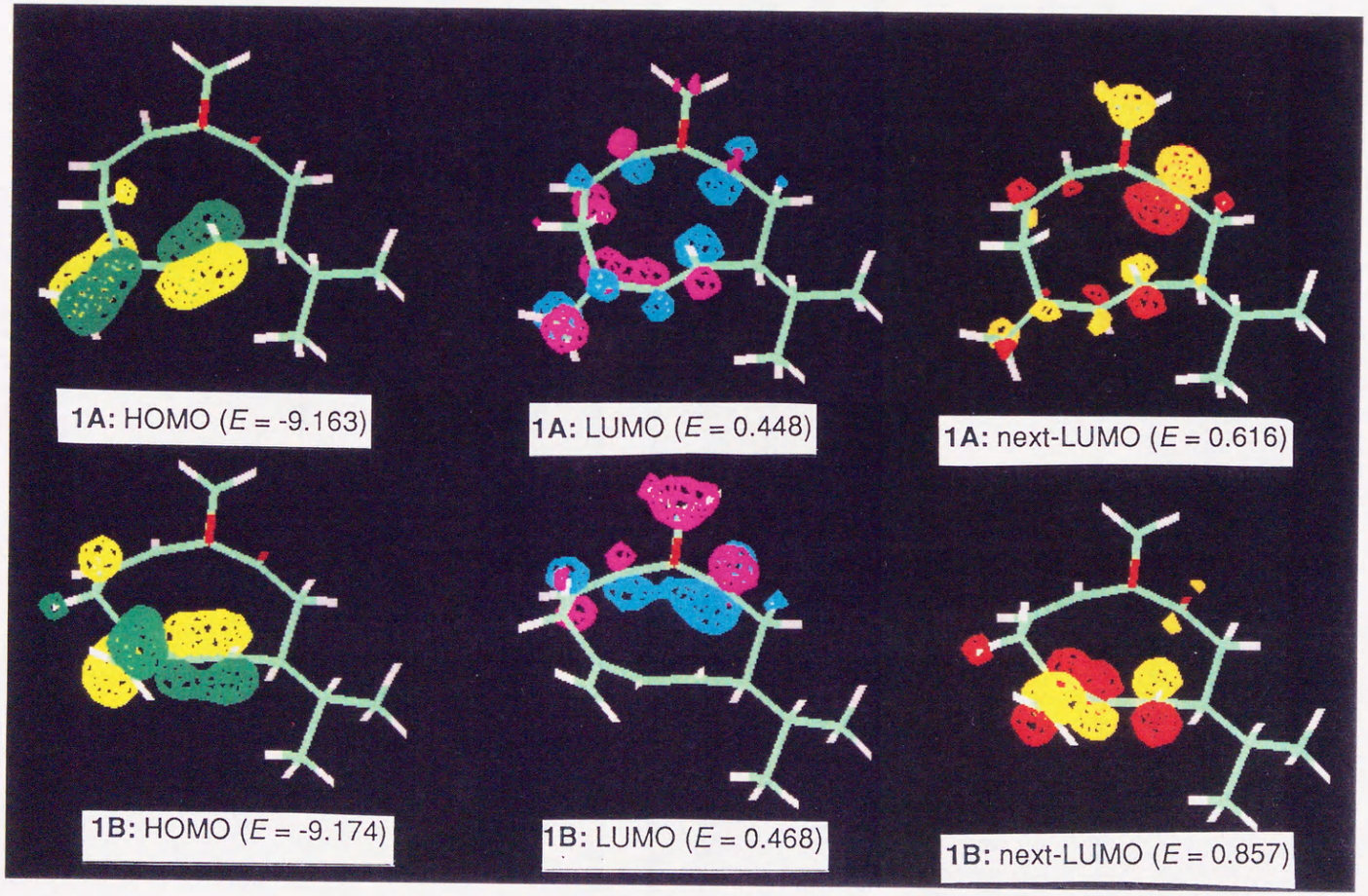

Fig. 9 Frontier orbitals of the global minimum and the second stable conformer of **1**, the value of each frontier orbital energy (*E*/eV) is shown in parentheses

As can be seen in Fig. 10, a better correlation between $EF^{(N)}_{(S)}$ values by using the two ring types with the biological activity is obtained as in the following equation.

$$\log_{10}[\text{Activity threshold(g)}] = -2.649 - 2.410 \times EF^{(N)}_{(S)} \quad (5)$$

($R = 0.969$, $\sigma = 0.91$, $F = 45.07$, SE = 0.36, $t_{static} = 6.71$ and $n = 5$)

The correlation is improved compared to that obtained by using only one ring type ($R = 0.929$).[7]

The biological activities of **1-3** are re-calculated from this new linear regression equation (Table 6). The predicted value of biological activity of **1** (threshold: $10^{-11.2}$g) was in good agreement with that observed in the bioassay. The drastic reduction on the biological activities of **2** and **3** from **1** also agrees with the predicted low values of biological activity. In the case of **2**, however, the observed value is higher than the predicted value. This may be explained by the 0.01% contamination of highly active **1**, which formed in the synthetic process of **2**. The predicted biological activity of **3** means that it has practically no activity in our bioassay system.

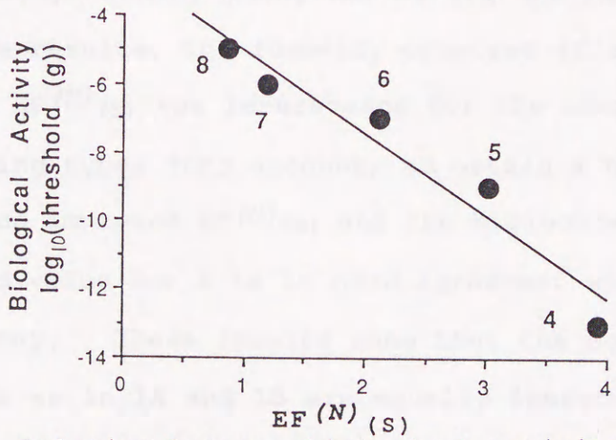

Fig. 10 Relation between biological activity and the value of improved $EF^{(N)}_{(S)}$ of **4-8**

Conclusion

By virtue of the new parameters and CONFLEX/MM2 calculations on periplanone-A (**1**), the epoxy epimer (**2**) and the analogue (**3**), their significantly populating conformers have been identified. The validity of the calculated results was confirmed by comparison with X-ray crystallographic and NMR analyses. The global minimum **1A** is well superimposable to that of periplanone-B (**4**). However, the second conformer **1B**, of which the exomethylene functional group is flapped upward is revealed to exist in comparable concentration as **1A** (1:0.92). In contrast, the corresponding ratio in **4** is 1:0.07. The geometries around the epoxy-carbonyl moiety are common between these two ring types. According to the AM1 study, the electronic distributions in the frontier unoccupied orbitals localized around the upper part of ten-membered ring ($FUMO_{upper}$) of the **1A** type conformers are different from those of **1B**. However the high density regions in $FUMO_{upper}$ are commonly distributed around the epoxy-carbonyl moiety among **1A**, **1B** and the case of **4** (**P-B**).[7] From these results, the formerly proposed effective frontier parameter $EF^{(N)}{}_{(S)}$ was re-assessed for the compounds **4-8** by taking the two ring types into account, to obtain a better correlation between the improved $EF^{(N)}{}_{(S)}$ and the biological activity. The calculated value for **1** is in good agreement with that observed in the bioassay. These results show that the conformers with the two ring types as in **1A** and **1B** are equally important to exhibit

biological activity. The improved effective frontier parameter $EF^{(N)}_{(S)}$ appears reliable.

In concluding this series of studies, we propose that the frontier unoccupied molecular orbitals localized around the epoxy-carbonyl moiety of periplanones must play an important role for the biological activity. We find no significant linear correlation between biological activities and electronic properties of HOMO and $FUMO_{lower}$, which are mainly located in the conjugated-diene moiety [C(5)-C(6) double bond in **5**] in all compounds examined.[7] However, the contributions of this electron rich region to pheromone recognition in the receptor site cannot be excluded in the view of π-π and hydrophobic interactions. Such discussion may be a subject in future study. As the coupling of computational chemical methods and structure-activity concepts must be potentially powerful, works along this line will provide valuable informations on the recognition of bioactive molecules, and will be linked to design new analogues.

References

1 H. Hauptmann, G. Mühlbauer and H. Sass, *Tetrahedron Lett.*, 1986, **27**, 6189.

2 S.Kuwahara and K.Mori, *Tetrahedron*, 1990, **46**, 8083, and references cited therein.

3 C. J. Persoons, F. J. Ritter and W. J. Lichtendonk, *Proc. Kon. Ned. Akad. Wetensch. Amsterdam*, 1974, C77, 201 (*Chem. Abstr.*, **81**, 88-209f); for a review on American cockroach sex pheromones, see C. J. Persoons, F. J. Ritter, P. E. J. Verwiel, H. Hauptmann and K. Mori, *Tetrahedron Lett.*, 1990, **31**, 1747, and references cited therein.

4 W. C. Still, *J. Am. Chem. Soc.*, 1979, **101**, 2493.
5 K. Okada, M. Mori, K. Shimazaki and T. Chuman, *J. Chem. Ecol.*, 1991, **17**, 695.
6 M. Mori, K. Okada, K. Shimazaki, T. Chuman, S. Kuwahara, T. Kitahara and K. Mori, *J. Chem. Soc., Perkin Trans. 1*, 1990, 1769.
7 K. Shimazaki, M. Mori, K. Okada, T. Chuman, H. Gotō, E. Ōsawa, K. Sakakibara and M. Hirota, *J. Chem. Soc., Perkin Trans. 2*, 1992, 811.
8 T. L. Macdonald, C. M. Delahunty, and J. S. Sawyer, *Heterocycles*, 1987, **25**, 305.
9 T. Harada, T. Takahashi and S. Takahashi, *Tetrahedron Lett.*, 1992, **33**, 369.
10 QCPE #506 AMPAC version 2.1
11 M. Mori, K. Okada, K. Shimazaki and T. Chuman, *Tetrahedron Lett.*, 1990, **31**, 4037.
12 *Gaussian 90*, M. J. Frisch, M. Head-Gordon, G. W. Trucks, J. B. Foresman, H. B. Schlegel, K. Raghavachari, M. A. Robb, J. S. Binkley, C. Gonzalez, D. J. Defrees, D. J. Fox, R. A. Whiteside, R. Seeger, C. F. Melius, J. Baker, R. L. Martin, L. R. Kahn, J. J. P. Stewart, S. Topiol, and J. A. Pople, Gaussian, Inc., Pittsburgh PA, 1990.
13 K. Sakakibara, H. Kawamura, T. Nagata, M. Hirota, K. Shimazaki and T. Chuman, submitted.
14 U. Burkert, and N. L. Allinger, *Molecular mechanics*, ACS Monograph 177, American Chemical Society, Washington, DC, 1982.
15 H. Gotō and E. Ōsawa, *J. Chem. Soc., Perkin Trans. 2*, 1993, 187.
16 H. Gotō and E. Ōsawa, *Tetrahedron*, 1993, **49**, 387.
17 C. A. G. Haasnoot, F. A. A. M. de Leeuw, and C. Altona, *Tetrahedron*, 1980, **36**, 2783.
18 S. Masamune, P. Ma, R. E. Moore, T. Fujiyoshi, C. Jaime, and E. Ōsawa, *J. Chem. Soc., Chem. Commun.* 1986, 261.
19 E. Ōsawa, T. Ouchi, N. Saito, M. Yamato, O. S. Lee and M.-K. Seo, *Org. Magn. Reson.* 1992, **30**, 1104.
20 H. Gotō, *Tetrahedron*, 1992, **48**, 7131.

Chapter 7

Conclusions

Insect pheromones, serricornin, periplanones, and related analogues have been studied by computational methods and the following conclusions have been obtained:

1)

The absolute configurations of acyclic and cyclic forms of serricornin are determined to be (*4S*,6S*,7S**) and (*3S*,5S*,6S**), respectively from comparison of the observed $^3J_{HH}$s values with those calculated for all possible diastereomers. It is revealed that the MM conformational analysis is useful in the determination of the unknown stereochemistry of natural products.

2)

X-ray crystallographic and NOE analyses have been performed on periplanone-A (**P-A**), -B (**P-B**) and their analogues to obtain the biologically active structures. The crystal structure of **P-A** established by X-ray analysis can be well superimposed on that of **P-B**. The results of the analyses by X-ray and NOE indicate that the conformation of the ten-membered ring of the analogues and the relative positions of the functionalities containing oxygen are analogous to those of **P-A** and **P-B**. However, the 2D NOESY spectrum of the epoxy-epimer of **P-A** is too complicated to permit a definition of the conformation.

In order to clarify the conformational properties, a complete analysis by molecular mechanics of **P-B** and its

related analogues was carried out by CONFLEX/MM2 with an additional set of MM2 force field parameters for the epoxy functional group. The validity of the calculated results was confirmed by comparison with X-ray and NMR results. The ring conformation of the global minimum of **P-B** is a dominant one among the stable conformers. The conformation of the global minimum of **P-B** is well superimposable on those of the analogues and of the third conformer of Germacrene-D. A hypothesis can be drawn as follows; the biological activities of **P-B** and the analogues depend on the total population of the conformers having the same ring conformation as the global minimum of **P-B**. CONFLEX/MM2 study suggests that the ring conformation of the global minimum of **P-B** is the biologically important structure.

An AM1 study on the stable conformers obtained by CONFLEX/MM2 was carried out to investigate the correlation between the electronic properties and their pheromone activity. Both HOMO and LUMO of the global minimum of **P-B** are localized around the conjugated diene moiety. The next-LUMO is localized around the spiro-epoxy and carbonyl groups. The extensions of the HOMO of the stable conformers of the analogues are similar to those of **P-B**. The distributions of the frontier unoccupied orbitals (LUMO and next-LUMO) of **P-B** and the analogues can be classified into two groups. The frontier unoccupied orbitals in the first group are distributed around the 'upper' part of the ten-membered ring in the structural formula, which include the next-LUMO of **P-B**. While those in the second group are localized around the 'lower' part of the ten-membered ring, including the LUMO of

P-B. For convenience, the former orbitals are called the frontier unoccupied orbital around the upper part of ten-membered ring (abbreviated as $FUMO_{upper}$). In the same manner, the latter orbitals are called the frontier unoccupied orbital around the lower part of ten-membered ring (abbreviated as $FUMO_{lower}$). Only the population-weighted orbital energy of $FUMO_{upper}$ shows a good correlation with biological activity (R=0.849). It suggests that the $FUMO_{upper}$ plays an important part in the biological activity.

A new parameter, effective frontier parameter ($EF^{(N)}_{(S)}$), is proposed as an index for the evaluation of pheromone activity; this takes into account the electronic properties in $FUMO_{upper}$ and the geometries of the stable conformers of **P-B** and the analogues. In the equation which defines $EF^{(N)}_{(S)}$, the conformational properties are given as the *structural factor*; 1, the ring structure of the stable conformer is superimposable on that of the global minimum of **P-B**; 0, the ring structure is not superimposable. The correlation between $EF^{(N)}_{(S)}$ and biological activities (R=0.929) is improved.

The same conformational analyses are performed on **P-A** and the related analogues to confirm the reliability of $EF^{(N)}_{(S)}$. A CONFLEX/MM2 calculation with a new set of the parameters for vinyl-epoxy functional group revealed the conformational properties of those compounds. The complicated NOESY spectrum of the epoxy-epimer of **P-A** can be explained on the basis of this calculated data. The conformation of the global minimum of **P-A** is well superimposable on that of **P-B**. However, the second conformer of **P-A**, of which exomethylene

group is flapped upwards, exists in comparable concentration with the global minimum. A comparison of the ring structure of the global minimum with that of the second one shows that the geometries around the epoxy-carbonyl moiety and the high density regions in $FUMO_{upper}$ are similar to each other. Therefore, $EF^{(N)}{}_{(S)}$ was reassessed for **P-B** and their analogues on the basis that these two ring structures are the biologically important ones. An even better correlation between improved $EF^{(N)}{}_{(S)}$ and biological activities is obtained (R=0.969). The predicted value of the biological activity for **P-A** calculated from the new linear regression equation is in good agreement with that observed in the bioassay. The improved $EF^{(N)}{}_{(S)}$ appears reliable as an index for the prediction of the biological activity of newly designed analogues.

In this thesis, computational methods are applied to the assignments of stereochemistry and to the structure-activity study of natural pheromones. The coupling of computational methods with experiments in insect pheromone studies may be extended to other biological molecules to give information on the nature of molecular recognition.

Acknowledgment

The author is sincerely grateful to Professor Eiji Ōsawa, Department of Knowledge-Based Information Engineering, Toyohashi University of Technology, for his guidance to the field of the study and reviewing her thesis.

The author would like to express her gratitude to Professor Terutsugu Abe, Department of Knowledge-Based Information Engineering, Professor Kenji Ito and Associate Professor Hisao Nishiyama, Department of Materials Science, Toyohashi University of Technology, for reviewing her thesis.

The author would also like to express her appreciation to Dr. Hitoshi Gotō, Department of Chemistry, Faculty of Science, Hokkaido University, Professor Minoru Hirota and Dr. Kazuhisa Sakakibara, Department of Synthetic Chemistry, Faculty of Engineering, Yokohama National University, Professor Kenji Mori and Associate Professor Takeshi Kitahara, Department of Agricultural Chemistry, Faculty of Agriculture, The University of Tokyo, Associate Professor Shigefumi Kuwahara, Laboratory of Agricultural Chemicals, Faculty of Agriculture, Ibaraki University, for their useful advice and encouragement.

The author gratefully acknowledges Dr. Tatsuji Chuman, General Manager of Technological Planning Dept. Head Office of Japan Tobacco Inc., Drs. Masana Noma and Hajime Matsushita, Deputy General Managers of Life Science Research Laboratory of Japan Tobacco Inc. by giving her a chance for organizing the thesis, Drs. Kunio Kato, Yukiteru Obi, and Tsuyoshi Sasaki (General Manager of Life Science Research Laboratory of Japan Tobacco Inc.) by their support during the work.

The author especially thanks Drs. Masataka Mori, Kentaro Okada and Akihiko Watanabe for their helpful cooperation in the study.

December first, 1993

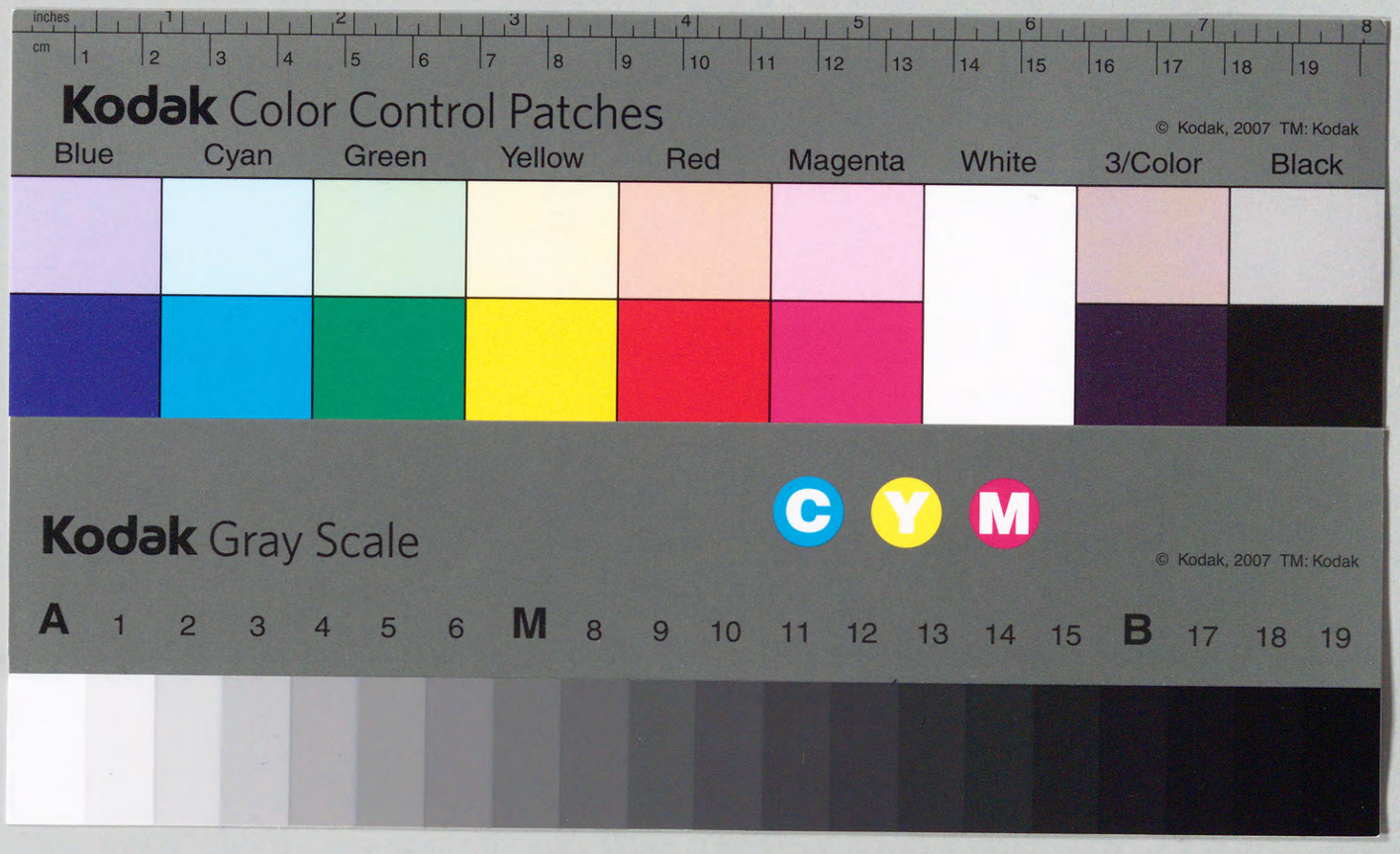
inches
cm
Kodak Color Control Patches
© Kodak, 2007 TM: Kodak
Blue
Cyan
Green
Yellow
Red
Magenta
White
3/Color
Black
Kodak Gray Scale
C
Y
M
© Kodak, 2007 TM: Kodak
A 1 2 3 4 5 6 M 8 9 10 11 12 13 14 15 B 17 18 19